FEDERAL UNIVERSITY OF CEARÁ
DEPARTMENT OF TELEINFORMATICS ENGINEERING
POSTGRADUATE PROGRAM IN TELEINFORMATICS ENGINEERING

WESKLEY VINICIUS FERNANDES MAURICIO

SCHEDULING FOR MASSIVE MIMO WITH HYBRID PRECODING BASED ON OPTIMIZATION AND CONTEXTUAL MULTI-ARMED BANDITS

FORTALEZA

2021

WESKLEY VINICIUS FERNANDES MAURICIO

SCHEDULING FOR MASSIVE MIMO WITH HYBRID PRECODING BASED ON OPTIMIZATION AND CONTEXTUAL MULTI-ARMED BANDITS

Thesis presented to the Postgraduate Program in Teleinformatics Engineering of the Federal University of Ceará as a partial requisite to obtain the Ph.D. degree in Teleinformatics Engineering.

Supervisor: Prof. Dr.-Ing. Tarcisio Ferreira Maciel

Co-supervisor: Prof. Dr. Francisco Rafael Marques Lima

FORTALEZA

2021

Dados Internacionais de Catalogação na Publicação
Universidade Federal do Ceará
Biblioteca Universitária
Gerada automaticamente pelo módulo Catalog, mediante os dados fornecidos pelo(a) autor(a)

F412s Fernandes Mauricio, Weskley Vinicius.
Scheduling for Massive MIMO with Hybrid Precoding Based on Optimization and Contextual Multi-armed Bandits / Weskley Vinicius Fernandes Mauricio. – 2021.
101 f. : il. color.

Tese (doutorado) – Universidade Federal do Ceará, Centro de Tecnologia, Programa de Pós-Graduação em Engenharia de Teleinformática, Fortaleza, 2021.
Orientação: Prof. Dr. Tarcisio Ferreira Maciel.
Coorientação: Prof. Dr. Francisco Rafael Marques Lima.

1. MIMO Massivo. 2. Alocação de recursos de Radio. 3. Qualidade de Serviço. 4. Equidade. 5. Contextual Multi-armed bandits. I. Título.

CDD 621.38

WESKLEY VINICIUS FERNANDES MAURICIO

SCHEDULING FOR MASSIVE MIMO WITH HYBRID PRECODING BASED ON OPTIMIZATION AND CONTEXTUAL MULTI-ARMED BANDITS

Thesis presented to the Postgraduate Program in Teleinformatics Engineering of the Federal University of Ceará as a partial requisite to obtain the Ph.D. degree in Teleinformatics Engineering.

Approved in: */*/*.

EXAMINATION BOARD

Prof. Dr.-Ing. Tarcisio Ferreira Maciel (Supervisor)
Universidade Federal do Ceará

Prof. Dr. Francisco Rafael Marques Lima (Co-supervisor)
Universidade Federal do Ceará

Prof. Dr.-Ing. Anja Klein
Technische Universität Darmstadt

Prof. Dr. Aldebaro Barreto da Rocha Klautau Júnior
Universidade Federal do Pará

Prof. Dr. Yuri Carvalho Barbosa Silva
Universidade Federal do Ceará

Acknowledgements

I would like to thank everyone that somehow contributed to this thesis and my personal development during my Ph.D. degree.

First and above all, I thank my family: my wife (Gabriela Leite), my mother (Veralucia), and my brother (Weslley). A special thanks to my wife, who believed and followed me around the world, cheering me up even in the hardest times. Also, a special thanks to my mother, who believed in me always investing in my studies. I would not have come this far without their support.

I would also like to thank my supervisor Prof. Dr. Tarcisio Ferreira Maciel. I greatly appreciate the support, guidance, and opportunities that you offered me. A special thanks go to my co-supervisor Prof. Dr. Francisco Rafael Marques Lima, who believed and guided me since graduation. You inspired me to follow the research area from the beginning.

I would like to thank PROBRAL (CAPES/DAAD) program to the opportunity to go abroad for the sandwich Ph.D. at Technische Universität Darmstadt in Germany. I would also like to thank my supervisor during the sandwich Ph.D. at Technische Universität Darmstadt in Germany - Prof. Dr.-Ing Anja Klein, for accepting to be my supervisor. She contributed immensely to increase the quality of my thesis and to me as a researcher. Also, thanks to you and the entire research group (Tobias, Andrea, Kilian, and the rest of the team) that received me warmly, making me feel at home.

I would also like to thank my colleagues at GTEL/UFC, mainly my friend Alexandre who always motivated me through his commitment. I also thank my old friend Laszlon, who always pioneered the paths I would follow.

A long stretch of road will teach you more about yourself than a hundred years of quiet introspection.

(Patrick Rothfuss)

Resumo

Nesta tese, estudamos os problemas de RRA (do inglês, *radio resource allocation*) em sistemas de quinta geração (5G) que utilizam a tecnologia MIMO (do inglês, *multiple-input multiple-output*) massivo. Focamos em resolver os problemas de otimização de desempenho (maximização da taxa de dados) dos sistemas MIMO massivo sujeitos a garantias de QoS (do inglês, *quality of service*). Contudo, estes problemas são extremamente difíceis em MIMO massivo, principalmente quando levamos em consideração os desafios práticos, dos quais podemos citar a limitação no número de cadeias de Rádio-Frequência (RF), precodificação híbrida e estimação de canal. Nesta tese aplicamos otimização numérica e CMABs (CMABs, do inglês *contextual multi-armed bandits*) para solucionar problemas de RRA. Também, esta tese é dividida em duas partes. A primeira parte tem por objetivo utilizar otimização para resolver os problemas de maximização de taxa de dados considerando cenários com e sem requisitos de QoS. Nesta parte, propomos um arcabouço para solução do problema composto de três passos - clusterização, agrupamento, e escalonamento. No passo da clusterização, criamos clusters de UEs (do inglês, *user equipment*) espacialmente compatíveis. No passo do agrupamento, selecionamos um conjunto de grupos SDMA (do inglês, *space-division multiple access*) de cada cluster. No passo do escalonamento, utilizamos estes grupos SDMA como candidatos para receber RBs (do inglês, *resource blocks*) com o objetivo de resolver um problema de RRA pré-definido. Nós propomos soluções ótimas e sub-ótimas para resolver os passos de agrupamento e escalonamento. As soluções propostas apresentaram um bom custo-benefício de desempenho em relação às soluções ótimas de alta complexidade e às soluções de referência. Na segunda parte, propomos um arcabouço utilizando CMAB dinamicamente adaptável para resolver três problemas de RRA: i) maximização da taxa de dados; ii) maximização da taxa de dados com garantias de justiça, e; iii) maximização da taxa de dados com garantias de QoS, que são problemas relevantes na área de comunicações sem fio. Nesta parte, utilizamos a clusterização e a precodificação híbrida para reduzir a complexidade do escalonamento considerando cada cluster como um agente de escalonamento CMAB virtual independente. Após isso, aplicamos um novo escalonador baseado em CMAB com objetivo de otimizar o desempenho desejado. Resultados de simulação mostram que o arcabouço proposto apresenta um bom custo-benefício de desempenho em termos de taxa de dados, justiça e QoS em relação às soluções de referência.

Palavras-chave: MIMO massivo, RRA, QoS, Equidade, CMAB.

Abstract

In this thesis, we study radio resource allocation (RRA) problems in fifth generation (5G) systems with massive multiple-input multiple-output (MIMO) technology. We focus on optimizing the system performance (data rate maximization) of massive MIMO systems subject to quality of service (QoS) guarantees. However, these problems are extremely difficult to solve in massive MIMO, especially when practical challenges are taken into account, such as the need of a large number radio frequency (RF) chains, hybrid precoding and channel estimation. In order to solve the studied RRA problems in this thesis, we use as main tools optimization and contextual multi-armed bandits (CMAB). Also, this thesis is divided into two parts. The first part utilizes optimization to solve the problems of maximizing the data rate with and without considering QoS requirements. In this part, we propose a framework composed of three steps: clusterization, grouping, and scheduling. In the clusterization step, we create cluster of spatially compatible user equipments (UEs). In the grouping step, we select a set of space division multiple access (SDMA) groups from each cluster. In the scheduling step, we utilize these SDMA groups as candidates to receive resource blocks (RBs) aiming at solving a predefined RRA problem. We propose optimum and suboptimum solutions to solve the grouping and scheduling steps. The low-complexity proposed solutions present a good performance trade-off in relation to the highly complex optimal solutions and reference solutions. In the second part, we propose a framework utilizing dynamically adaptable CMAB to solve three RRA problems: i) data rate maximization; ii) data rate maximization with fairness guarantees, and; iii) data rate maximization with QoS guarantees, which are relevant problems in wireless communications. In this part, we utilize the clusterization and hybrid precoding to reduce the scheduling problem complexity by considering each cluster as an independent virtual CMAB scheduling agent. Next, we apply a new CMAB-based scheduler aiming to optimize the desired system performance metric. The solution for each problem utilizing our proposed framework is evaluated separately with UEs moving at different speeds. Simulation results showed that the proposed framework presents a good performance trade-off in data rate, fairness, and QoS in relation to the reference solutions.

Keywords: Massive MIMO, RRA, QoS, Fairness, CMAB.

List of Figures

List of Tables

List of Abbreviations and Acronyms

1G	first generation
3GPP	3rd generation partnership project
4G	fourth generation
5G	fifth generation
BB	branch and bound
BET	blind equal throughput
BF	best fit
BS	base station
CDF	cumulative distribution function
CMAB	contextual multi-armed bandits
CSI	channel state information
E2E	end-to-end
eMBB	enhanced mobile broadband
EPA	equal power allocation
FDD	frequency division duplexing
G-OPT	optimal grouping
G-PROP	proposed grouping
ILP	integer linear problem
IoT	internet of things
JSM	joint satisfaction maximization
LOS	line-of-sight
LTE	long-term evolution
M2M	machine-to-machine
MAB	multi-armed bandits
MIMO	multiple-input multiple-output
mMTC	massive machine-type communication
mmWave	millimiter wave
MT	maximum throughput

MTFG	maximum throughput with fairness guarantees
MTQG	maximum throughput with QoS guarantees
NLOS	non line-of-sight
NR	new radio
OC	only clustering
OFDM	orthogonal frequency division multiplexing
OFDMA	orthogonal frequency division multiple access
PF	proportional fair
QAM	Quadrature Amplitude Modulation
QoS	quality of service
QuaDRiGa	quasi deterministic radio channel generator
RAN	radio access network
RB	resource block
RF	radio frequency
RL	reinforcement learning
RRA	radio resource allocation
S-OPT	optimal scheduling
S-PROP	proposed scheduling
SDMA	space division multiple access
SE	spectral efficiency
SINR	signal to interference-plus-noise ratio
SISO	single input single output
SLNR	signal to leakage plus noise ratio
SVD	singular value decomposition
TDD	time division duplex
TTI	transmit time interval
UE	user equipment
UMi	urban micro
UPA	uniform planar array
URLLC	ultra-reliable and low latency communication
ZF	zero-forcing

List of Symbols

$\mathcal{J}$	Set of user equipments (UEs)
J	Number of UEs
$\lvert\cdot\rvert$	Set cardinality
$\mathcal{S}$	Set of services
S	Number of services
$\mathcal{J}_s$	Number of UEs belonging to service s
K	Number of scheduled UEs
N_t	Number of transmission antenna elements
N_symb	Number of orthogonal frequency division multiplexing (OFDM) symbols
N_sc	Number of adjacent orthogonal frequency division multiple access (OFDMA) subcarriers
$\mathcal{N}$	Number of available resource blocks (RBs)
x_k	Symbol to be sent to UE k
$\boldsymbol{f}_k$	Precoding vector employed on data for UE k
$\boldsymbol{h}_k$	Channel vector between the base station (BS) and UE k
p_k	Power allocated to UE k
$\mathcal{M}$	Set containing the UEs receiving information from BS
z_k	Additive Gaussian white noise
$\boldsymbol{\Omega}_j$	Covariance matrix associated to the channel between base station and UE j
$\boldsymbol{h}_{t,j}$	Downlink channel vector between the BS and the UE j at transmit time interval (TTI) t
τ	Number of channel samples considered to estimate the covariance matrix
$\boldsymbol{D}_j$	Matrix containing eigenvectors from channel covariance of UE j
$\boldsymbol{\Lambda}_j$	Matrix containing eigenvalues from channel covariance of UE j

N_C	Number of clusters
G_g	Number of UEs in a given space division multiple access (SDMA) group g
$\bar{J}_c$	Number of UEs selected in each SDMA group in cluster c
$\boldsymbol{E}_c$	Average of the eigenvector matrices $\boldsymbol{D}_j$ belonging to cluster c
$\mathcal{J}_c$	Set of UEs belonging to cluster c
J_c	Number of UEs belonging to cluster c
$\boldsymbol{K}_c$	Matrix containing the $\bar{J}_c$ strongest eigenvectors of matrix $\boldsymbol{E}_c$
$\boldsymbol{e}_{c,b}$	Strongest eigenvector b from matrix $\boldsymbol{E}_c$ of cluster c
$\boldsymbol{F}_g^{\mathrm{RF}}$	Analog precoder from SDMA group g
$\boldsymbol{H}_g$	Group channel matrix of the UEs belonging to SDMA group g
$\zeta_{k,g}$ k^{th}	UE of SDMA group g
$\bar{\boldsymbol{H}}_g$	Equivalent channel matrix formed by $\boldsymbol{H}_g$ and $\boldsymbol{F}_g^{\mathrm{RF}}$ of SDMA group g
$\boldsymbol{F}_g^{\mathrm{BB}}$	Digital precoder of SDMA group g
$\|\cdot\|_{\mathrm{F}}$	Frobenius norm
p_{RB}	Total power constraint per RB
$\boldsymbol{P}_g$	Diagonal power matrix of each UE belonging to the SDMA group g
N_{s}	Total number of streams
$\boldsymbol{F}_g$	Hybrid precoding of SDMA group g
$\hat{\boldsymbol{y}}_g$	Receive information vector of SDMA group g
$\boldsymbol{x}_g$	Group symbol vector of SDMA group g
$\boldsymbol{z}_g$	Group noise vector of SDMA group g
$\Gamma_{i,g}$	Average signal to interference-plus-noise ratio (SINR) perceived by UE i from SDMA group g
σ_i^2	Noise power of UE i
R_i	Data rate of UE i
B	Bandwidth of the RB
R_{f}	Number of radio frequency (RF) chains
N_{g}	Number of generated SDMA groups
$\hat{\boldsymbol{D}}$	Matrix containing the eigenmodes from channel covariance of all UEs
$\boldsymbol{d}_{j,1}$	Vector containing the dominant eigenvector from channel covariance of UE j
λ_j	Highest eigenvalue of UE j
$\boldsymbol{a}$	Attenuation vector containing the inverse of the dominant eigenmode of all UEs in a cluster
$\boldsymbol{C}$	Spatial correlation matrix of all UEs in a cluster
$\boldsymbol{u}$	Binary selection vector of UEs to compose an SDMA group

u_j	Binary variable that assumes the value 1 if UE j is selected to compose an SDMA group and 0 otherwise
$m(\hat{\Pi})$	Convex combination of the total spatial correlation and channel gains
$\hat{\Pi}$	Set of UEs belonging to an SDMA group
β	Control parameter establishing the trade-off between spatial correlation and channel gain
$\boldsymbol{u}^{\star}$	Solution containing the best SDMA groups
$\hat{\Pi}_c$	Set of UEs belonging to SDMA group of cluster c
$\mathcal{O}(\cdot)$	Worst-case computational complexity
$\tilde{\boldsymbol{D}}$	Matrix containing the concatenation of all UEs eingenmodes of a given cluster measured for the middle RB
$\tilde{\boldsymbol{a}}$	Attenuation vector for the middle RB of all UEs in a given cluster
$\tilde{\boldsymbol{C}}$	Spatial correlation matrix of all UEs in a cluster for the middle RB
$\hat{\boldsymbol{C}}$	Block diagonal spatial correlation matrix for a given cluster of each SDMA group
$\boldsymbol{I}_n$	$n \times n$ identity matrix
$\otimes$	Kronecker product operator
$\mathbf{1}_n$	$n \times 1$ vector composed of 1's
$\hat{\boldsymbol{a}}$	Block diagonal attenuation vector for a given cluster of each SDMA group
$\boldsymbol{T}$	Fairness constraint matrix of the SDMA groups
$\boldsymbol{V}_i$	Matrix to guarantee the diversity of UEs in the SDMA groups
$\boldsymbol{O}$	Binary assignment matrix of RBs and SDMA groups
$o_{g,n}$	Element of $\boldsymbol{O}$ that assumes the value 1 if the RB n is assigned to the SDMA group g and 0 otherwise
$\boldsymbol{R}$	Tensor containing the Shannon capacity of UEs, RB, and SDMA groups
$r_{g,j,n}$	System data rate of the UE j in RB n belonging to SDMA group g and 0 otherwise
$\boldsymbol{\rho}$	Binary selection vector of the UEs selected to be satisfied
ρ_j	Element of $\boldsymbol{\rho}$ that assumes the value 1 if UE j is selected to be satisfied and 0 otherwise
$\boldsymbol{l}$	Vector containing the UEs required data rate
l_j	Required data rate of UE j
$\boldsymbol{w}$	Vector containing the minimum number of UEs necessary to be satisfied per service
w_s	Required minimum number of UEs of service s

$\mathcal{G}$	Set containing the available SDMA groups
υ	Number of linear programming subproblems
$\Gamma_{g,j,n}$	SINR perceived by UE j in RB n from SDMA group g
κ_j	Number of SDMA groups that UE j belongs to
N_{RB}	Number of available RBs to be allocated
$\mathcal{R}$	Receiver set of UEs that needs to receive RBs to get satisfied
$\mathcal{D}$	Available resource set containing all RBs that can be donated from the donors
$\mathcal{F}$	Contains the pairs of $\mathcal{G}$ and $\mathcal{D}$ that maximize the number of satisfied UEs
$\mathcal{R}_{j^\star}$	Set of receivers that belong to the SDMA group g of the chosen UE $j^\star$
$\hat{l}_j$	Required data rate of UE j according to the current resource assignment
Φ^{cur}	Sum of data rates achieved by all allocated UEs in all RBs according to the current resource assignment
$\Phi^{new}_{g,n}$	Sum of the data rates when the SDMA group g receives via reallocation the RB n without modifying the assignment on the other RBs
π_g	Number of receivers in SDMA group g
g'	SDMA group chosen to a given RB in the unconstrained maximization part
$r_{g',j,n}$	Data rate of UE j on RB n in SDMA group g'
$j^\star$	UE to be disregarded
α	Reward (system data rate)
A	Number of possible actions
$\mathcal{A}$	Action space
A_c	Number of possible actions of cluster c
$\mathcal{A}_c$	Action space of cluster c
$\boldsymbol{d}_c$	Action value of cluster c
a_c	Given action of cluster c
$P_j(\cdot)$	Priority function to obtain the priority of UE j
v^{avg}	Arithmetic mean of the throughput obtained by the UEs
v_j	Throughput of the $j-$ th UE
δ	Variable to control the shape of the priority function
$q_c(a_c)$	Arithmetic mean priority of the UE belonging to a given action a_c
$\mathcal{U}_c(a_c)$	Set containing the UEs composing the action a_c
K_c	Number of scheduled UEs of cluster c

v^{req}	Required throughput of UE j
μ	Value between 0 and 1 that refers to the system satisfaction desired by the system operator
Ω	Value between 0 and 1 that refers to the security threshold for the priority function to start changing its shape
η	Variable that determines the shape of the function P_j
ϵ	Probability of the algorithm performing the exploration phase

Table of Contents

Chapter 1

Introduction

Over the last decades, mobile communications experienced an incredible development moving from the analog voice-only first generation (1G) of cellular systems to the commercial deployment of fifth generation (5G) networks in 2019 [1]. Some of the requirements that 5G is designed to support are [2]–[5]:

- Massive connectivity - Massive number of connected devices supporting internet of things (IoT) and machine-to-machine (M2M) communications.
- Higher data rates - Devices achieving data rates 10 to 100 times higher than in fourth generation (4G).
- Lower latency - End-to-end latency reaching 1 millisecond, supporting real-time processing and transmission.
- Energy efficiency - Increased energy saving and battery lifetime with gains of 10-fold over 4G networks. Also, it is expected to achieve an energy efficiency of 0.01 J/bit.
- Flexibility - Supports the coexistence of different radio access network (RAN) technologies.

Therefore, 5G has the challenge to achieve higher data rates and lower latency, not exceeding 4G costs, while perfectly supporting heterogeneous networks. In order to achieve these requirements, new technologies have been studied in the past few years, and several 4G technologies have been improved to address 5G challenges. Among them we mention:

- **Massive multiple-input multiple-output (MIMO)** - It is a key technology capable of meeting the data rate requirements of 5G systems [6], [7].

This technology allows the base station (BS) to be equipped with tens to hundreds of antennas, enabling them to create many narrow beams to serve multiple user equipments (UEs) at the same resource block (RB), thus increasing spatial reuse and spectral efficiency [8], [9].

- **Millimiter wave (mmWave)** - Free microwave spectrum is scarce since this band has been used by the past cellular generations. Therefore, 5G should rely on new bands to meet the strict requirements mentioned above. mmWave provides large bandwidth, making it possible to achieve the high data rate requirements of 5G systems [10], [11]. Therefore, its availability and large bandwidth make it a key technology for 5G systems [3].

- **Network slicing** - It is a common physical or virtual network that supports different end-to-end (E2E) logical networks, known as slices. These slices can be created on demand and can be controlled/managed independently of each other. Also, it reduces the hardware cost of 5G by allowing the support of different RANs. Therefore, its flexibility makes it a key technology of 5G networks [12].

This thesis focuses on massive MIMO and mmWave technologies since they solve many technical challenges of 5G networks. Despite the benefits of those technologies, each one of them has its own challenges. In the next section, we detail the technologies considered in this thesis, as well as their benefits and challenges. In general, the application of those technologies is expected to make 5G support three general types of use cases [2], [13]:

- **Enhanced mobile broadband (eMBB)** - In this use case 5G networks are capable of fulfilling the quality of service (QoS) of data-hungry UEs by delivering data rates 10 to 100 times higher than in 4G. It will support higher UE mobility, enabling broadband access in vehicles, such as cars, trains, and planes. Also, it provides enhanced connectivity, making broadband access available everywhere, which creates the concept of ultra-dense networks. From the aforementioned technologies, we highlight mmWave and massive MIMO as promising to achieve this service requirement.

- **Massive machine-type communication (mMTC)** - This use case will provide connectivity solutions for a massive number of devices, such as weather and medical sensors, machines, and so on. Therefore, from the aforementioned technologies, we highlight massive MIMO as a promising technology to achieve this service requirement.

- **Ultra-reliable and low latency communication (URLLC)** - This use case will support services with extreme requirements on reliability, availability, and low latency, such as health care, smart city, and self-driving cars. From the aforementioned technologies, we highlight network slicing as a promising technology to achieve these service requirements.

Figure 1.1 shows the general type of use cases and some services provided by them.

Figure 1.1 – 5G use cases.

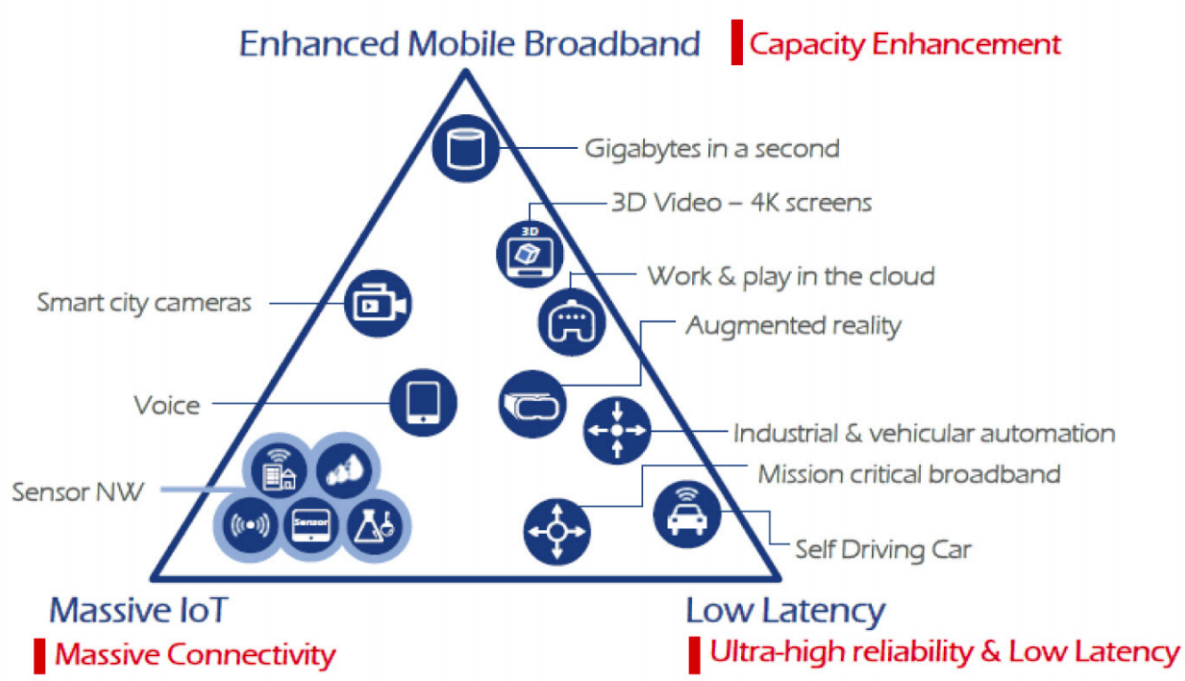

Source: ITU-R IMT 2020 requirements [14].

1.1 Background

1.1.1 Massive MIMO

MIMO is a multiplexing technique that provides the spatial dimension as a new resource for wireless communication. The combination of this additional spatial dimension and multiplexing techniques allows the transmission of several data streams, which increases the system data rate. As mentioned before, massive MIMO for 5G differs from the conventional MIMO used on 4G by the very large number of antennas at each BS [15]. The higher number of antenna elements and, therefore, spatial streams, leads to an increase in the data rate and number of served UEs. This increase in data streams fits very well in the new 5G systems, where a massive number of connected devices and the use of data hungry applications are expected. Figure 1.2 shows a multiuser

massive MIMO system with UEs using different kinds of services and being served by the BS with a massive number of antennas in the same RB.

Figure 1.2 – Example of a multiuser massive MIMO System.

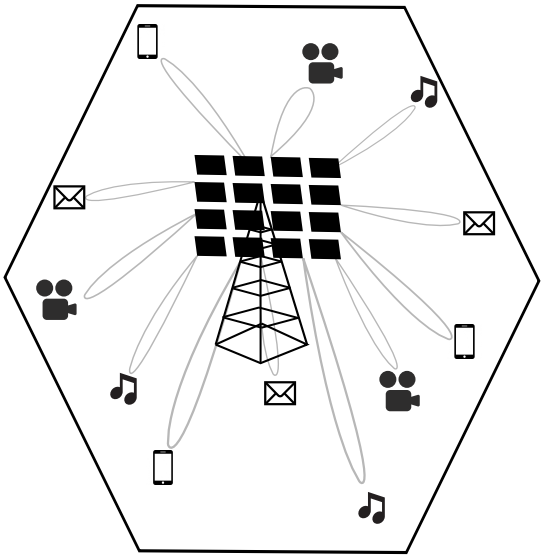

Source: Created by the author.

Another benefit of massive MIMO is the channel hardening effect [16], [17]. Due to the channel hardening, the randomness of wireless communications can become negligible, i.e., the channel can behave almost deterministically. This effect makes itself present by the deployment of many antennas, which minimizes the small-scale fading problem, leaving to be handled only the large-scale fading problem. The small-scale fading is one of the major issues in wireless communications. This effect may simplify the radio resource allocation (RRA), channel estimation, and other wireless communications procedures.

We highlight here that this thesis focuses on massive MIMO considering frequency division duplexing (FDD). Therefore, despite the benefits of massive MIMO, there are some issues [18]:

- **Large amount of required radio frequency (RF) chains** - In conventional MIMO, there is one RF chain per antenna element. Important to notice that an RF chain is a circuit composed of analog/digital converters, mixers, and power amplifiers. These circuits tend to be costly in high frequencies. Also, the number of RF chains at the BS determines the maximum number of supported streams. Therefore, the usage of the classical fully-digital precoding in massive MIMO is impractical since it needs as many RF chains as antennas, which results in unsustainable costs and power consumption [18], [19]. However, [20] says that hybrid beamforming will be replaced by digital beamforming in a few years, leading the

hybrid beamforming studies to take other directions in the future such as satellite communications.

- **Feed back channel** - In massive MIMO based on FDD, the UEs perform the channel estimation by reporting the channel state information (CSI) to the BS. However, the amount of information that each UE needs to feed back increases largely with the number of antennas, which can easily cause an overhead at the feedback channel since it is limited. Considering that this problem affects the available information at the BS, the precoder design is also affected [18], [19].

One way to counteract these issues is to split precoding into analog and digital domains, an approach also known as hybrid precoding [18], [19], [21].

1.1.2 Hybrid Precoding

Hybrid precoding is a two-stage precoding scheme that splits the beamforming between analog and digital domains, and which leads to employ less RF chains than transmit antennas. Therefore, this scheme allows the use of massive MIMO by using a small number of RF chains, which reduces the system design complexity and energy consumption. Otherwise, massive MIMO has prohibitive power consumption and cost. Also, this scheme provides great reduction in the CSI feedback [18].

There are two main architectures for hybrid precoding, which differ in the signal mapping of RF chains and transmit antennas [22]. The first one is called fully-connected hybrid precoding, where all transmitting antennas are connected to each RF chain, as illustrated in Figure 1.3a. Therefore, each RF chain uses the phase shifters to send signals to all transmitting antennas. This architecture fully exploits the precoding gain that can be obtained by each RF chain. The second one is called partially-connected hybrid precoding, where each RF chain is connected to a subset of transmitting antennas, as illustrated in Figure 1.3b. Therefore, each RF chain uses the phase shifters to send signals only to a reduced number of transmitting antennas. This architecture reduces the hardware complexity at the cost of losing beamforming gain. Therefore, there is a trade-off between these two structures, which has to be carefully taken into account in the implementation of hybrid precoding massive MIMO systems. In this thesis we consider that our system uses the fully-connected architecture.

The massive MIMO with hybrid precoding architecture brings several challenges, such as the joint optimization of analog and digital precoding, which

Figure 1.3 – Hybrid precoding architectures

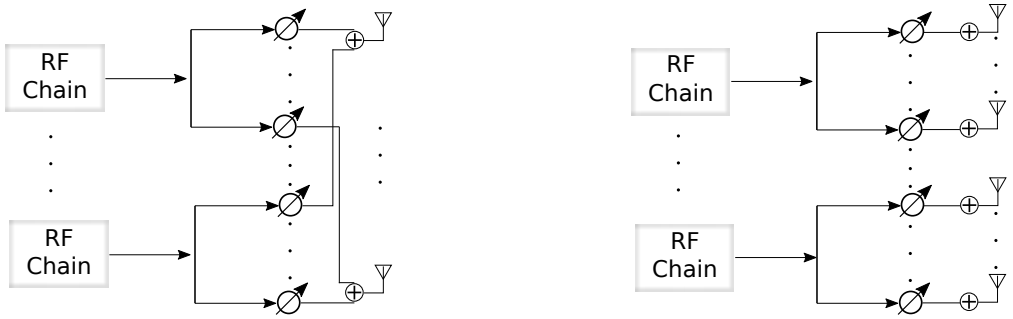

(a) Hybrid precoding fully connected. (b) Hybrid precoding partially connected.

Source: Created by the author.

leads to non-convex optimization problems. Moreover, phase shifters and other elements can be used to implement the analog precoder, which imposes additional constraints in the precoding design.

1.1.3 Radio Resource Allocation

RRA manages the available radio resources among the UEs in the system. In single input single output (SISO) wireless systems, the available resources can be frequency, transmit power, and time slots. In MIMO wireless systems, the use of beams adds the spatial resource dimension to the existing ones [23]. In particular, the RRA algorithms that manage the spatial resources are called space division multiple access (SDMA) schemes. SDMA solutions exploit the spatial compatibility among different UEs, placing UEs whose channels are nearly orthogonal in the same group and if the algorithm succeeds in grouping the users, increases the system spectral efficiency (SE) [24], [25]. In general, those resources need smart management, otherwise, they will negatively impact system performance. Also, managing these resources in the MIMO scenario leads to solutions with high computational complexity [26].

The way in which the SDMA groups are formed affects directly the precoding capability to reduce the interference among UEs. The characteristics of the selected UEs' channels dictate the performance achieved by the precoder, i.e., forming spatially compatible SDMA groups is fundamental to help the precoders to guarantee the best attainable signal to interference-plus-noise ratio (SINR).

The main drawback in SDMA problems is the number of possible groups that can be created [27]. Usually, the exhaustive search for the best groups is prohibitive. Over the years, two approaches for the SDMA grouping problem stood out:

- Classical iterative SDMA grouping approach - UEs are placed in the SDMA group in a sequential manner based on some spatial compatibility metric [24], [28].
- Clustering before scheduling - spatially correlated UEs are divided into clusters before being scheduled into an SDMA group [29], [30].

We highlight mathematical optimization as a key tool to handle the RRA problems. This tool provides a general framework to determine a possible solution (in many cases, the optimal one) to a well-defined problem. Optimization problems are expressed in terms of variables, objective function, and constraints [31].

Moreover, the large dimensionality of multi-user massive MIMO systems, on its own, drastically increases RRA complexity and, when combined with the stringent target requirements of 5G, RRA problems become even more difficult to be solved. Also, RRA in massive MIMO systems is challenging due to the inherent non-orthogonality among UEs, which can lead to high multi-user interference and affects the system performance negatively. Another challenge is that the problem is combinatorial and the number of scheduling possibilities grows exponentially with the number of UEs and available RF chains [32]. Therefore, the development of new RRA algorithms is particularly challenging in those scenarios [33], [34].

1.1.4 Reinforcement Learning

Reinforcement learning (RL) is a paradigm from machine learning that emulates human intelligence learning by trial and error when interacting with the environment. RL maps situations into actions aiming at maximizing a predefined objective [35]. There is a learning agent that interacts with the environment taking actions and obtaining a reward from it. In general, the agent does not have the entire information of the environment. The rewards the agent receives from each action it takes define which actions are good or bad for the agent (system). Therefore, the learning agent needs to keep trying the actions to discover which actions maximize the reward. These actions may change the actual state of the environment, affecting not only the immediate situations but also the future ones. Therefore, the learning agent will learn over time the best possible action it should take in a specific situation to maximize its reward [35].

The environment, learning agent, state, reward, and actions are some of the main elements of the RL field. However, there are some other important

elements as [35]:

- **Policy** - it is the brain of the learning agent, defining how it will behave at a given time. Therefore, the policy maps into an action the perceived state of the environment, i.e., the learning agent takes a specific action for a given policy and state [35].
- **Value function** - despite the fact that the reward indicates what is good in an immediate state, it does not give us any information about what is good in the long run. The value function comes to fill this gap since it provides information about how good an action is in the long term. Therefore, it is the expected reward that a learning agent will accumulate over time by taking a given action. For example, a given action can have a high-value function even if it has a low immediate reward at a given future state. It happens if, regularly, this action yields high rewards in some time instants [35].
- **Model of environment** - this element tries to give some information about the behavior of the environment. For example, for a given state and action, the best model will perfectly predict the next state and reward. The models are used to look at possible future states before trying them, making it easier for the learning agent to select the next action [35].

The RL solutions can deal with another difficulty of RRA in massive MIMO systems, which is how to perform it efficiently only with partial CSI, since UEs often have to be scheduled without complete knowledge of their full instantaneous channel at the BS. In this context, RL appears as a very suitable tool to this problem due to its capability of operating under limited/scarce information and still achieving good performance in the long run [36]. Also, RL is very suitable for RRA solutions since it aims to make an agent learn how to behave in an environment to optimize a predetermined objective, such as the system performance metrics considered by the scheduler, e.g., throughput, fairness or QoS [8].

Herein, we highlight contextual multi-armed bandits (CMAB) [37] as an RL method suitable to our studied problems. In CMAB, the learning agent observes some side information (e.g., outdated CSI) called context (state), and, based on that, chooses an action (e.g., schedules certain UEs) obtaining a reward (e.g., throughput) from it [37]. Then, the expected reward, called action value, can be calculated by averaging the obtained rewards of that action over time. Therefore, at each iteration, a decision is made based on the current context

Figure 1.4 – Reinforcement learning (RL) and CMAB problems.

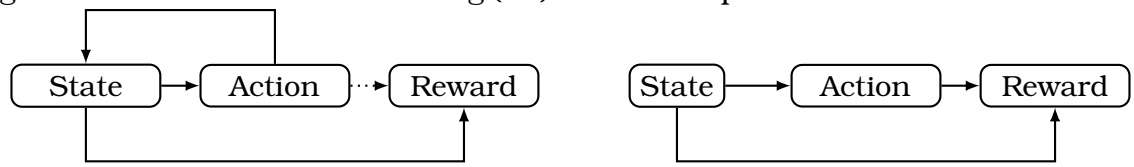

(a) RL problem. (b) CMAB problem.

Source: Created by the author.

and current action values aiming at maximizing the expected cumulative (long run) reward. CMAB solutions have to obtain a balance between increasing the information about the action values of different actions (exploration) and selecting the actions with higher action values (exploitation) to reach this goal [37]. The main difference between CMAB and other RL techniques is that in most RL techniques the agent can take multiple consecutive actions before obtaining the reward while in CMAB solutions the agent will use the state as context to decide which action to take and it will give a reward. Figure 1.4a shows the RL and CMAB. The RL have environmental states, where the next states depend on previous actions with the rewards being able to be delayed over time. Differently from RL The CMAB the actions that are taken in a given state affect only its reward and the reward cannot be delayed over time.

problem where an action affects state and both of them affect the reward and Figure 1.4b shows the CMAB problem where state and action affect reward.

Also we can cite the multi-agent feature that may help some wireless communications problems. The introduction of multi-agents in the model was shown to fit very well to solve wireless communication problems, such as interference coordination [38], [39].

1.2 Objectives and Thesis Structure

Considering the overview about massive MIMO, hybrid precoding, RRA and RL presented in previous sections of this chapter, the main objective of this thesis is to study RRA problems for massive MIMO subject to QoS guarantees using optimization and RL tools.

In Chapter 2, we describe the common system model that is employed in the following chapters of this thesis. In this chapter, we describe how the spatial covariance matrix and its eigendecomposition are used as statistical CSI by the clustering algorithm that is applied by the resource scheduling algorithm. Also, we present the hybrid precoding and received signal models followed by how the SINR and data rate are calculated.

Chapter 3 of this thesis is divided into two parts. The first part evaluates the problem of maximizing the system data rate considering only one RB and service. The second part evaluates the problem of maximizing the system data rate considering QoS constraints with multiple RBs and services. More specifically, in the first part of Chapter 3, we propose a scheduling based on a metric that accounts for the trade-off between their spatial channel correlation and channel gain. The corresponding scheduling is optimally solved by using branch and bound (BB) [40]. However, since the BB solution has high computational complexity, we propose a suboptimal scheduling algorithm that presents a reduced complexity. This scheduling is performed after the creation of clusters composed of spatially compatible UEs, as explained in Chapter 2. Moreover, we compare the proposed solutions with the random scheduler that performs clustering and chooses the UEs to compose the groups at random. In the second part of Chapter 3, we propose a framework composed of three steps - *clustering, grouping, and scheduling*. The clustering step is done as explained in Chapter 2. The grouping step is based on the previous metric utilized earlier in that chapter. However, to address this more complex problem containing multiple RBs, services, and QoS, new constraints are required. Also, we make use of the channel hardening phenomenon in massive MIMO to generate candidate SDMA groups independent of RBs. The scheduling step uses the candidate SDMA groups from the grouping step to solve the data rate maximization problem considering QoS requirements. We reformulate the problem in order to be solved by the BB algorithm. In order to avoid the BB complexity, we propose an efficient low complexity solution. In the simulation results, we evaluate the performance of each part of the proposed framework using both optimal and suboptimal solutions, as well as an adaptation of the joint satisfaction maximization (JSM) scheduler [41] to a massive MIMO scenario.

Chapter 4 of this thesis presents different scheduling problems using RL tools. More specifically, we propose a scheduling framework using CMAB that can dynamically adapt itself to solve three scheduling problems, which are: i) throughput maximization; ii) throughput maximization with fairness guarantees, and; iii) throughput maximization with QoS provisioning, which are well-known relevant problems in the area. The first step is to exploit the statistical CSI to create clusters of spatially compatible UEs, as explained in Chapter 2. Next, we apply a new learning-based scheduler aiming at optimizing the desired system performance metric. Moreover, only scheduled UEs need to feed back instantaneous equivalent CSI, which also reduces the signaling overhead of the proposal. The superiority of the proposed framework is demonstrated through

numerical simulations in comparison with reference solutions.

1.3 Related Works

In this section we present a literature review of works related to this thesis. Many works have investigated scheduling with QoS guarantees [41]–[43]. In [41], the authors study the problem of throughput maximization with QoS guarantees considering multiple services. The proposed scheduler, termed JSM, utilizes derivatives of a sigmoidal function that is dynamically adapted to protect the most prioritized service satisfying the UEs' QoS requirements. In [42], the authors proposed a new low-complex scheduling method based on graph theory aiming at maximizing the throughput considering QoS requirements in an orthogonal frequency division multiple access (OFDMA) wireless network. In [43], the authors propose a scheduling with the objective of balancing energy-efficiency and fairness among UEs considering QoS requirements in an OFDMA system. Therein, the scheduler is divided into two parts: the first part schedules the UEs aiming at achieving fairness among UEs and the QoS requirements, whereas the second part employs a power allocation algorithm to achieve the maximum energy efficiency with the already scheduled UEs. Despite their relevant contributions, the aforementioned works [41]–[43] do not consider a MIMO scenario, which includes the challenge of managing spatial resources besides the already considered time and frequency resources.

As it will be discussed in the sequel, several works propose scheduling solutions for massive MIMO systems considering fully digital precoding. In [29], the authors propose a solution that first creates clusters of UEs with similar spatial channel covariance (statistical CSI) using K-means algorithm [44]. Then, this statistical CSI of the UEs in a cluster is used to create an outer precoder that nearly suppresses the inter-cluster interference. Afterwards, UEs are suitably polled by the BS for their equivalent instantaneous CSI, which takes into account the UEs' channels and the cluster outer precoder. This equivalent instantaneous CSI has a smaller dimension than the full instantaneous channel (implying less signaling) and it is used to create an inner precoder that suppresses the UEs intra-cluster interference. In [45], the authors propose an algorithm that performs joint dynamic clustering and CSI acquisition, and a scheduler that selects semi-orthogonal UEs. In [46], the authors use graph theory to propose a clustering and scheduling method. Their solution has polynomial computational complexity and deals with fairness among UEs. In [47], the authors propose a new hierarchical clustering method that builds the groups by merging clusters. In [48], the

authors propose a method to jointly optimize the number of clusters, the clustering procedure, and the beamforming strategy. Furthermore, the authors in [47] and [48] propose a scheduler that utilizes a metric based on signal to leakage plus noise ratio (SLNR) to suppress inter-cluster and intra-cluster interference. In [49], the authors propose a greedy UE scheduling aiming at mitigating the inter-cluster and intra-cluster interference. However, the digital precoders of this method are calculated for each UE until the number of UEs per cluster is reached. Therefore, computational complexity becomes prohibitive as the number of UEs and cluster size increase. In [50], a graph theory-based clustering and scheduling method is proposed to maximize the system throughput while guaranteeing fairness. This same objective of maximizing the system throughput while guaranteeing fairness has also been study in [51] and [52]. In [51] the authors propose an RL-based scheduling solution, where each UE is considered as an autonomous agent that makes its own RB allocation. In [52] the authors propose a greedy scheduling that selects the UEs based on their channel gains. Although the proposals in [29], [45]–[52] have their own merits, the assumption of fully-digital precoding is hard to hold in practice when massive MIMO is considered as previously explained.

In [32], [53]–[55], new scheduling schemes using hybrid precoding are proposed for massive MIMO. In [32], the authors propose a scheduler that uses only statistical CSI to select the UEs aiming at maximizing the system throughput. It schedules the UEs using a parameter that controls a trade-off between channel gain and spatial channel correlation. The authors in [53] propose a new scheduling method based on matrix vectorization. The scheduler vectorizes the channel matrix and creates groups of UEs based on Pearson's correlation coefficient. Afterwards, a set of UEs is selected from existing groups aiming at maximizing the throughput. In [54] the authors also propose a scheduler based only on statistical CSI, however, their objective was to maximize the throughput while guaranteeing the fairness among UEs. The problem is formulated based on Lyapunov-drift optimization, which models the UEs priority based on their transmission history creating virtual queues. Afterwards, a low-complexity greedy algorithm is proposed to obtain near-optimal performance. In [55], the authors analyze two scheduling strategies based on statistical CSI aiming at maximizing the throughput in a scenario where the UEs are moving at high speeds. The scheduling strategies are semi-orthogonal user selection and a greedy algorithm. Since the schedulers are based on statistical CSI, the same scheduled UEs are served in subsequent transmit time intervals (TTIs) without rescheduling while the UEs are moving. Simulation results showed that rescheduling is necessary, otherwise throughput drops over time. Despite

their contributions, the aforementioned works [32], [53]–[55] do not take into account the mandatory features of modern wireless networks, such as QoS provisioning and support of multiple services. These features impose additional constraints on the optimization problem as well as more challenges since the UEs have different QoS demands and channel quality states.

Since obtaining CSI is one of the principal issues of massive MIMO, the CSI usage by schedulers should be taken into account. It is important to notice that most of the presented works assume that instantaneous CSI is always available in the scheduler part, such as [41]–[43], [50], [51], [53]. Among the aforementioned works, the ones that use only the statistical information for scheduling are [32], [54] and [55]. The advantage of using statistical CSI is that it reduces the signaling overhead since the estimation can be done without dedicated pilots and the statistical CSI variation speed is much lower than that of the instantaneous CSI [54].

RL-based scheduling has gained popularity and has been applied in different contexts with different objectives [56]–[58]. In [56], the authors propose a combinatorial multi-armed bandits (MAB) based scheduler to solve the joint mode selection and resource allocation in a device-to-device system. They reduced the action space and improved the algorithm learning speed dividing the problem into two stages, which reduced the complexity of the problem. The first stage is responsible for scheduling only the cellular UEs and aims at maximizing the throughput. The second stage is responsible for scheduling the device-to-device pairs aiming at maximizing the system throughput. In [57], the authors propose an actor-critic RL-based scheduling aiming at maximizing the fairness among UEs maintaining QoS in long-term evolution (LTE) systems. In [58], the authors propose an RL and neural networks based framework aiming at guaranteeing the QoS requirements for different types of services in OFDMA ultra-reliable low-latency communications. They evaluate the framework performance over different RL algorithms. The aforementioned RL-based schedulers [56]–[58], as many other RL-based schedulers, model their problem, environment, action, state, and reward space, taking into account their predetermined scenario and assumptions. Thus, their modeling does not fit on our problem. Therefore, we consider that a novel RL-based scheduler is needed to address this complex scenario containing a massive number of antennas, hybrid beamforming, different objectives, and services.

1.4 Scientific Productions

During this Ph.D., the following papers have been published or submitted:

- **W. V. F. Mauricio**, T. F. Maciel, A. Klein, and F. R. M. Lima, "Scheduling for Massive MIMO with Hybrid Precoding using Contextual Multi-Armed Bandits", in *IEEE Transactions on Vehicular Technology (SUBMITTED)*, 2021
- **W. V. F. Mauricio**, D. C. Araujo, T. F. Maciel, and F. R. M. Lima, "A framework for radio resource allocation and SDMA grouping in massive MIMO systems", *IEEE Access*, vol. 9, pp. 61 680–61 696, 2021. DOI: 10.1109/ACCESS.2021.3074360
- **W. V. F. Mauricio**, T. F. Maciel, A. Klein, and F. R. M. Lima, "Learning-based scheduling: contextual bandits for massive MIMO systems", in *2020 IEEE International Conference on Communications Workshops (ICC Workshops)*, 2020, pp. 1–6. DOI: 10.1109/ICCWorkshops49005.2020.9145188
- **W. V. F. Mauricio**, F. R. M. Lima, A. Taufik, T. F. Maciel, and A. S. Diego, "Resource allocation for energy efficiency and QoS provisioning", *Journal of Communication and Information Systems*, vol. 34, no. 1, pp. 224–238, Oct. 2019. DOI: 10.14209/jcis.2019.24. [Online]. Available: https://jcis.sbrt.org.br/jcis/article/view/665
- A. S. Diego, **W. V. F. Mauricio**, R. Antonioli, F. R. M. Lima, and T. F. Maciel, "Improved joint resource and power allocation algorithm with QoS provisioning", in *XXXVI SIMPÓSIO BRASILEIRO DE TELECOMUNICAÇÕES E PROCESSAMENTO DE SINAIS*, Sep. 2018, pp. 1–5. DOI: 10.14209/sbrt.2018.345
- **W. V. F. Mauricio**, D. C. Araujo, F. H. C. Neto, F. R. M. Lima, and T. F. Maciel, "A low complexity solution for resource allocation and SDMA grouping in massive MIMO systems", in *Proceedings of the IEEE International Symposium on Wireless Communications Systems (ISWCS)*, Aug. 2018, pp. 1–6. DOI: 10.1109/ISWCS.2018.8491076
- **W. V. F. Mauricio**, F. R. M. Lima, T. F. Maciel, and F. R. P. Cavalcanti, "Proposta alternativa para obtenção da solução ótima do problema de maximização da eficiência energética com restrições de QoS", in *XXXVI SIMPÓSIO BRASILEIRO DE TELECOMUNICAÇÕES E PROCESSAMENTO DE SINAIS*, Sep. 2017, pp. 1–5. DOI: 10.14209/sbrt.2017.82

It is worth mentioning that this thesis was developed under the context of the following Ericsson/UFC technical cooperation project:

- Nov/2016-Oct/2018: *HYBEAM - Formatação Híbrida de Feixes em MIMO Massivo para Sistemas de Comunicação Móveis 5G*,

in which a number of four technical reports have been delivered. Furthermore, a sandwich Ph.D. internship took place during this period:

- Nov/2019-Oct/2020: sandwich Ph.D. at Technische Universität Darmstadt, Germany.

Chapter 2

System Model

We consider the downlink of a cellular multi-user MIMO system based on OFDMA composed of a BS serving a set $\mathcal{J}$ of UEs randomly distributed within linearly spaced hotspots with a determined radius, where $|\mathcal{J}| = J$ and $|\cdot|$ denotes the set cardinality. As we are dealing with a multiservice scenario, we assume that the number of services provided by the system operator is S and that $\mathcal{S}$ is the set of all services. We consider that the set of UEs from service $s \in \mathcal{S}$ is $\mathcal{J}_s$ and that $J_s = |\mathcal{J}_s|$. Note that $\bigcup_{s\in\mathcal{S}} \mathcal{J}_s = \mathcal{J}$ and $\sum_{s\in\mathcal{S}} J_s = J$. Moreover, we consider that the BS is equipped with a uniform planar array (UPA) composed of N_t antenna elements.

The UEs are equipped with a single omnidirectional antenna. We consider that the smallest allocable resource unit, termed RB, has N_symb consecutive orthogonal frequency division multiplexing (OFDM) symbols and N_sc adjacent OFDMA subcarriers. At each TTI, K out of the J UEs are selected to receive data at the same RB. We are going to use the eigenmode as the analog precoder and the technique that makes it possible requires the combination of two RF chains[59]. Therefore, we consider that the number of scheduled UEs K is equal to half the number of available RF chains at the BS. Moreover, $\mathcal{N}$ is the set of available RBs and $|\mathcal{N}| = N_\mathrm{RB}$. Before transmission, for a given RB and TTI, the symbol x_k to be sent to UE k is prefiltered at the BS by the precoding vector $\boldsymbol{f}_k \in \mathbb{C}^{N_\mathrm{t}\times 1}$. The filtered symbols are then transmitted through the channel associated with the RB. Figure 2.1 illustrates the considered system model.

In order to simplify our notation, we omit the index for the RB. Later, when referring to channel and precoding matrices, these will be indexed to a specific RB whenever necessary. The downlink channel vector between the BS and the UE k is denoted by $\boldsymbol{h}_k \in \mathbb{C}^{N_\mathrm{t}\times 1}$, where this UE k belongs to a given SDMA group. The coefficients in the channel vector of a given RB refer to the corresponding

Figure 2.1 – System model with massive MIMO system serving K UEs distributed in a set of linearly spaced hotspots. These UEs are using one of the different services provided by the system operator.

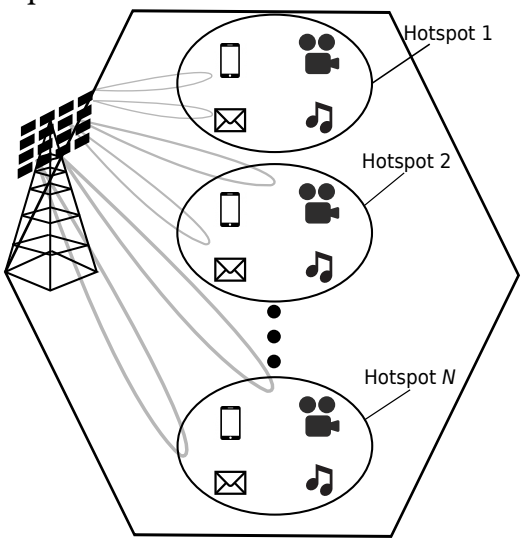

Source: Created by the author.

channel of the middle subcarrier of the RB and the first OFDM symbol in a TTI, and these channel coefficients are assumed to remain constant within a TTI. Thus, the prior-filtering receive symbol y_k at the k^{th} selected UE is

$$y_k = \boldsymbol{h}_k^{\mathrm{T}} \boldsymbol{f}_k \sqrt{p_k}\, x_k + \sum_{i \neq k\ ,\ i \in \mathcal{M}} \boldsymbol{h}_k^{\mathrm{T}} \boldsymbol{f}_i \sqrt{p_i}\, x_i + z_k, \tag{2.1}$$

where p_k is the power allocated to the UE k; where $\mathcal{M}$ is the set containing the UEs receiving information from BS; the second term on the right-hand side of (2.1) represents the multi-user interference, also known as intra-cell interference, generated by the other $K-1$ UEs sharing the same RB; and z_k is the additive Gaussian white noise, which is distributed as $\mathcal{CN}(0, \sigma^2)$, with standard deviation σ.

2.1 Clustering

As adopted in [29], [32], [47], we assume that UEs are split into clusters based on statistical CSI only. As we will show in Section 2.2, the clustering process greatly simplifies the analog precoder design. The use of statistical CSI is highly beneficial in FDD systems since this information changes at a slow pace and, therefore, reduces the frequency at which CSI estimation is required.

Herein, the covariance matrix is given as in [29], [32] by

$$\boldsymbol{\Omega}_j = \frac{1}{\tau} \sum_{t=1}^{\tau} \boldsymbol{h}_{t,j} \boldsymbol{h}_{t,j}^{\mathrm{H}}, \tag{2.2}$$

where $\boldsymbol{h}_{t,j} \in \mathbb{C}^{N_{\mathrm{t}} \times 1}$ is the channel vector between the BS and UE j at TTI t and τ indicates the number of channel samples considered to estimate the covariance

matrix. The eigendecomposition of the covariance matrix is expressed as

$$\boldsymbol{\Omega}_j = \boldsymbol{D}_j \boldsymbol{\Lambda}_j \boldsymbol{D}_j^{\mathrm{H}}, \tag{2.3}$$

where $\boldsymbol{D}_j \in \mathbb{C}^{N_{\mathrm{t}} \times N_{\mathrm{t}}}$ and $\boldsymbol{\Lambda}_j \in \mathbb{C}^{N_{\mathrm{t}} \times N_{\mathrm{t}}}$ contain the eigenvectors and the eigenvalues of $\boldsymbol{\Omega}_j$, respectively.

In the following, we describe the K-means clustering algorithm, which partitions the J UEs into N_{C} clusters [60], i.e., N_{C} is the number of clusters. Note that, although we use K-means, we are not limited to it; other clustering methods could be employed such as agglomerative clustering [47], fuzzy c-means [61] or K-medoids [62]. Herein, the K-means algorithm uses the dominant eigenvector of each UE j from the covariance matrix $\boldsymbol{\Omega}_j$ of (2.3) as input. Firstly, the algorithm randomly chooses N_{C} UEs and considers their dominant eigenvectors as the initial cluster's centroids. After that, the UEs are associated to the cluster that minimizes the Euclidean distance between their dominant eigenvectors, i.e., to the nearest cluster. Then, the mean of the dominant eigenvectors from the UEs belonging to each cluster determines the cluster's new (updated) centroid. The K-means algorithm repeats this process until there is no change in the UE-to-cluster association, or a maximum number of iterations is reached. For more details on K-means, please refer to [60]. A pseudo-code for K-means is presented in Algorithm 1.

Algorithm 1 K-means algorithm.

1: Randomly choose the dominant eigenvector of N_{C} UEs as the initial clusters' centroids;
2: **while** UEs-to-cluster assignments and clusters' centroids do not converge or the maximum number of iterations is not reached **do**
3: Assign UEs to the closest cluster;
4: Update clusters' centroids;
5: Increment the iteration counter;
6: **end while**

One specific drawback of K-means is the determination of the number of clusters, N_{C}. This is an important issue in clustering analysis since most of the clustering algorithms assume that they know a priori the number of clusters N_{C}. There is a variety of clustering validation measures and methods in the literature for evaluating clustering algorithms. These measures and methods are used to obtain the optimal number of clusters. In [63], the authors evaluate and compare 30 proposed methods to determine the optimal number of clusters. The silhouette index, proposed in [64], shows how good each item (UE, in our case) is classified. However, although there are some works in the literature that focus on the clustering algorithm design and, therefore, on the optimum number of clusters, our work uses clustering as part of a more complex framework. More specifically, our focus lies on the scheduling and

resource allocation, which is performed after the clustering stage. Therefore, for the sake of simplicity, we used the well-known K-means algorithm to solve the clustering problem, which needs, as many other clustering algorithms, the desired number of clusters as input. Also, other clustering algorithms could perform better depending of the considered scenario such as non line of sight scenario.

2.2 Analog and Digital Precoding Design

In general, in order to schedule UEs, the potential transmit data rate should be estimated. However, to calculate the data rate, we need to know a priori the hybrid beamforming filters so as to estimate SINR. Therefore, in this section, we present the hybrid precoding scheme and the data rate calculation. We assume that the BS already performed the clustering step and built the SDMA groups. Consider a given SDMA group g that is composed of G_g UEs and consider that $\bar{J}_c$ is the number of UEs from SDMA group g belonging to cluster c. We would like to highlight that g is the notation for the SDMA group that can be scheduled and c is the notation for a given cluster. Then, let us define the matrix $\boldsymbol{E}_c \in \mathbb{C}^{N_\mathrm{t} \times N_\mathrm{t}}$ as the average of the eigenvector matrices $\boldsymbol{D}_j$, defined in (2.3) belonging to the cluster c, i.e.

$$\boldsymbol{E}_c = \frac{1}{\mathrm{J_c}} \sum_{j \in \mathcal{J}_c} \boldsymbol{D}_j, \tag{2.4}$$

where $\mathcal{J}_c$ is the set of UEs belonging to cluster c and $|\mathcal{J}_c| = J_\mathrm{c}$. Thus, let us define $\boldsymbol{K}_c \in \mathbb{C}^{N_\mathrm{t} \times \bar{J}_c}$ as the matrix containing the $\bar{J}_c$ strongest eigenvectors of matrix $\boldsymbol{E}_c$ for each cluster c as

$$\boldsymbol{K}_c = \begin{bmatrix} \boldsymbol{e}_{c,1} & \boldsymbol{e}_{c,2} & \dots & \boldsymbol{e}_{c,\bar{J}_c} \end{bmatrix}, \tag{2.5}$$

where the vector $\boldsymbol{e}_{c,b}$ is the b^{th} strongest eigenvector from matrix $\boldsymbol{E}_c$ of cluster c. Therefore, $\boldsymbol{K}_c$ contains the $\bar{J}_c$ best beams of cluster c.

In the following, we present the computational complexity analysis to obtain the $\bar{J}_c$ strongest eigenvectors of the covariance matrix. We are using the singular value decomposition (SVD) to decompose (2.3) and, according to [65], the computational complexity to compute the SVD of an $m \times n$ matrix is $O(m^2 n + mn^2 + n^3)$. After that, we need to employ a sorting algorithm in the eigenvalue matrix. In general, according to [66], the worst-case computation complexity to sort a vector of size m is $O(m^2)$. Substituting m and n by N_t, the computational complexity to obtain the strongest eigenvectors of a UE is $O(N_\mathrm{t}^3)$. Therefore, we perform those operations $\bar{J}_c$ times to obtain the $\bar{J}_c$ strongest eigenvectors, which give us a worst case computational complexity of $O(\bar{J}_c N_\mathrm{t}^3)$.

Herein, the analog precoder $\boldsymbol{F}_g^{\mathrm{RF}} \in \mathbb{C}^{N_{\mathrm{t}} \times G_g}$ from SDMA group g is obtained using (2.5) for each cluster, and can be written as

$$\boldsymbol{F}_g^{\mathrm{RF}} = \begin{bmatrix} \boldsymbol{K}_1 & \boldsymbol{K}_2 & \dots & \boldsymbol{K}_{N_{\mathrm{C}}} \end{bmatrix}. \tag{2.6}$$

Since the UEs of different clusters are highly spatially uncorrelated, the analog precoder nearly eliminates the inter-cluster interference [29], [32]. Note that the elements of the precoder (2.6) do not fulfill the unity amplitude constraint of analog precoders. However, it is possible to implement such a precoder by combining two RF chains for each UE stream, as discussed in [59]. According to [59], this approach achieves the same performance of digital precoding with the requirement that the number of RF chains should be twice the number of spatial streams. There are other methods, such as those presented in [59] that enable the use of one RF chain per stream up to a negligible performance loss. We choose the simplest approach that consists in constructing the analog precoding using the phases of each entry in the matrix defined in (2.6), i.e., using twice the number of chains.

Let us define the group channel matrix $\boldsymbol{H}_g \in \mathbb{C}^{G_g \times N_{\mathrm{t}}}$ of the UEs belonging to the SDMA group g as

$$\boldsymbol{H}_g = \begin{bmatrix} \boldsymbol{h}_{\zeta_{1,g}} & \boldsymbol{h}_{\zeta_{2,g}} & \dots & \boldsymbol{h}_{\zeta_{G_g,g}} \end{bmatrix}^{\mathrm{T}}, \tag{2.7}$$

where $\zeta_{k,g}$ is the k^{th} UE of SDMA group g. The group channel matrix defined as $\boldsymbol{H}_g$ and the group analog precoder $\boldsymbol{F}_g^{\mathrm{RF}}$ form the equivalent channel matrix

$$\bar{\boldsymbol{H}}_g = \boldsymbol{H}_g \boldsymbol{F}_g^{\mathrm{RF}} \quad \in \mathbb{C}^{G_g \times G_g}. \tag{2.8}$$

To suppress the residual intra-cluster interference, we exploit the digital precoder, that is part of hybrid precoding by using the zero-forcing (ZF) digital filter defined as [67]

$$\boldsymbol{F}_g^{\mathrm{BB}} = \frac{(\bar{\boldsymbol{H}}_g^H)^{-1}}{\|(\bar{\boldsymbol{H}}_g^H)^{-1}\|_{\mathrm{F}}}, \tag{2.9}$$

where $\|\cdot\|_{\mathrm{F}}$ represents the Frobenius norm. However, the data throughpput is decreased if the scheduled UEs have highly correlated channels. Therefore, in Chapters 3 and 4 we are going to see different techniques to select the scheduled UEs in order to decrease the loss in throughput related to correlated channels.

The total power constraint is enforced by normalizing the digital and analog filters, such that $\|\boldsymbol{F}_g^{\mathrm{RF}} \boldsymbol{F}_g^{\mathrm{BB}} \sqrt{\boldsymbol{P}_g}\|_{\mathrm{F}}^2 = p_{\mathrm{RB}}$, where $\boldsymbol{P}_g \in \mathbb{R}_+^{G_g \times G_g}$ is a diagonal power matrix with the power allocated to each UE belonging to the SDMA group g and p_{RB} is the transmit power for a given RB. We consider that the number of

UEs in the SDMA group is equal to the number of streams N_{s}, i.e., there is one stream per UE in an SDMA group. Finally, $\boldsymbol{F}_g^{\mathrm{RF}}$ and $\boldsymbol{F}_g^{\mathrm{BB}}$ can be combined to compose the hybrid precoding matrix $\boldsymbol{F}_g = \boldsymbol{F}_g^{\mathrm{RF}} \boldsymbol{F}_g^{\mathrm{BB}} \in \mathbb{C}^{N_{\mathrm{t}} \times G_g}$.

Note that, one limitation of the scheme that we are proposing is that it is not designed to support pure non line-of-sight (NLOS) channels since the NLOS channel does not have one dominant path. The reason for that is due to usage of clustering and analog precoders based on the dominant eigenvectors of the UE statistical channels. To address the pure NLOS case, we should consider the following modifications: another clustering algorithm or a modification in the K-means algorithm should be considered, and a different analog precoder design that considers not only the dominant eigenvector but an average of the strongest ones.

The receive information vector $\hat{\boldsymbol{y}}_g \in \mathbb{C}^{G_g \times 1}$ of the SDMA group is given by

$$\hat{\boldsymbol{y}}_g = \boldsymbol{H}_g \boldsymbol{F}_g \sqrt{\boldsymbol{P}_g}\, \boldsymbol{x}_g + \boldsymbol{z}_g, \tag{2.10}$$

where $\boldsymbol{x}_g \in \mathbb{C}^{G_g \times 1}$ is the SDMA group symbol vector and $\boldsymbol{z}_g \in \mathbb{C}^{G_g \times 1}$ is the SDMA group noise vector. We are considering that the symbols have unitary variance, therefore, the average SINR perceived by a selected UE i from SDMA group g can be calculated as

$$\Gamma_i = \frac{|q_{i,i}|^2}{\sum\limits_{j \neq i} |q_{i,j}|^2 \, + \, \sigma_i^2}, \tag{2.11}$$

where $q_{i,j}$ is the element at the row i and column j of $\boldsymbol{Q}_g = \boldsymbol{H}_g \boldsymbol{F} \sqrt{\boldsymbol{P}_g} \in \mathbb{C}^{G_g \times G_g}$ and σ_i^2 is the noise power of UE i. The data rate of UE i is calculated according to Shannon capacity formula [68] and is given by

$$r_k = N_{\mathrm{sc}} N_{\mathrm{symb}} \min\left\{\log_2(1 + \Gamma_k), 8\right\} \text{ bits/TTI/RB}, \tag{2.12}$$

where $\min\{x, 8\}$ refers to our modulation order upper bound using 256-Quadrature Amplitude Modulation (QAM), which is the highest modulation order supported by 5G new radio (NR) systems [69].

Note that, when RRA is concerned, our presented scenario has similar challenges to the conventional MIMO scheduling, which is combinatorial. However, there are additional issues in our scenario, such as the higher number of antennas and, therefore, the number of multiplexed UEs, as well as the assumption of hybrid precoding. In this scenario, the data rate of each UE thus depends on the employed analog and digital precoders, which, in their turn, depend on the chosen SDMA group and clusterization. So, there is a hard inter-dependence of scheduling and hybrid precoding. Consequently, in order to find an optimal solution, it would be necessary to use brute force enumeration to estimate the

data rate of each UE at each possible SDMA group, which is impracticable for massive MIMO systems. Some challenges of precoding design will be discussed in Section 3.2.

Chapter 3

RRA in Massive MIMO Systems Using Optimization Tools

In the present chapter, we deal with RRA problems for massive MIMO networks proposing scheduling algorithms using optimization tools to optimize the system performance. More specifically, we propose a framework to solve RRA problems in massive MIMO composed of clustering, grouping and scheduling. In the first part of this chapter, we deal with the problem of maximizing the data rate considering only one RB. This problem is formulated as a binary quadratic problem which is solved using BB and a proposed low-complexity algorithm. In the second part of this chapter, we deal with the problem of maximizing the throughput and satisfying QoS constraints considering multiple RBs and services. This problem is divided into SDMA grouping and scheduling parts which are optimally solved by exhaustive search and BB algorithm, respectively. Due to the exponential complexity of exhaustive search and BB solutions, low-complexity solutions with polinomyal complexity are proposed.

3.1 Contributions and Chapter Organization

This chapter has the following main contributions:

- Proposal of a framework for RRA in massive MIMO systems that is divided into three parts: clustering, grouping and scheduling. The clustering and grouping steps aim at reducing the scheduling search space by creating low-correlated clusters of UEs and, afterwards, exploiting the channel hardening characteristic to generate a suitable set of SDMA groups that are going to be used in the scheduling step. The scheduling step assigns RBs to the SDMA groups generated in the previous step aiming at maximizing a given objective;

- Mathematical formulation of the grouping problem aiming at maximizing the throughput considering only one RB and reducing the intra-cluster interference. Also, it uses only statistical CSI;
- Mathematical formulation of the grouping problem aiming at maximizing the throughput and satisfying QoS constraints considering multiple RBs, services, and reducing the intra-cluster interference. Also, it uses only statistical CSI and exploits the channel hardening effect;
- Adaptation of the data rate maximization problem with QoS guarantees from [70] to a scenario with massive MIMO using hybrid beamforming;
- Proposal of efficient and low-complexity solutions for the considered problems;
- Calculation of the computational complexity of the involved algorithms and their performance evaluation by means of computational simulations.

This chapter is organized as follows. Section 3.2 defines the main problem. Afterwards, we propose a general framework to solve it. Section 3.3 describes the problem of maximizing the system data rate considering one RB. Next, we propose a low-complexity solution to this problem and evaluate it against the optimum and baseline solutions. Furthermore, Section 3.4 describes the problem of maximizing the system data rate considering multiple RBs, services and QoS requirements. Afterwards, we propose a low-complexity solution to this problem and evaluate it against the optimum solution and a solution adapted from the literature. Finally, Section 3.5 presents the main chapter conclusions.

3.2 Problem Definition

Note that a smart design of precoders needs to be considered to avoid the degradation of system SE caused by the intra-cell interference. The creation of SDMA groups containing spatially compatible UEs can avoid poor SE. In this sense, the total number of possible groups assuming J single-antenna UEs and the double of stream number is given by [70]

$$\sum_{l=1}^{\min(2\cdot streams, J)} \binom{J}{l}. \tag{3.1}$$

The exhaustive search can be used to evaluate the best SDMA group among all possibilities. However, this brute force method leads to high computational

costs. Therefore, low-complexity solutions to obtain the SDMA groups are required.

As previously mentioned in this thesis, we propose a general framework for RRA in massive MIMO systems. The proposed framework is divided into three parts and summarized in Figure 3.1.

Figure 3.1 – Proposed framework composed of three steps: clustering, grouping and scheduling.

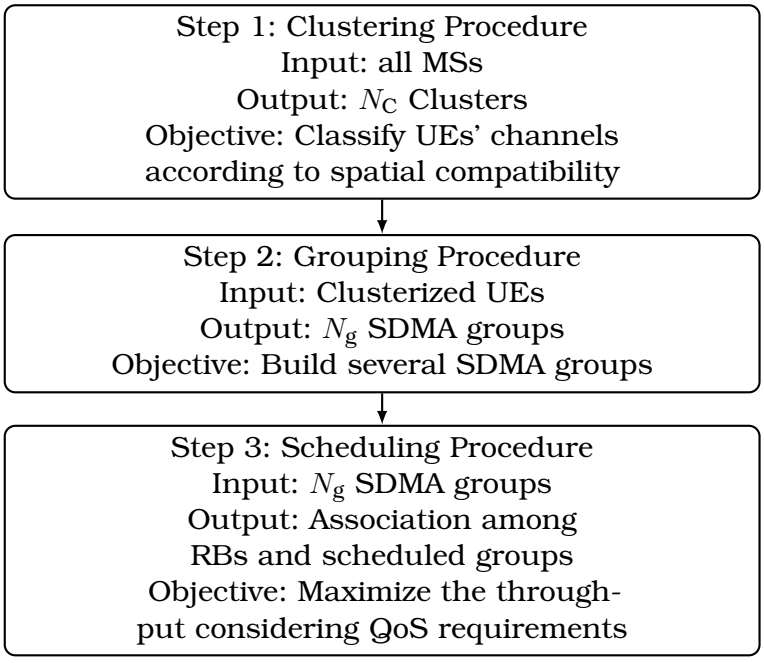

Source: Created by the author.

The first one, called *clustering procedure*, divides all UEs into N_C clusters, where each cluster contains UEs with compatible spatial channel characteristics (correlated channels), as explained in Section 2.1. This step can make the grouping process easier since, in general, UEs from different clusters will have spatially compatible (not similar) channels. In this way, a grouping procedure after clustering is able to reduce the search space of SDMA groups. However, the resulting number of SDMA groups might still remain impracticable. In the second part, called *grouping procedure*, we select UEs from each cluster to form several SDMA groups. Intelligent strategies to build efficient groups in terms of SE are employed here since the number of SDMA groups should be limited in order not to increase the complexity of the next step. Therefore, we build a total of N_g SDMA groups according to a metric that will be defined in details in Section 3.3, i.e., we drastically reduce the number of candidate SDMA groups through clusterization and grouping procedures. Finally, in the third part called *scheduling procedure*, we assign RBs to the SDMA groups selected in the second step aiming at optimizing a predefined objective. Thus,

we allocate RBs to those built SDMA groups aiming to satisfy QoS requirements and maximizing the total system data rate.

3.3 Maximization of System Data Rate Considering One RB

In this section we deal with the problem of maximizing the system data rate considering only one RB. Compared to the case with multiple RBs, this problem is less complex and can be used to gain insights about solutions to the more complex problem with multiple RBs studied in Section 3.4. Since this section only deals with one RB, the grouping and scheduling procedures of our proposed framework are done jointly.

The clustering procedure of Section 2.1 reduces the number of possible candidate SDMA groups since selecting too many UEs from the same cluster can lead to higher interference among UEs. However, the number of possible SDMA groups still remains unpractical. Therefore, a solution for further reducing the number of possible SDMA groups is necessary and we formulate a grouping problem that deals with such a challenge. This step is applied in each cluster separately to choose a set of UEs to compose an SDMA group assuming that the inter-cluster interference is negligible since UEs of different clusters are chosen to have low-correlated channels. Since more than one UE of the same cluster is part of an SDMA group, the scheduler needs to select less spatially correlated UEs (even knowing that these UEs already have high correlation) to deal with the intra-cluster interference. It is possible to make this assumption due to the massive MIMO technology and higher frequencies that allows the creation of narrow beams which reduces the interference of the scheduled UEs in the same cluster. Note that, the main objective is to have UEs with higher data rate when scheduling them together in an SDMA group. However, to estimate the data rate it is necessary to calculate the filters before calculating the SINR and then calculate the data rate. Therefore, these calculations are avoided by using the proposed SDMA grouping and metrics, i.e., this solution avoids computing digital precoders for every possible candidate group of UEs inside each cluster.

Next, we describe an assumption that is used to drastically reduce the number of possible compositions of scheduled UEs in a given TTI. For a group of UEs scheduled in the same resource, ZF precoding sends the signal of a served UE in the joint null space projection of the other scheduled UEs. Therefore, the channel correlation among UEs directly impacts on the channel gain of each UE after ZF precoding [67]. Figure 3.2 illustrates this behavior, where $\mathcal{S}_k = \text{Span}(\boldsymbol{h}_k)$, and $\theta_{\mathcal{S}_k,\boldsymbol{h}_k}$ is the angle between the channel vectors $\boldsymbol{h}_k$ and $\mathcal{S}_k$. Using $\theta_{\mathcal{S}_k,\boldsymbol{h}_k}$, the channel correlation coefficient between UE k and the subspace

$\mathcal{S}_k$ is given by $\cos(\theta_{\mathcal{S}_k,\boldsymbol{h}_k})$, with the channels becoming more uncorrelated as $\theta_{\mathcal{S}_k,\boldsymbol{h}_k}$ approaches $\frac{\pi}{2}$, which increases the effective channel gains after ZF precoding [67]. The channel $\boldsymbol{h}_k$ can be decomposed into two projections: projection into the null space projection and space projection. As previously mentioned, UEs belonging to different clusters are supposed to be low-correlated (i.e., $\cos(\theta_{\mathcal{S}_k,\boldsymbol{h}_k})$ tends to be close to zero for UEs of different clusters). Then, the interference from the signals transmitted from the BS serving UEs belonging to different clusters becomes negligible [32]. The channel correlation among UEs of different clusters will be briefly analyzed in Section 3.3.2. Note that, this assumption allows us to split the problem making it possible to schedule the UEs for each cluster separately reducing the search space. Moreover, one simple and possible solution that could be used as a baseline solution is to make several clusters and randomly schedule one UE of each cluster. However, this solution will lose in data rate since the UEs could have spatially correlated channels increasing the interference among them.

Figure 3.2 – Projection of channel $\boldsymbol{h}_i$ onto interference and null interference spaces [67].

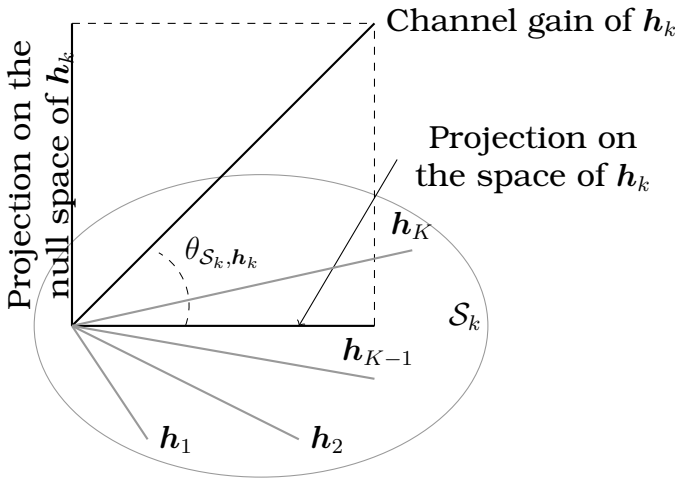

Source: Modified from [67].

In the sequel, we define the variables used to formulate the problem of maximizing the data rate. Let us define the matrix $\hat{\boldsymbol{D}} \in \mathbb{C}^{J_c \times N_\mathrm{t}}$ containing all UEs dominant eigenmodes of a given cluster:

$$\begin{aligned}\hat{\boldsymbol{D}} &= \begin{bmatrix}(\boldsymbol{d}_{1,1}\lambda_1) & (\boldsymbol{d}_{2,1}\lambda_2) & \dots & (\boldsymbol{d}_{J_c,1}\lambda_{J_c})\end{bmatrix}^{\mathrm{T}} \\ &= \begin{bmatrix}\hat{\boldsymbol{d}}_{1,1} & \hat{\boldsymbol{d}}_{2,1} & \dots & \hat{\boldsymbol{d}}_{J_c,1}\end{bmatrix},\end{aligned} \tag{3.2}$$

where $\boldsymbol{d}_{j,1}$ is the dominant eigenvector of UE j, λ_j is the highest eigenvalue obtained from $\boldsymbol{\Lambda}_j$, and $\hat{\boldsymbol{d}}_{j,1}$ is the dominant eigenmode of UE j.

Consider $\boldsymbol{a} \in \mathbb{R}^{J_c \times 1}$ as the attenuation vector containing the inverse of the dominant eigenvalue (channel gain) of all J_c UEs in a cluster. Then, we can

express $\boldsymbol{a}$ using $\hat{\boldsymbol{d}}$ as:

$$\boldsymbol{a} = \left[\|\hat{\boldsymbol{d}}_{1,1}\|_2^{-2} \quad \|\hat{\boldsymbol{d}}_{2,1}\|_2^{-2} \quad \dots \quad \|\hat{\boldsymbol{d}}_{J_c,1}\|_2^{-2}\right]^{\mathrm{T}}. \tag{3.3}$$

Then using (3.2) and (3.3), we can write the spatial correlation matrix $\boldsymbol{C} \in \mathbb{R}^{J_c \times J_c}$ as

$$\boldsymbol{C} = \left|\sqrt{\mathrm{diag}(\boldsymbol{a})}\hat{\boldsymbol{D}}\hat{\boldsymbol{D}}^{\mathrm{H}}\sqrt{\mathrm{diag}(\boldsymbol{a})}\right|. \tag{3.4}$$

Let the binary selection vector $\boldsymbol{u}$ be defined as

$$\boldsymbol{u} = \begin{bmatrix} u_1 & u_2 & \dots & u_{J_\mathrm{c}} \end{bmatrix}^{\mathrm{T}}, \tag{3.5}$$

where the element u_j assumes the value 1 if UE j is selected to compose an SDMA group and 0 otherwise. Then, combining (3.4) and (3.5), the convex combination $m(\hat{\Pi})$ of the total spatial correlation and channel gains is defined as

$$m_c(\hat{\Pi}_c) = (1-\beta)\frac{\boldsymbol{u}^{\mathrm{T}}\boldsymbol{C}\boldsymbol{u}}{\|\boldsymbol{C}\|_{\mathrm{F}}} + \beta\frac{\boldsymbol{a}^{\mathrm{T}}\boldsymbol{u}}{\|\boldsymbol{a}\|_{\mathrm{F}}}, \tag{3.6}$$

where $\hat{\Pi}_c$ is the set of UEs belonging to the SDMA group of cluster c, and $0 \leq \beta \leq 1$ is a control parameter establishing the trade-off between spatial correlation and channel gain. The terms $\frac{1}{\|\boldsymbol{C}\|_{\mathrm{F}}}$ and $\frac{1}{\|\boldsymbol{a}\|_{\mathrm{F}}}$ are normalization factors intended to balance $\boldsymbol{C}$ and $\boldsymbol{a}$, i.e., to try to compensate for their absolute difference and to have a likely unbiased β [24]. Therefore, β tries to establish a trade-off between spatial compatibility and channel gain.

Using the definitions above, the UE selection per cluster is made by solving the following optimization problem:

$$\boldsymbol{u}^{\star} = \arg\min_{\boldsymbol{u}} \left\{(1-\beta)\frac{\boldsymbol{u}^{\mathrm{T}}\boldsymbol{C}\boldsymbol{u}}{\|\boldsymbol{C}\|_{\mathrm{F}}} + \beta\frac{\boldsymbol{a}^{\mathrm{T}}\boldsymbol{u}}{\|\boldsymbol{a}\|_{\mathrm{F}}}\right\} \tag{3.7a}$$

subject to:

$$\mathbf{1}_{J_\mathrm{c}}^{\mathrm{T}}\boldsymbol{u} = \left\lfloor\frac{N_\mathrm{s}}{N_\mathrm{C}}\right\rfloor, \tag{3.7b}$$

$$\boldsymbol{u} \in \mathbb{B}^{J_\mathrm{c}}, \tag{3.7c}$$

where $\boldsymbol{u}^{\star}$ is the solution that can be directly mapped to the best cluster SDMA group $\hat{\Pi}_c$ containing $\left\lfloor\frac{N_s}{N_\mathrm{C}}\right\rfloor$ UEs that have low total spatial correlation and low total channel attenuation. Equation (3.7b) ensures that only $\left\lfloor\frac{N_\mathrm{s}}{N_\mathrm{C}}\right\rfloor$[1] UEs per cluster are selected, i.e., we ensure that the same number of UEs per clusters are scheduled. The last constraint assures that $\boldsymbol{u}$ is binary. This problem is

[1] Since we need to select at least one UE, this ratio should be equal or greater than 1.

solved by each cluster. After all clusters do it, the BS puts these SDMA groups in an unified SDMA group to transmit information to them.

The problem in (3.7) is a binary quadratic problem that can be optimally solved using the BB algorithm. However, the BB algorithm might be prohibitively complex, since it computes the grouping metric $m(\hat{\Pi}_c)$ for each cluster and according to (3.1), the number of SDMA groups increases combinatorially with the number of UEs J. Therefore, efficient suboptimal algorithms are required.

Figure 3.3 – Illustrative example of BF algorithm for SDMA grouping considering 6 UEs, 2 clusters and 4 streams. The gray and white boxes represent UEs that already belong to the group and candidate UEs, respectively. From the picture, after the clustering and grouping steps, the SDMA group is composed of UEs {1,3,4,5}.

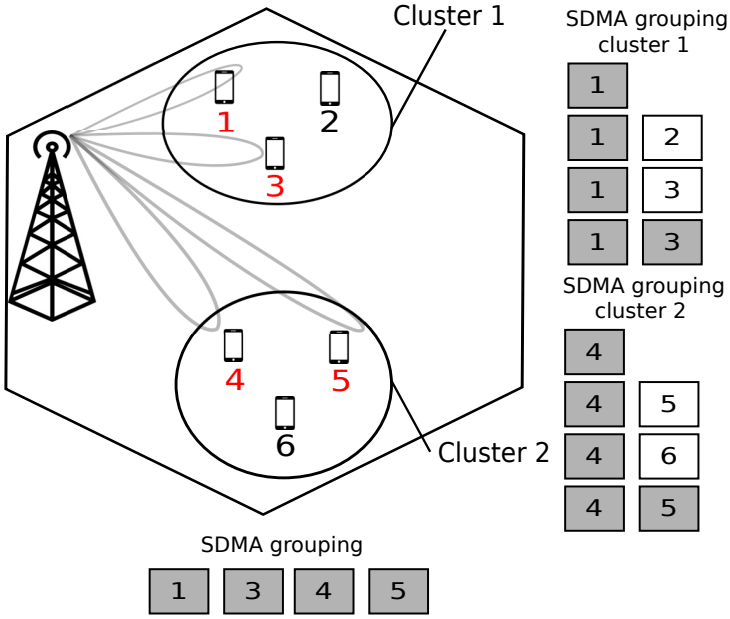

Source: Created by the author.

3.3.1 BF Algorithm

The best fit (BF) algorithm first selects an initial UE in order to calculate the correlation metric $m(\hat{\Pi}_c)$. The chosen UE is the one with strongest dominant eigenmode (highest channel gain). After that, the algorithm employs a greedy search to find the UE that minimizes the metric $m(\hat{\Pi}_c)$ when this UE is added to the group. Thus, the metric is calculated for each candidate UE of cluster c that does not belong to the SDMA group formed by the already selected UEs. Then, the same procedure is repeated until $\left\lfloor \frac{N_S}{N_C} \right\rfloor$ UEs associated with each cluster are selected, as to respect constraints (3.7b). The pseudo-code of the BF algorithm is presented in Algorithm 2.

At this point, it is also important to present a computational complexity analysis for the proposed algorithm. Therefore, as in [70], we consider summations, multiplications, and comparisons as the most relevant and time-consuming

Algorithm 2 BF Algorithm.

for $c = 1$ until $c = N_{\mathrm{C}}$ **do**
  $\boldsymbol{u} \leftarrow \mathbf{0}_{J_{\mathrm{C}}}$
  $\mathcal{J}_c$ is the set of UEs belonging to cluster c
  $\hat{\Pi}_c$ is the group of UEs that are in the SDMA group and belong to cluster c
  $j^{\star} \leftarrow \arg\max_{j} \left\{ \|\hat{\boldsymbol{d}}_j\| \right\}, \forall j \in \mathcal{J}_c$
  $u_{j^{\star}} \leftarrow 1$
  $\hat{\Pi}_c \leftarrow \{j^{\star}\}$ ▷ SDMA group updated
  $\mathcal{J}_c \leftarrow \mathcal{J}_c \setminus \{j^{\star}\}$ ▷ Set of UEs updated
  while $\mathbf{1}_{J_{\mathrm{C}}}^{\mathrm{T}} \boldsymbol{u} \neq \left\lfloor \frac{N_{\mathrm{s}}}{N_{\mathrm{C}}} \right\rfloor$ **do** ▷ Constraints (3.7b)
    $j^{\star} \leftarrow \arg\min_{j} \left\{ m(\hat{\Pi}_c) \right\}, \forall j \in \mathcal{J}_c$
    $u_{j^{\star}} \leftarrow 1$
    $\hat{\Pi}_c \leftarrow \hat{\Pi}_c \cup \{j^{\star}\}$
    $\mathcal{J}_c \leftarrow \mathcal{J}_c \setminus \{j^{\star}\}$
  end while
end for
$\hat{\Pi} = \left[\hat{\Pi}_1 \ \hat{\Pi}_2 \ \ldots \ \hat{\Pi}_{N_{\mathrm{C}}}\right]$

operations. We use the asymptotic notation $\mathcal{O}(\cdot)$ to represent the worst-case computational complexity. The algorithm searches within a cluster which UE has the strongest eigenmode. Note that, J_{C} comparisons per cluster are necessary. Then, the selected UE is excluded from the search for the next UE to compose the SDMA group. If the number of streams or required number of selected UEs per cluster $\left\lfloor \frac{N_s}{N_c} \right\rfloor \geq 2$, the algorithm chooses another user that minimizes the compatibility metric in (3.6). The process is repeated until number of users selected per cluster is equal to number of streams per cluster. Based on this, the total number of comparisons considering all the clusters is $N_{\mathrm{C}} \sum_{i=0}^{\lfloor N_{\mathrm{s}}/N_{\mathrm{C}} - 1 \rfloor} (J_{\mathrm{C}} - i)$. Note that this solution has a polynomial complexity while solvers based on the well-known BB method have exponential complexity [71]. Figure 3.3 shows a simple example of the BF algorithm applied to the problem (3.7) for a scenario with $J = 6$ UEs, $N_{\mathrm{C}} = 2$ clusters and $N_{\mathrm{s}} = 4$ streams.

3.3.2 Performance Evaluation

In this section, we compare the proposed solution with the only clustering (OC) algorithm, which applies the clustering procedure and after that randomly selects $\left\lfloor \frac{N_{\mathrm{S}}}{N_{\mathrm{C}}} \right\rfloor$ UEs to compose the SDMA group. Furthermore, we solve the problem defined in (3.7) using BF and BB methods. We utilized the IBM ILOG CPLEX Optimizer [40] to solve problem (3.7).

The scenario considered herein is shown in Figure 3.4, where a massive MIMO BS at coordinate $(0, 0)$ is equipped with an 8×8 UPA ($N_{\mathrm{t}} = 64$). It services

100 UEs which are randomly distributed inside two hotspots, each with a radius of 15 m, located inside a $60°$ cell sector with 200 m of radius. The centers of the hotspots are 100 m away from the BS and $30°$ apart. Also, we consider that the UEs are moving at a speed of $0.833m/s$, which is close to a typical walking pedestrian speed [72]. Moreover, as in [8], [32], [53], [73], [74], we consider at most 20% of the number of transmit antennas as the quantity of available RF chains. Furthermore, the number of simulated UEs is limited by the complexity to obtain the optimal solution, which is exponential.

Figure 3.4 – Scenario considering 2 hotspots with a determined angle θ between their centers.

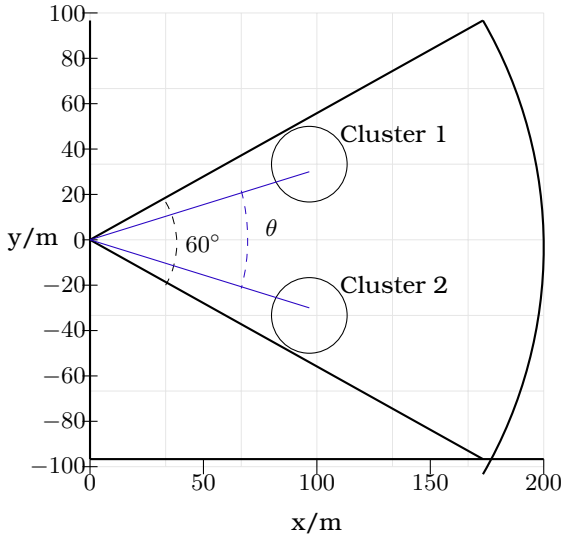

Source: Created by the author.

We adopt the quasi deterministic radio channel generator (QuaDRiGa) urban micro (UMi) line-of-sight (LOS) channel model [75] and assume the BS power to be evenly divided among 125 RBs. However, in this section, we are assuming only one RB available for transmission. Also, we are considering a simulation time of 25 ms and 100 simulations rounds, the reason for considering only 25 ms is to analyze the performance of the algorithms at the end of this time in a given TTI. The most relevant parameters used in our simulations are shown in Table 4.1.

In order to support the considered assumption of low interference among UEs of different clusters, in Figure 3.5 we applied the K-means clustering algorithm to observe the behavior of the channel correlation among the UEs' channels belonging to different clusters varying the angle θ where the center of the clusters are disposed.

Therefore, applying K-means for varying angle θ (see Figure 3.5), one can see that it clusters UEs with low correlated channels even for very close hotspots, with correlation being inversely proportional to the angular distance between

Table 3.1 – Simulation Parameters for Section 3.3

Parameter	**Value**	**Unit**
Simulation time	25	ms
Number of simulation rounds	100	–
Cell radius	200	m
Total transmit power	35	dBm
Noise figure	9	dB
Noise spectral density	-174	dBm/Hz
Shadowing standard deviation	3.1	dB
Number of UEs	100	-
Number of clusters	2	-
UEs speed	0.833	m/s

Source: Created by the author.

hotspots. Thus, as mentioned before, our assumption that the interference among clusters is negligible becomes increasingly true as the distance angle θ between clusters increases.

Figure 3.5 – Average channel correlation for UEs from two distinct clusters for different values of θ.

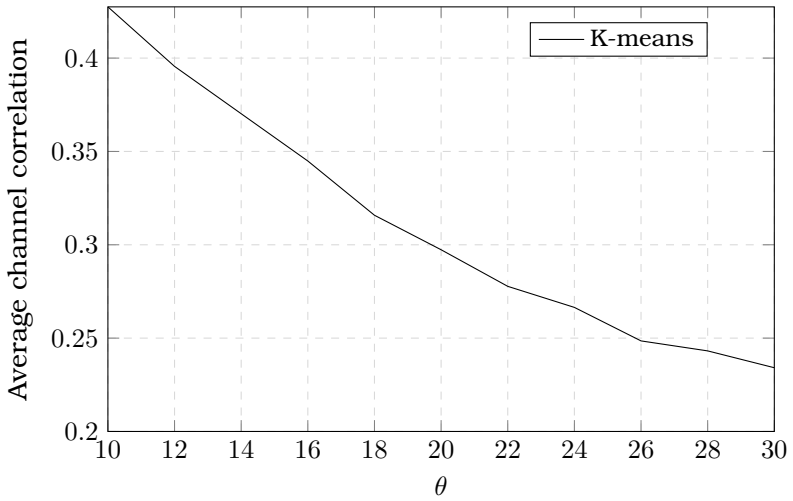

Source: Created by the author.

In Figure 3.6 we evaluate the system data rate at the 50^{th} percentile of the cumulative distribution function (CDF) of system data rate, which is the sum of the data rate in (2.12) of all selected UEs, for BB, BF and OC solutions when the β parameter in (3.6) varies from 0 to 1. We also vary the number of streams from 2 to 3 per cluster.

As we can see, the selection of β impacts the system performance and different system data rate values are achieved as β is varied. For example, we can see that a better system performance can be achieved with $\beta = 0$ (selection of UEs with low channel correlation within a cluster) than $\beta = 1$ (selection of UEs with high channel gains). According to this, the spatial correlation cannot

Figure 3.6 – System data rate at 50th percentile of BB, BF, and OC solutions.

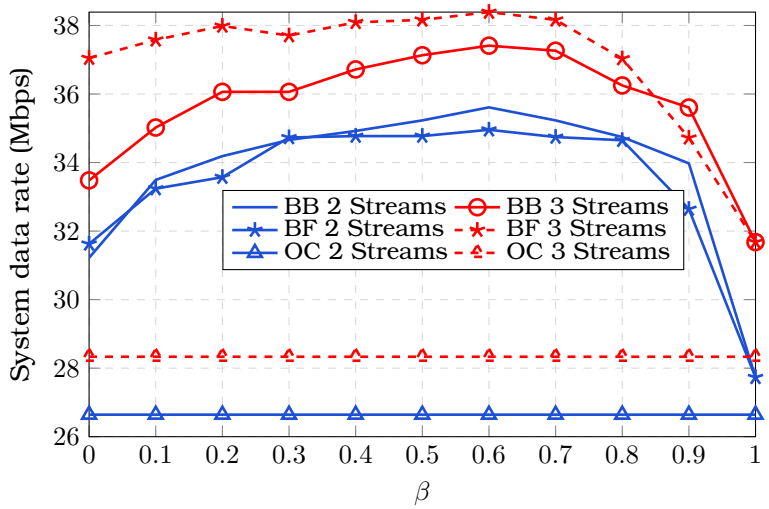

Source: Created by the author.

be completely neglected as with $\beta = 1$ since this increases the intra-cluster interference. However, this figure also shows that the optimal performance is achieved for an intermediate value of β (β = 0.6), showing that both channel correlation and channel gain should be carefully taken into account to improve the system performance. Note that we can serve more UEs by increasing the number of streams from 2 to 3. However, the UE data rate decreases because the intercluster interference increases. Finally, the transmission of multiple streams per cluster using BB and BF can lead to a performance gain of 32% and 35.5% over OC, respectively.

Figure 3.7 evaluates the average grouping metric defined in (3.6) using BB and BF solutions versus the β parameter varying from 0 to 1. We also vary the number of streams from 2 to 3 per cluster.

Figure 3.7 – Metric average of our proposed solutions.

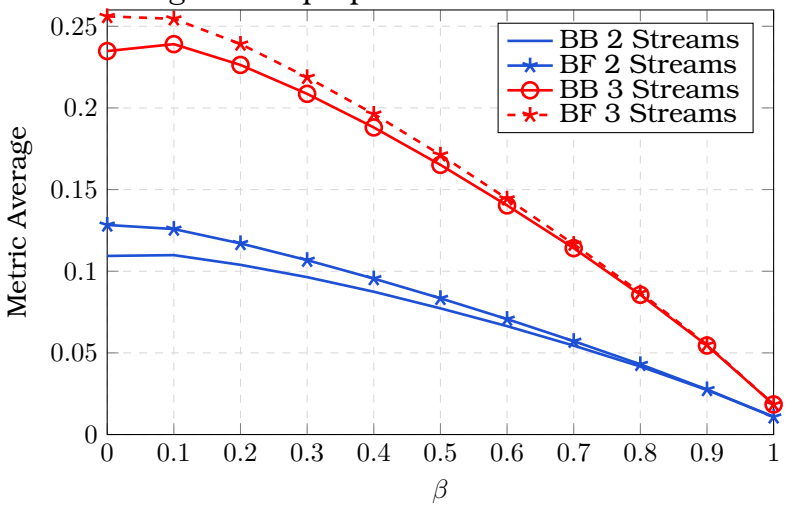

Source: Created by the author.

In the whole beta range, the BF algorithm presents a close-to-optimal

performance, especially when $\beta = 1$. Basically, the problem (3.7) becomes linear and, therefore, easier to solve when β approaches the value 1. Also, a smaller value for the metric means higher optimality. Another important aspect to mention is that the optimization of the grouping metric presented in (3.6) does not necessarily lead to capacity maximization. However, despite its suboptimality, the employed grouping metric was shown to be well correlated to the system capacity according to the presented simulation results.

3.4 Maximization of System Data Rate Considering Multiple RBs, Services, and QoS Requirements

In this section we deal with the problem of maximizing the system data rate considering multiple RBs, services, and QoS requirements. Motivated by the higher problem complexity when compared to the one studied in Section 3.3, the grouping and scheduling procedures of our proposed framework Figure 3.1 are done separately in this section.

3.4.1 Grouping Procedure

We start by explaining the step 2 (grouping procedure) of our proposed framework in Figure 3.1 since the step 1 (clustering procedure) was explained in Section 2.1. As in Section 3.3, we are going to deal with the challenge of having an unpractical number of possible SDMA groupings. However, differently from Section 3.3, in this section the goal consists in generating N_g spatially compatible groups to maximize the sum-rate and meet QoS constraints since the RBs are allocated later to these SDMA groups. Therefore, instead of having the scheduling step scan the whole search space to find the best SDMA group per RB, the grouping step will reduce the number of possible SDMA groups (N_g) that are pre-selected with the objective of maximizing the sum rate.

Assuming that the inter-cluster interference is negligible thanks to clustering and precoding, a grouping problem is applied to each cluster separately where a set of UEs is selected to form SDMA groups. In this selection process, we choose spatially compatible UEs to keep the intra-cluster interference at acceptable levels, if possible. One of the advantages of the grouping step is to evaluate spatial compatibility, without computing the precoding vectors, as described in Section 2.1, for all possible UEs groups. Moreover, our grouping method exploits the channel hardening characteristic, which avoids the computation of SDMA groups for each RB. Therefore, by exploiting channel hardening in the massive MIMO system, where the instantaneous channel gain of each UE can be approximated by its mean in the frequency domain, we can reduce

the complexity of this task [76].

Let us define the matrix $\tilde{\boldsymbol{D}} \in \mathbb{C}^{J_c \times N_\mathrm{t}}$ containing all UEs' dominant eigenmodes of a given cluster measured for the RB in the center of the bandwidth (middle RB):

$$\tilde{\boldsymbol{D}} = \begin{bmatrix} \tilde{\boldsymbol{d}}_1 & \tilde{\boldsymbol{d}}_2 & \dots & \tilde{\boldsymbol{d}}_{J_c} \end{bmatrix}. \tag{3.8}$$

where $\tilde{\boldsymbol{d}}_j$ is the dominant eigenmode for the middle RB of the j^{th} UE from cluster c, which index was dropped out for simplicity sake.

Consider $\tilde{\boldsymbol{a}} \in \mathbb{R}^{J_c \times 1}$ as the attenuation vector containing the inverse of the dominant eigenvalue (channel gain) for the middle RB of all J_c UEs from cluster c. Then, we can express $\tilde{\boldsymbol{a}}$ using $\tilde{\boldsymbol{d}}$ as:

$$\tilde{\boldsymbol{a}} = \begin{bmatrix} \|\tilde{\boldsymbol{d}}_1\|_2^{-2} & \|\tilde{\boldsymbol{d}}_2\|_2^{-2} & \dots & \|\tilde{\boldsymbol{d}}_{J_c}\|_2^{-2} \end{bmatrix}^{\mathrm{T}}. \tag{3.9}$$

Due to the channel hardening effect that allows massive MIMO to use average channel gains and using (3.8) and (3.9), we can write the spatial correlation matrix $\boldsymbol{C} \in \mathbb{R}^{J_c \times J_c}$ for the middle RB as [77]

$$\boldsymbol{C} = \left| \sqrt{\mathrm{diag}(\tilde{\boldsymbol{a}})} \tilde{\boldsymbol{D}} \tilde{\boldsymbol{D}}^{\mathrm{H}} \sqrt{\mathrm{diag}(\tilde{\boldsymbol{a}})} \right|. \tag{3.10}$$

Therefore, using (3.10) and considering N_g as the number of groups to be generated as output of the grouping step, we can define the following block diagonal spatial correlation matrix $\hat{\boldsymbol{C}} \in \mathbb{R}^{J_c N_\mathrm{g} \times J_c N_\mathrm{g}}$ as

$$\hat{\boldsymbol{C}} = \boldsymbol{I}_{N_\mathrm{g}} \otimes \boldsymbol{C}, \tag{3.11}$$

where $\boldsymbol{I}_{N_g}$ is the $N_g \times N_g$ identity matrix and $\otimes$ is the kronecker product.

Analogously, let us define the following attenuation vector $\hat{\boldsymbol{a}} \in \mathbb{R}^{J_c N_\mathrm{g} \times 1}$ as

$$\hat{\boldsymbol{a}} = \mathbf{1}_{N_\mathrm{g}} \otimes \tilde{\boldsymbol{a}}, \tag{3.12}$$

where $\mathbf{1}_{N_\mathrm{g}}$ is the $N_\mathrm{g} \times 1$ vector composed of 1's and $\hat{\boldsymbol{a}}$ is a concatenation of attenuation vectors from all UEs of each SDMA group. Therefore, the block diagonal spatial correlation matrix $\hat{\boldsymbol{C}}$ and the stacked vector of channel gains $\hat{\boldsymbol{a}}$ refers to N_g independent SDMA groups.

Consider the binary selection vector

$$\boldsymbol{u} = \begin{bmatrix} u_1 & u_2 & \dots & u_{J_c \cdot N_\mathrm{g}} \end{bmatrix}^{\mathrm{T}}, \tag{3.13}$$

which selects UEs for each SDMA group, where u_i is equal to 1 when the k^{th} UE of a given cluster is chosen to compose SDMA group g with $i = g \cdot N_\mathrm{g} + k$.

We can formulate a convex combination that takes into account both the total spatial correlation and channel gains of all SDMA groups. Such a combination is defined as

$$m(\hat{\Pi}) = (1-\beta)\frac{\boldsymbol{u}^{\mathrm{T}}\hat{\boldsymbol{C}}\boldsymbol{u}}{\|\hat{\boldsymbol{C}}\|_{\mathrm{F}}} + \beta\frac{\hat{\boldsymbol{a}}^{\mathrm{T}}\boldsymbol{u}}{\|\hat{\boldsymbol{a}}\|_{\mathrm{F}}}, \tag{3.14}$$

where the normalization factors $\frac{1}{\|\hat{\boldsymbol{C}}\|_{\mathrm{F}}}$ and $\frac{1}{\|\hat{\boldsymbol{a}}\|_{\mathrm{F}}}$ are responsible to balance $\hat{\boldsymbol{C}}$ and $\hat{\boldsymbol{a}}$, i.e., to make the β parameter unbiased [24].

Let us define the matrix $\boldsymbol{T} \in \{0,1\}^{J_c \times J_c N_{\mathrm{g}}}$ as

$$\boldsymbol{T} = \mathbf{1}_{N_{\mathrm{g}}}^{\mathrm{T}} \otimes \boldsymbol{I}_{J_c}, \tag{3.15}$$

where $\boldsymbol{T}$ is a matrix that we introduce to cope with fairness constraints of the SDMA groups. Indeed each row of the matrix $\boldsymbol{T}$ is associated to UE j and all SDMA groups, and it will be used to guarantee that each UE will be present in at least one of the N_{g} generated SDMA groups.

Let us define the following matrix $\boldsymbol{V}_i \in \{0,1\}^{J_c N_{\mathrm{g}} \times J_c N_{\mathrm{g}}}$

$$\boldsymbol{V}_i = \boldsymbol{G}_i \otimes \boldsymbol{I}_{J_c}, \forall i \in \{1, N_{\mathrm{g}}\}, \tag{3.16}$$

where $\boldsymbol{G}_i \in \{0,1\}^{N_{\mathrm{g}} \times N_{\mathrm{g}}}$ is a diagonal matrix whose unique non-zero element corresponds to the i^{th} element in the main diagonal and its value is 1; and $\boldsymbol{V}_i$ is a matrix introduced to guarantee the UE diversity in the SDMA groups as it will be explained later, which helps to satisfy the QoS requirements.

Using the definitions above, the multiple groups and fairness optimization problem, which should be solved separately for each cluster, can be formulated as

$$\boldsymbol{u}^{\star} = \arg\min_{\boldsymbol{u}} \left\{ (1-\beta)\frac{\boldsymbol{u}^{\mathrm{T}}\hat{\boldsymbol{C}}\boldsymbol{u}}{\|\hat{\boldsymbol{C}}\|_{\mathrm{F}}} + \beta\frac{\hat{\boldsymbol{a}}^{\mathrm{T}}\boldsymbol{u}}{\|\hat{\boldsymbol{a}}\|_{\mathrm{F}}} \right\} \tag{3.17a}$$

subject to:

$$(\boldsymbol{I}_{N_{\mathrm{g}}} \otimes \mathbf{1}_{J_c}^{\mathrm{T}})\boldsymbol{u} = \mathbf{1}_{N_{\mathrm{g}}}\bar{J}_c, \tag{3.17b}$$

$$\boldsymbol{T}\ \boldsymbol{u} \geq \mathbf{1}_{N_{\mathrm{g}}}\left\lfloor \frac{N_{\mathrm{g}}}{J_c} \right\rfloor, \tag{3.17c}$$

$$\mathbf{1}_{N_{\mathrm{g}}J_c}(\boldsymbol{V}_i - \boldsymbol{V}_g)\boldsymbol{u} \neq 0, \quad \forall i, g \in \{1, N_{\mathrm{g}}\}, \text{ and } i \neq g, \tag{3.17d}$$

$$\boldsymbol{u} \in \{0,1\}^{J_c N_{\mathrm{g}}}, \tag{3.17e}$$

where $\boldsymbol{u}^{\star}$ is the solution containing the best N_{g} SDMA groups containing $\bar{J}_c$ UEs of a given cluster that have low total spatial correlation and low total channel attenuation, depending on the chosen β. Constraint (3.17b) ensures

that only $\bar{J}_c$ UEs per group are selected, totalizing a number of $N_{\mathrm{g}}\bar{J}_c$ UEs selected per cluster assuming all SDMA groups. Constraint (3.17c) ensures that every UE is present in at least $\left\lfloor \frac{N_{\mathrm{g}}}{J_c} \right\rfloor$ SDMA groups, i.e., we impose a fairness constraint among UEs. Constraint (3.17d) ensures that we do not form groups containing the same UEs, i.e., we impose a variability constraint among SDMA groups. The last constraint assures that $\boldsymbol{u}$ is binary. Problem (3.17) can be solved by exhaustive search, which consists in enumerating all the possible SDMA group compositions and choosing the best one. However, this method has impractical computational complexity. Therefore, efficient suboptimal algorithms are required, as presented in the following.

3.4.2 Grouping Procedure Proposed Algorithm

The proposed low-complexity solution for the grouping part is presented in Algorithm 3. The main idea here is to select UEs from each cluster to compose all N_{g} SDMA groups that will be used in the scheduling part. In lines 7 to 13, the proposed algorithm firstly selects an initial UE in order to calculate the correlation metric $m(\hat{\Pi})$. The chosen UE is the one with highest eigenmode gain. This selected UE will have a low priority to be chosen as the initial UE of other SDMA groups to fulfill constraint (3.17c). After that, in lines 14 to 18, the algorithm employs a greedy search to find the UE which can form a possible and different combination (constraint (3.17d)) that minimizes the metric $m(\hat{\Pi})$ when the UE is added to the group. Thus, the metric is calculated for each UE that does not belong to the SDMA group formed by the already selected UEs of the cluster. Then, the same procedure is repeated until $\bar{J}_c$ UEs associated with each cluster are selected, as to respect constraint (3.17b). In line 19, we remove the selected combination from the set of all possible combinations. In lines 20 to 24, if a given UE is already part of all of its possible SDMA groups, then this UE cannot be chosen to compose another SDMA group. These steps are repeated until N_{g} groups are formed for each cluster. The pseudo-code of the proposed algorithm is presented in Algorithm 3.

In the following we calculate the worst-case computational complexity of Algorithm 3. It sorts the UEs within a cluster based on the dominant eigenmode. Note that, in the worst-case a simple sorting of the J_c UEs can have a complexity of $\mathcal{O}(J_c \log(J_c))$ per cluster. Then, Algorithm 3 selects the first UE, i.e., the UE with highest dominant eigenmode. Note that, $N_{\mathrm{C}}N_{\mathrm{g}}$ selections are done. Then, the selected UE is excluded from the search for the next UE to compose the SDMA group. If we need to select more than one UE per cluster, i.e., if the number of streams per cluster is greater than one, the algorithm chooses another UE that minimizes the compatibility metric in (3.14). The

Algorithm 3 Proposed algorithm for grouping

Define $\hat{\Pi}_{c,g}$ as the set of UEs from cluster c that belongs to SDMA group g
for $c = 1$ to $c = N_{\mathrm{C}}$ **do**
  Define $\mathcal{J}_c$ as the set of UEs belonging to cluster c
  Sort $\mathcal{J}_c$ in descending order of dominant eigenmode
  Define $\mathcal{A}$ as the set with all possible combinations of $\bar{J}_c$ UEs taken from $\mathcal{J}_c$ ▷ Constraint (3.17d)
  for $g = 1$ until $g = N_{\mathrm{g}}$ **do**
    $\hat{\Pi} = \emptyset$
    Define $\boldsymbol{u}$ as the binary selection vector for group g
    $\boldsymbol{u} \leftarrow \mathbf{0}_{J_c}$
    $j^\star \leftarrow$ first element of $\mathcal{J}_c$ ▷ Constraint (3.17c)
    Put $j^\star$ in the last position in the set $\mathcal{J}_c$ ▷ Constraint (3.17c)
    $u_{j^\star} \leftarrow 1$
    $\hat{\Pi} \leftarrow \{j^\star\}$
    while $\mathbf{1}_{J_c}^{\mathrm{T}} \boldsymbol{u} \neq \bar{J}_c$ **do** ▷ Constraints (3.17b)
      $j^\star \leftarrow \arg\min_{j} \left\{ m(\hat{\Pi}) \right\}, \forall \hat{\Pi} \subseteq \mathcal{A}$
      $u_{j^\star} \leftarrow 1$
      $\hat{\Pi} \leftarrow \hat{\Pi} \cup \{j^\star\}$
    end while
    $\mathcal{A} \leftarrow \mathcal{A} \setminus \{\hat{\Pi}\}$
    for each UE j in $\hat{\Pi}$ **do**
      if $j \notin \mathcal{A}$ **then**
        $\mathcal{J}_c \leftarrow \mathcal{J}_c \setminus \{j\}$
      end if
    end for
    $\hat{\Pi}_{c,g} \leftarrow \hat{\Pi}_{c,g} \cup \hat{\Pi}$
  end for
end for
return $\hat{\Pi}$

process is repeated until the number of UEs selected per cluster is equal to the number of streams per cluster. Based on this, the total number of comparisons considering all the clusters and SDMA groups are $N_{\mathrm{C}} N_{\mathrm{g}} \sum_{i=0}^{\bar{J}_c - 1} (J_c - i)$. Therefore, the algorithm worst-case complexity is $\mathcal{O}(N_{\mathrm{C}} N_{\mathrm{g}} (1 + \sum_{i=0}^{\bar{J}_c - 1} (J_c - i)))$, which is polynomial. Note that this solution has a very low complexity compared to solvers based on the well-known BB methods that have exponential complexity [71].

3.4.3 Scheduling Procedure Optimal Solution

This section presents the maximization of total data rate considering QoS and a multiservice scenario. This problem has been already studied in [70] for a conventional MIMO system. However, in [70], the authors optimize the system performance by evaluating the possible transmit data rates considering all possible combinations of SDMA groups, as shown in (3.1), which is impracticable in real systems, especially with massive MIMO.

Let us define some relevant variables. Assume that $\boldsymbol{O} \in \{0,1\}^{N_{\mathrm{g}} \times N_{\mathrm{RB}}}$ is an

assignment matrix whose element $o_{g,n}$ assumes the value 1 if the RB n is assigned to the SDMA group g and 0 otherwise. Let $\boldsymbol{R} \in \mathbb{R}^{N_{\mathrm{g}} \times J \times N_{\mathrm{RB}}}$ be a tensor whose element $r_{g,j,n}$ is the Shannon capacity of the UE j in RB n if UE j belongs to SDMA group g and 0 otherwise. Let us define the vector $\boldsymbol{\rho} \in \{0,1\}^{J \times 1}$ as a binary selection vector whose element ρ_j assumes the value 1 if UE j is selected to be satisfied and 0 otherwise. The vector $\boldsymbol{l} \in \mathbb{R}^{J \times 1}$ is defined as a vector whose element l_j is the required data rate necessary to satisfy UE j. Note that, as in [70], we map the long-term data rate requirements as instantaneous data rate requirements. The minimum satisfaction constraint for each service is defined as a vector $\boldsymbol{w} \in \mathbb{Z}^{S \times 1}$, whose element w_s is the minimum number of UEs from service s that should be satisfied. Note that, we sequentially dispose the index of UEs in $r_{g,j,n}$ and in l_j according to the service, i.e, the UEs $j = J_{s-1} + 1$ to $j = J_s$ are from service s, where J_s is the number of UEs from service s.

According to the previous considerations, the resource assignment problem can be formulated as the following optimization problem:

$$\arg\max \{\boldsymbol{o}, \boldsymbol{\rho}\} \left(\sum_{g \in \mathcal{G}} \sum_{n \in \mathcal{N}} \sum_{j \in \mathcal{J}} o_{g,n} r_{g,j,n} \right), \tag{3.18a}$$

subject to:

$$\sum_{g \in \mathcal{G}} o_{g,n} = 1, \forall n \in \mathcal{N}, \tag{3.18b}$$

$$\sum_{g \in \mathcal{G}} \sum_{n \in \mathcal{N}} o_{g,n}\, r_{g,j,n} \geq \rho_j\, l_j, \forall j \in \mathcal{J}, \tag{3.18c}$$

$$\sum_{j \in \mathcal{J}_s} \rho_j \geq w_s, \forall s \in \mathcal{S}, \tag{3.18d}$$

$$o_{g,n} \in \{0,1\}, \forall g \in \mathcal{G} \text{ and } \forall n \in \mathcal{N}, \tag{3.18e}$$

$$\rho_j \in \{0,1\}, \forall j \in \mathcal{J}. \tag{3.18f}$$

The objective function shown in (3.18a) is the maximization of the total downlink data rate transmitted by the BS. The first constraint (3.18b) assures that an RB will not be shared by different SDMA groups. Constraints (3.18c) and (3.18d) state that a minimum number of UEs should be satisfied for each service.

Problem (3.18) is a combinatorial optimization problem with linear constraints. Hence, depending on the problem dimension, its optimal solution has prohibitive computational complexity [70]. In order to write this problem in a compact form we will represent the problem variables and inputs in vector and

matrix forms. Thus, let us define the matrix $\tilde{\boldsymbol{R}} \in \mathbb{Z}^{J \times N_{\mathrm{g}} N_{\mathrm{RB}}}$ as follows

$$\tilde{\boldsymbol{R}} = \begin{bmatrix} r_{1,1,1} & r_{2,1,1} & \cdots & r_{N_{\mathrm{g}},1,1} & r_{1,1,2} & \cdots & r_{N_{\mathrm{g}},1,N_{\mathrm{RB}}} \\ r_{1,2,1} & r_{2,2,1} & \cdots & r_{N_{\mathrm{g}},2,1} & r_{1,2,2} & \cdots & r_{N_{\mathrm{g}},2,N_{\mathrm{RB}}} \\ \vdots & \vdots & \ddots & \vdots & \vdots & \ddots & \vdots \\ r_{1,J,1} & r_{2,J,1} & \cdots & r_{N_{\mathrm{g}},J,1} & r_{1,J,2} & \cdots & r_{N_{\mathrm{g}},J,N_{\mathrm{RB}}} \end{bmatrix}.$$

Therefore, we can rewrite problem (3.18) as

$$\arg\max \{\boldsymbol{O}, \boldsymbol{\rho}\} \left(\mathbf{1}_J^{\mathrm{T}} \tilde{\boldsymbol{R}} \operatorname{vec}(\boldsymbol{O}) \right), \tag{3.19a}$$

subject to:

$$(\mathbf{1}_{N_{\mathrm{g}}}^{\mathrm{T}} \otimes \boldsymbol{I}_{N_{\mathrm{RB}}}) \operatorname{vec}(\boldsymbol{O}) = \mathbf{1}_{N_{\mathrm{RB}}}, \tag{3.19b}$$

$$\tilde{\boldsymbol{R}} \operatorname{vec}(\boldsymbol{O}) \geq \operatorname{diag}(\boldsymbol{l})\, \boldsymbol{\rho}, \tag{3.19c}$$

$$(\mathbf{1}_{J_s} \otimes \boldsymbol{I}_S)^{\mathrm{T}} \boldsymbol{\rho} \geq \boldsymbol{w}, \tag{3.19d}$$

$$\boldsymbol{O} \in \{0,1\}^{N_{\mathrm{g}} \times N_{\mathrm{RB}}}, \tag{3.19e}$$

$$\boldsymbol{\rho} \in \{0,1\}^{J}, \tag{3.19f}$$

where the operator $\operatorname{vec}(\cdot)$ maps a matrix to a vector by stacking its columns on top of each other and returns a column vector. Therefore, the original problem is recast as a standard integer linear problem (ILP) and can be solved using BB methods.

In the following, we calculate the worst-case computational complexity to obtain the optimal solution of problem (3.19). For an arbitrary number of integer variables υ, the number of linear programming subproblems to be solved is at least $(\sqrt{2})^{\upsilon}$ [71]. Since in problem (3.19) there are $N_{\mathrm{g}} N_{\mathrm{RB}} + J$ integer variables and $N_{\mathrm{RB}} + J + S$ constraints, and by retaining only the high order operations, the worst-case computational complexity for problem (3.19) is $O\left(\sqrt{2}^{(N_{\mathrm{g}} N_{\mathrm{RB}} + J)}\right)$. Motivated by this exponential computational complexity, we present in the next section a low-complexity suboptimal solution.

3.4.4 Scheduling Procedure Low-Complexity Solution

In this section, we propose a low-complexity heuristic algorithm for the scheduling, which is divided into two parts: unconstrained maximization and reallocation. The unconstrained maximization part is responsible for allocating the RBs into groups to maximize the throughput without taking into account the QoS constraints. The reallocation part is responsible for distributing the RBs that have been assigned in the previous part to another group to satisfy the QoS constraints. Flowcharts describing unconstrained maximization and reallocation parts are shown in Figures 3.8 and 3.9, respectively.

Before initializing our proposed algorithm, we consider that the achievable data rates of all UEs on all resources when belonging to any SDMA group formed by the grouping problem (3.17) are known. One way to do this is by calculating the precoders (as explained in Section 2.2), then the SINR and the data rate according to (2.12). In the unconstrained maximization part, the basic idea is to have a good initial solution that gives us a capacity upper bound. Firstly, in step 1, we define the set of available UEs composed of all UEs that is used along the algorithm. In step 2, we assign the RBs to the SDMA groups with the highest data rate (maximum rate allocation). After that, we define a set with the UEs that have fulfilled their data rate requirements and another set with the ones that are still unsatisfied. If the minimum number of satisfied UEs for all services is fulfilled (according to the constraint (3.18d)), we have found the optimum solution to problem (3.18). However, in general, only a few groups get assigned most of the RBs due to the unfairness of the employed assignment.

If the satisfaction constraint for any service is not fulfilled, a UE of the available UE set will be disregarded. By disregarding a UE, we mean it will not contribute to the reallocation metric (3.21) at the current TTI, i.e., the algorithm will not try to satisfy this UE. The criterion to select the UE $j^\star$ to be disregarded is given by

$$j^\star = \arg\min_{j \in \mathcal{J}} \frac{\left(\sum_{g \in \mathcal{G}} \sum_{n \in \mathcal{N}} \frac{\Gamma_{g,j,n}}{\kappa_j \cdot N_{\mathrm{RB}}} \right)}{l_j}, \tag{3.20}$$

where $\Gamma_{g,j,n}$ is the SINR of the UE j in RB n belonging to the SDMA group g, κ_j is the number of SDMA groups that UE j belongs to and N_{RB} is the number of available RBs. The adopted criterion to disregard a UE is quite reasonable: we disregard the UE that requires, on average, more RBs to be satisfied. The selected UE is taken out of the available UE set. After that, if the SDMA groups that contain the UE $j^\star$ have only disregarded UEs, then these groups are also disregarded.

The next step is to check whether the service of the UE $j^\star$, chosen using (3.20), can have another UE disregarded without infringing the minimum number of UEs necessary to satisfy the QoS constraint (3.18d). If so, we perform the maximum rate allocation considering the remaining SDMA groups. Otherwise, no UEs from this service will be disregarded anymore and all the UEs from this service are taken out of the available UE set. This procedure is repeated until we find a feasible solution, or no UE can be disregarded anymore.

Finally, we check if at least one UE is satisfied. If so, we define the receiver set $\mathcal{R}$ and available resource set $\mathcal{D}$. The receiver set is composed of the unsatisfied UEs, which have to receive RBs from the donors to satisfy their data rate requirements, where the donors are the satisfied UEs, which can donate/share RBs to/with unsatisfied UEs. Finally, the available resource set is composed of all RBs that are assigned to UEs of the donors, and which can be donated/shared to/with UEs of the receiver set. In case there is no satisfied UE after executing the first part, the proposed algorithm is not able to find a feasible solution, i.e., the algorithm is not able to satisfy the constraints of problem (3.18).

Since the unconstrained maximization part does not deal with QoS guarantees, it is necessary to reallocate the RBs that were previously allocated in order to satisfy the QoS requirements. Therefore, in the reallocation part, we exchange RBs among SDMA groups, changing the initial allocation provided by the unconstrained maximization part, to satisfy the UEs from the receiver set.

We start by creating the set $\mathcal{G}$ that is composed of all SDMA groups that contain the UE $j^\star$, which is the most difficult UE to be satisfied from receiver set $\mathcal{R}$. This UE can be found according to (3.20). The main motivation for choosing the most difficult UE to be served firstly is to assign the minimum number of RBs to satisfy the UEs in an unfavorable situation and assign the remaining RBs to UEs with better channel conditions. After that, we must identify the SDMA groups and RB pairs that are candidate to be chosen in the reallocation procedure. Therefore, the next step is to calculate the number of UEs that each pair of SDMA group from $\mathcal{G}$ and available RB from $\mathcal{D}$ can satisfy. Then, we can compose the set $\mathcal{F}$ containing the pairs of $\mathcal{G}$ and $\mathcal{D}$ that maximize the number of satisfied UEs.

The step 3 is to define a metric to reallocate an RB to the SDMA group that leads the receivers ($\mathcal{R}$) to satisfaction, while not causing a high SE loss. This can be achieved by the following metric

$$\varphi_{g,n} = \left(\frac{\sum\limits_{j \in \mathcal{R}_{j^\star}} |l_j - (\hat{l}_j + r_{g,j,n} - r_{g',j,n})|}{\sum\limits_{j \in \mathcal{R}_{j^\star}} |l_j - \hat{l}_j|} \right) \frac{\Phi^{cur}}{\Phi^{new}_{g,n} \cdot \pi_g}, \tag{3.21}$$

where $\mathcal{R}_{j^\star}$ is the set of receivers that belong to the SDMA group g of the chosen UE $j^\star$, $\hat{l}_j$ consists in the required data rate of UE j according to the current resource assignment, Φ^{cur} is the sum of the data rate achieved by all UEs in all RBs according to the current resource assignment, $\Phi^{new}_{g,n}$ is the sum of the data rate when the SDMA group g receives via reallocation the RB n without

Figure 3.8 – Unconstrained maximization part.

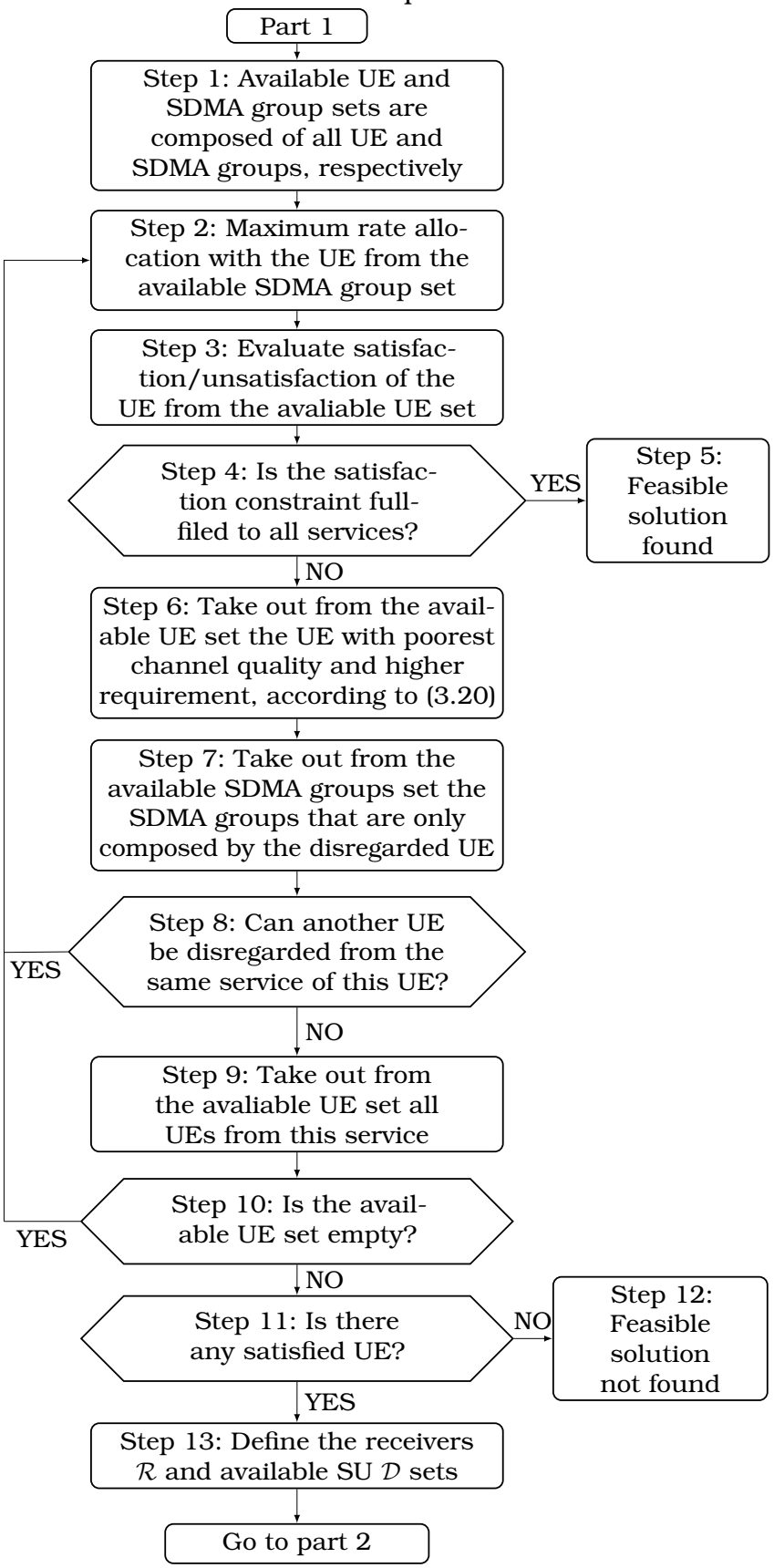

Source: Created by the author.

modifying the assignment on the other RBs, and π_g is the number of receivers in SDMA group g. This is an adaptation of the reallocation metric used in [70].

We consider that g' is the SDMA group that was chosen to RB n in the first part of the proposed solution (unconstrained maximization). Also, $r_{g',j,n}$ is the data rate of UE j on RB n when present in SDMA group g'. Note that $\Phi_{g,n}^{new} \leq \Phi^{cur}$ since we begin with the maximum rate solution in the unconstrained maximization part of our solution and to satisfy UEs we lose spectral efficiency. The SDMA group and RB chosen in the reallocation part are those that minimize the reallocation metric (3.21).

The step 4 is to check whether the reallocation would lead any UE from the donor SDMA group to become unsatisfied. If so, the reallocation is not performed, and the chosen RB is removed from the available RB set and cannot be chosen anymore. Otherwise, the reallocation is performed, and the UEs' data rates are updated. Then, the algorithm checks whether any receiver has become satisfied after reallocation. If so, these UEs are taken out from the receiver set. After that, the RB that was assigned to a new SDMA group is removed from the available RB set. Then, it is checked whether the UEs of all services became satisfied. If so, the algorithm ends, and a feasible solution is found. Otherwise, the reallocation process should continue. An outage event happens when there still exist UEs in the receiver set, and there is no RB for reallocation.

In the following, we present the computational complexity analysis of the proposed algorithm. Part 1 of the proposed solution in Figure 3.8 is clearly dominated by the maximum rate allocation, which needs $N_{\mathrm{RB}}N_{\mathrm{g}}$ comparisons. Part 2 is dominated by the calculation of the reallocation metric in (3.21), which is calculated for every available RB and group. This is repeated until the RB set becomes empty. Therefore, as the reallocation metric needs to be calculated for each available RB and UE, the worst-case computational complexity is $\mathcal{O}(N_{\mathrm{RB}}N_{\mathrm{g}} + N_{\mathrm{RB}}^2 N_{\mathrm{g}})$. Thus, by retaining only the high order operations, the worst-case computational complexity is $\mathcal{O}(N_{\mathrm{RB}}^2 N_{\mathrm{g}})$.

3.4.5 Performance Evaluation

In this section, we evaluate step-by-step the proposed framework. In Section 3.4.5.1 we evaluate the step 1 using the K-means algorithm. In Section 3.4.5.2 we evaluate the step 2 comparing the proposed grouping (G-PROP) algorithm against the optimal grouping (G-OPT) solution, considering that the K-means algorithm was utilized in step 1. In Section 3.4.5.3 we evaluate the step 3 comparing the proposed scheduling (S-PROP) algorithm presented in

Figure 3.9 – Reallocation part.

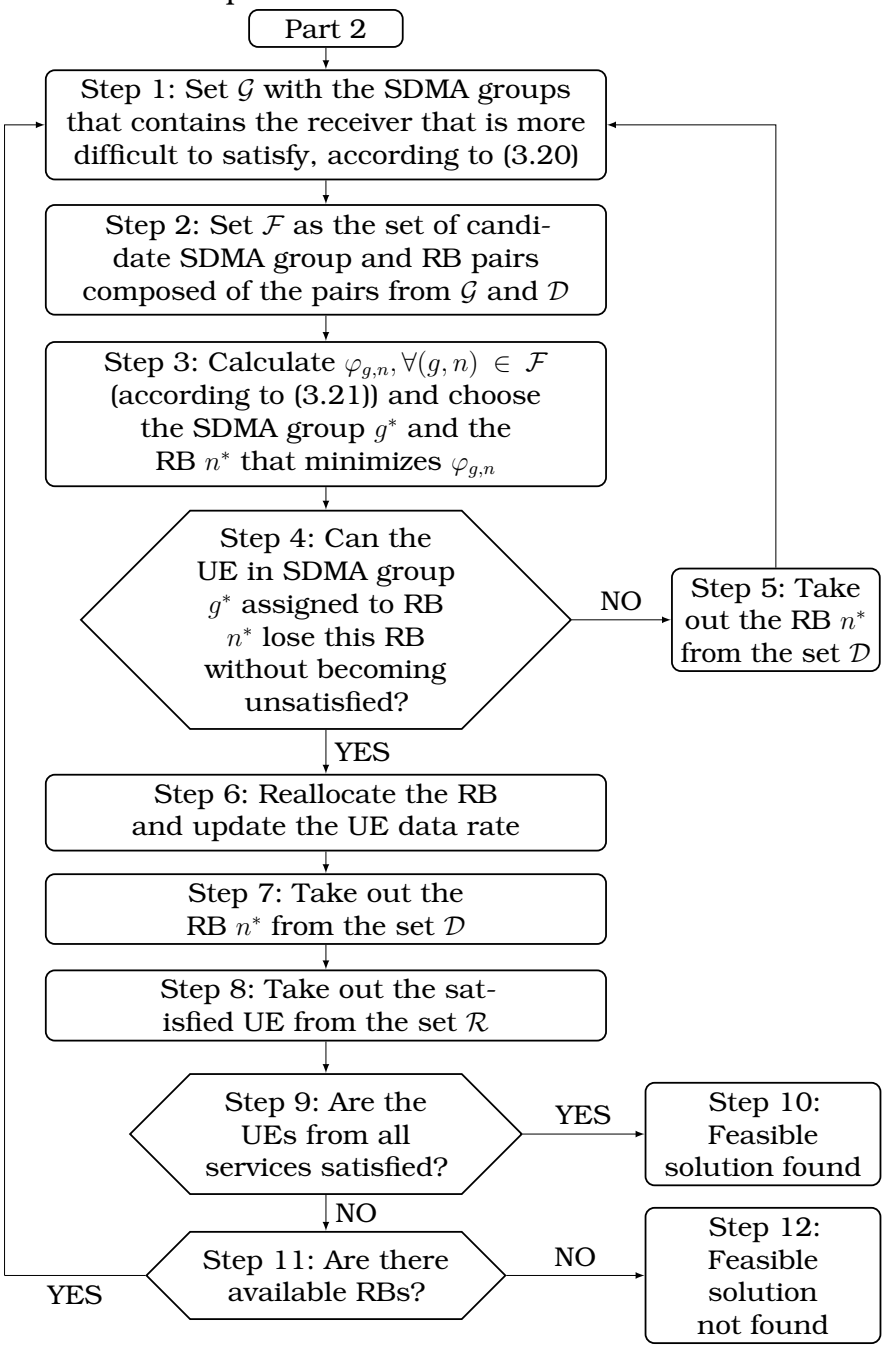

Source: Created by the author.

Section 3.4.4 against the optimal scheduling (S-OPT) solution obtained using the CPLEX solver [40] and against an adaptation of the JSM algorithm [41]. The JSM algorithm [41] determines the UEs' priority using the derivative of a sigmoidal function. Since the JSM solution needs to estimate the instantaneous data rate, we estimate it by using the dominant eigenvalue and eigenvector that are the CSI available for the other algorithms. Furthermore, in order to deal with the interference among clusters and keep fairness when comparing with our proposed framework, the JSM algorithm is employed after step 1.

The simulation scenario consists in a UMi LOS [75] single cell system with an 8×8 UPA ($N_{\mathrm{t}} = 64$). We also assume that the system works with a bandwidth of 100 MHz, a frequency of 28 GHz and that the UEs are equipped with a single-antenna[2]. Based on [78, Table 2], we generate a set of 125 RBs, each composed of 12 equally spaced subcarriers of 60 kHz. Moreover, each frame has 10 subframes carrying 14 symbols each and the TTI duration is 0.25 ms. The considered channel model is the 3-dimensional QuaDRiGa [75]. We consider that a set of 40 UEs is equally divided into two groups (forming two circular hotspots) with 15 m of radius. The UEs are uniformly disposed inside hotspots, which are linearly distributed in a 60° cell sector[3]. The total power is fixed and equal power allocation (EPA) among RBs and among spatial subchannels is employed. Since we are using hybrid precoding, as many other works in literature [8], [32], [53], [73], [74], we are considering the number of available RF chains as at most 10% of the number of BS antennas. Also, we are considering that the BS serves 2 or 3 UEs per RB and cluster. Therefore, the BS can simultaneously serve more than 100 UEs since we are considering in our simulations 2 clusters and 25 RBs. Furthermore, the number of simulated UEs is limited by the complexity to obtain the optimal solution, which has an exponential computational complexity. Also, we are considering a simulation time of 25 ms and 100 simulations rounds, the reason for considering only 25 ms is to analyze the performance of the algorithms at the end of this time in a given TTI. Other relevant simulation parameters are listed in Table 3.2.

Table 3.2 – Simulation parameters for Section 3.4.

Parameter	**Value**	**Unit**
Simulation time	25	ms
Number of TTIs	100	–
Number of simulation rounds	2000	–
Cell radius	200	m
Total transmit power	35	dBm
Noise figure	9	dB
Noise spectral density	-174	dBm/Hz
Shadowing standard deviation	3.1	dB
Number of UEs	40	-
Number of Clusters	2	-
UEs speed	3	km/h
Total Number of RBs	125	-
Used Number of RBs	25	-
Number of services	2	-
Number of UEs per service	20	-

Source: Created by the author.

[2] The study of UEs with more than one antenna is out of the scope of this thesis, leaving it as the perspective of study for future works.

[3] Note that a UPA with 64 antenna elements radiating with the 3rd generation partnership project (3GPP) antenna model has an effective coverage of a 60° sector.

Note that, in this chapter, firstly the BS create the set of possible SDMA group as presented in Section 3.4.1. Secondly, the UEs feed back their CSI using the analog precoders (2.6) and eigenvectors of equivalent channel (2.3) presented in Section 2.2. After that, the digital precoder (2.9) is computed following Section 2.2 for each set of SDMA group. Finally, the UEs are scheduled using the algorithm presented in Section 3.4.4, and the data is sent to the scheduled UEs using (2.12). Therefore, this solution reduces the signaling overhead since it requires only to calculate the digital precoders of the smaller set of SDMA groups computed previously instead of all possible SDMA groups.

3.4.5.1 K-means Algorithm Evaluation (Step 1)

In Figure 3.10 we evaluate the effectiveness of the employed clustering (step 1 of the proposed framework) in the proposed scenario with two hotspots. Let us clarify the difference between the terms hotspot and group of UEs: a hotspot is a group of UEs in a confined area, and the cluster is the grouping done by the clustering step, which can even select UEs of different hotspots. For this analysis, basically, we increase the angle between the line segments from the BS to the center of the two hotspots. With this, the channel among UEs of different hotspots tends to be more uncorrelated. As the angle increases, we expect that the probability of the clustering algorithm to group UEs of different hotspots decreases. We define the expected clustering difference as the probability of clustering together UEs that do not belong to the same hotspot. Focusing on performance, we can see that as the angle between hotspots increases, the formed clusters get closer to the given physical clusters (hotspots).

In Figure 3.11 we evaluate the step 1 (clustering step) of our algorithm by means of the mean-squared error between the centroids formed in each iteration and those formed when the stop criterion is met (clusters do not change or a maximum number of iterations is reached). We can see that the mean-squared error decays very fast over the iterations and converges in 8 iterations. This happens because the UEs are already disposed in a defined number of hotspots and an angle of 15° was assumed between clusters, which helps the algorithm to converge. Therefore, from the analyses provided in this subsection, the K-means algorithm can reach a good clusterization with a small number of iterations in the considered scenarios.

3.4.5.2 Grouping Algorithm Evaluation (Step 2)

In this section we evaluate the step 2 (grouping step) in terms of the system data rate. After this step, the RBs are allocated to the SDMA groups aiming at maximizing the system data rate. For the sake of comparison, we implemented

Figure 3.10 – Expected clustering difference of K-means clustering for different hotspots dispositions.

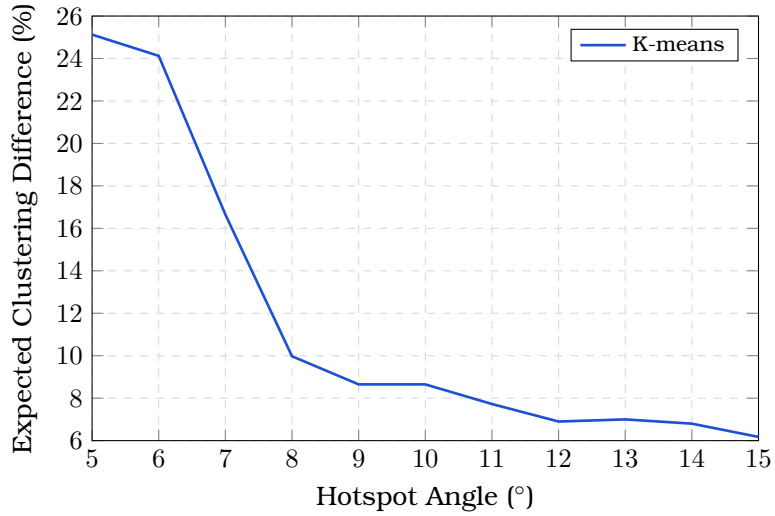

Source: Created by the author.

Figure 3.11 – Convergence of K-means clustering.

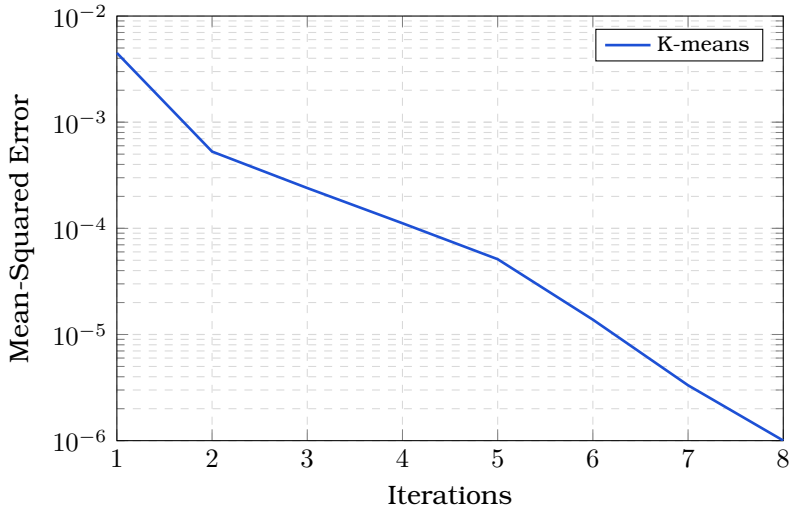

Source: Created by the author.

the optimal SDMA grouping solution (G-OPT), that is obtained by enumerating all the possible SDMA group compositions and choosing the best one for each RB. Note that, due to the complexity to obtain the G-OPT solution, we had to reduce the number of SDMA groups of the problem. For this reason, we decided to reduce the number of UEs per cluster. For example, considering 20 UEs in each cluster, 2 clusters and 2 UEs served per cluster, the number of possible SDMA groups is $36,100$, which is impracticable. Motivated by this, the performance analysis of the G-PROP algorithm against the G-OPT solution considers a reduced scenario with 2 clusters each one containing 10 UEs.

In Figure 3.12, we evaluate the step 2 (grouping step) in terms of total system data rate for the G-PROP and G-OPT solution for a scenario considering 2 UEs selected per cluster when the required number of SDMA groups N_g

varies. As we can see, the impact of β on the system performance decreases as the number of SDMA groups N_g increases. This behavior happens due to the fairness constraint (3.18d), which avoids aiming only at maximizing the system data rate, i.e., the algorithm tries to select SDMA groups that include in a balanced way all UEs and not only groups that maximize the SE. Focusing on performance, selecting the best β of each curve, the G-PROP algorithm compared with the G-OPT solution has a loss of 21%, 8% and 6% for $N_g = 1$, $N_g = 10$ and $N_g = 40$, respectively.

Figure 3.12 – System data rate of G-PROP and G-OPT solutions for a scenario considering 2 UEs selected per cluster and different numbers of SDMA groups.

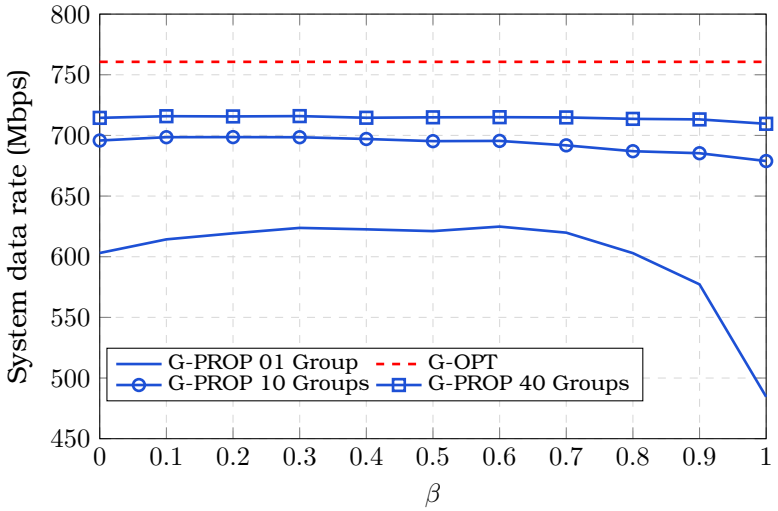

Source: Created by the author.

In Figure 3.13, we evaluate the step 2 (grouping step) in terms of total system capacity for the G-PROP and G-OPT solutions for a scenario considering 3 UEs selected per cluster when the required number of SDMA groups N_g varies. Note that, as we increased the number of UEs selected per cluster, the setting of β parameter should be performed more carefully than in the previous scenario (considering 2 UEs selected per cluster). Therefore, differently of Figure 3.12, the impact of β on the system performance can be seen even considering 40 SDMA groups. Focusing on performance, selecting the best β of each curve, the G-PROP algorithm compared with the G-OPT solution has a loss of 51%, 20% and 14% for $N_g = 1$, $N_g = 10$ and $N_g = 40$, respectively. The reason for the increase in the performance gap between solutions is the increase in the complexity (search space) of the problem, since the search space grows combinatorially with the number of selected UEs per cluster.

The total number of possible SDMA groups evaluated by G-OPT are $2,025$ and $14,400$ for the scenarios considering 10 UEs in each cluster serving 2 and 3 UEs per cluster, respectively. Therefore, from the analyses of the results, the G-PROP algorithm achieves good performance even when a very small percentage

Figure 3.13 – System data rate of G-PROP and G-OPT solutions for a scenario considering 3 UEs selected per cluster and different number of SDMA groups.

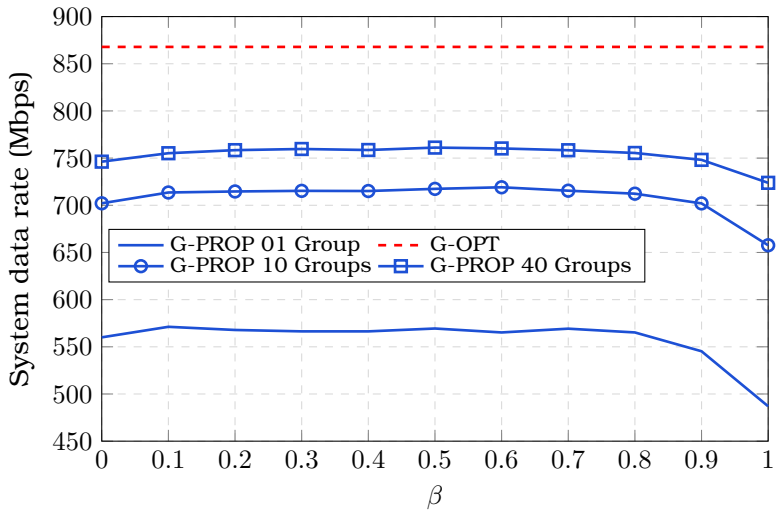

Source: Created by the author.

of the possible SDMA compositions is considered. Furthermore, as shown in Section 3.4.2, the computational complexity of the G-PROP suboptimal algorithm is polynomial and much lower than that of the G-OPT solution, thus offering a good performance-complexity trade-off.

3.4.5.3 Scheduling Algorithm Evaluation (Step 3)

In this section we evaluate the proposed step 3 (scheduling step) considering 40 UEs in the system, 2 clusters, 2 UEs selected per cluster, and 25 available RBs which makes possible to serve all 40 UEs simultaneously. Note that, the total number of scheduled UEs in an RB (4 in this section) is limited by the number of available RF chains. In all figures of this section, the β parameter in (3.14) varies from 0 to 1. We consider three performance metrics: the total system data rate, the outage rate and the average number of satisfied UEs. Note that, only solutions that are feasible for all β are utilized. An outage event happens when the problem constraints cannot be fulfilled by the algorithm. Note that, the problem itself can be infeasible, depending on the UEs' positions, channel gains, and data rate requirements. Thus, we can define the outage rate as the ratio between the number of outage events and the total number of simulation rounds. Therefore, this performance metric indicates if the algorithms are capable of finding a feasible solution to the studied problem. The third and final metric is the ratio between the total number of satisfied UEs and the total number of UEs in the system.

In Figure 3.14, we evaluate the step 3 (scheduling step) in terms of outage rate and the total system data rate for the S-PROP, JSM and S-OPT solutions when the number of groups N_g varies. As we can see, the selection of β impacts

Figure 3.14 – System outage and capacity of our proposed and OPT solutions for a scenario considering 2 UEs selected per cluster, requirement of 5 Mbps per UE, requirements of 100% of satisfied UEs and different number of SDMA groups.

(a) Outage. (b) System capacity at 50th percentile.

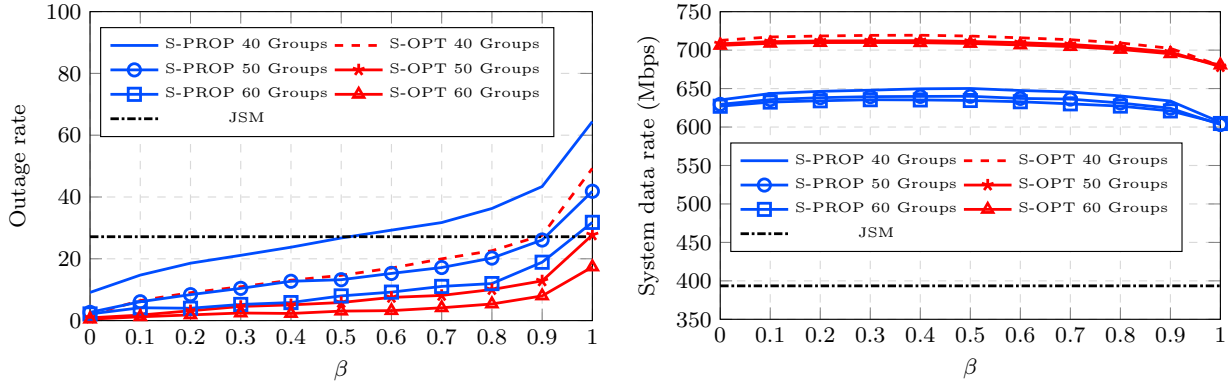

Source: Created by the author.

on the system performance achieving different system data rate and outage values as β varies. For example, we can see that the lowest outage rate can be achieved with $\beta = 0$ (selection of UEs with lowest channel correlation within a cluster). This behavior occurs for the rest of the figures in this section. According to this, the spatial correlation cannot be neglected, e.g., $\beta = 1$, since this increases the intra-cluster interference. However, this figure also shows that the best system outage and data rate are achieved for values of $\beta = 0$ and $\beta = 0.5$, respectively, showing that both channel correlation and channel gain should be carefully taken into account, depending on the performance objectives of the system. Moreover, the performance loss of the JSM algorithm in comparison with other solutions is due to the fact that this solution does not take into account the intra-cluster interference. This behavior occurs for the rest of the figures in this section.

As we can see in Figure 3.14a, it is possible to reduce the outage rate by increasing the number of candidate SDMA groups. Focusing on the relative performance among algorithms we can see that, when the β parameter is close to 0, the S-PROP algorithm performs near optimally for 50 and 60 groups, while a higher performance loss can be seen for 40 SDMA groups. Therefore, depending on the number N_g of SDMA groups, the grouping procedure can return a solution where the constraint (3.18d) might be unfeasible or hard to be solved, i.e., as the number of SDMA groups increases the QoS constraints become easier to be fulfilled. However, to increase the number of SDMA groups leads to an increase in the search space for the scheduling step and, consequently, the complexity of both scheduling and SDMA grouping procedures increases. Thus, as the number of SDMA groups increases, a trade-off between complexity and performance takes place. Another observation is that we consider only a small

Figure 3.15 – System outage and satisfaction of our proposed and OPT solutions for a scenario considering 2 UEs selected per cluster, $N_g = 60$, requirement of 100% of satisfied UEs and different data rate requirements.

(a) Outage.

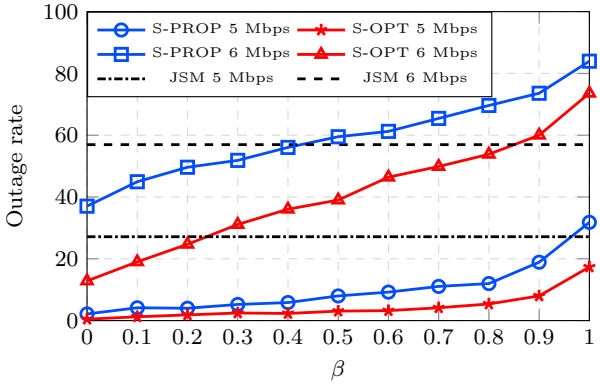

(b) Percentage of satisfied UEs.

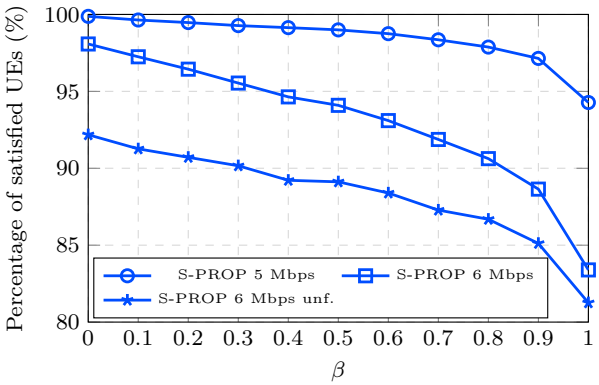

Source: Created by the author.

fraction of the total number of possible SDMA groups, which for the considered scenario is $91,390$, according to (3.1). Therefore, it is unpractical to solve the problem considering all possible SDMA groups.

Analyzing Figure 3.14b, we can see that the system data rate is almost unchanged and does not depend on the number of SDMA groups, i.e., the increase of N_g has more impact on the outage than on the capacity. This can be justified due to the grouping metric (3.17a), which tries to create SDMA groups that maximize capacity. Due to that, the capacity for the feasible solutions has a similar behavior. Focusing on the relative performance among algorithms, the S-PROP and JSM algorithms have a loss of approximately 15% and 43%, respectively, in comparison to the S-OPT solution.

In Figure 3.15, we evaluate the step 3 (scheduling step) in terms of outage rate for the S-PROP, JSM, and S-OPT solutions and the average number of satisfied UEs for the S-PROP solution when the required data rate (l_j) varies from 5 to 6 Mbps. As we can see in Figure 3.15a, the outage rate increases when the required data rate per UE increases. Focusing on the relative performance among algorithms, the S-PROP algorithm performs near optimally for the requirement of 5 Mbps, and a performance loss is noted for a requirement of 6 Mbps.

In the next analyses, we evaluate the performance of the S-PROP algorithm in scenarios which do not have a feasible solution, or in which it is hard to obtain a feasible solution. We denote this case as "unf.". An unfeasible case happens when the analyzed algorithm is not able to find a solution that satisfies all the constraints of problem (3.18). Note that, it is interesting to analyze this scenario since an important feature that a QoS constrained RRA algorithm

Figure 3.16 – System outage and satisfaction of our proposed and OPT solutions for a scenario considering 2 UEs selected per cluster, $N_g = 60$, requirement of 6 Mbps per UE and different requirements of satisfied UEs per service.

(a) Outage.

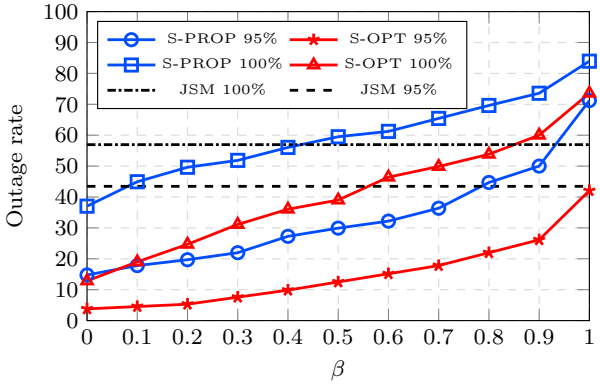

(b) Percentage of satisfied UEs.

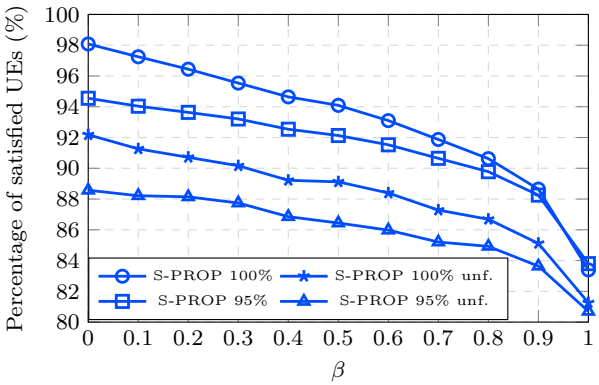

Source: Created by the author.

should seek is to provide a good result within the presented circumstances. This "unf." case is compared against the scenario considering all the simulation rounds. Therefore, as we can see in Figure 3.15b, even when the S-PROP algorithm is not able to find a solution, it provides a result that satisfies a good number of UEs. Focusing on performance, the average percentage of satisfied UEs is almost 100% for a requirement of 5 Mbps and 98% for a requirement of 6 Mbps considering all simulation rounds. When only unfeasible simulation rounds are considered, the S-PROP algorithm satisfies in average 92% of the UEs for $\beta = 0$, which is reasonable considering the hard nature of the scenario. This happens due to step 3 of part 2 of the proposed RRA algorithm in Figure 3.9, wherein at each iteration the algorithm tries to satisfy with only one RB reallocation a high number of unsatisfied UEs. Therefore, although in Figure 3.15a we can see a high outage rate when the required data rate is 6 Mbps, most of the UEs are satisfied. Thus, a way to deal with these unsatisfied UEs is to satisfy them in the upcoming TTIs, i.e., the UEs can receive a priority inversely proportional to the data rate obtained until now. Note that we do not present results for the S-OPT solution regarding the percentage of satisfied UEs since the solver only returns a valid solution when the problem is feasible. Therefore, the average percentage of satisfied UEs cannot be analyzed for the S-OPT algorithm. In Figure 3.15a we can see an outage of approximately 0% when we consider the requirements of 5 Mbps, therefore, the number of simulation rounds containing only unfeasible solutions is very low (close to 0). Thus an analysis containing only unfeasible solutions cannot be performed for those requirements. Moreover, we skip the analysis of the average percentage of satisfied UEs for the JSM algorithm since it has a higher loss in outage rate in comparison to our proposed algorithm depending of β.

In Figure 3.16, we evaluate the step 3 (scheduling step) in terms of outage rate for the S-PROP, JSM, and S-OPT solutions and the percentage of satisfied UEs for the S-PROP solution when the required number of satisfied UEs per service varies. As we can see in Figure 3.16a, the outage rate increases with the number of UEs that need to be satisfied. Note that the gap among S-PROP, JSM, and S-OPT solution is reduced when the number of satisfied UEs decreases. This behavior is similar to that one seen in Figure 3.15a when the required data rate decreases. Focusing on the relative performance among algorithms, when β is close to 0, the S-PROP and JSM solutions present a higher performance loss. However, despite this higher loss in Figure 3.16a, we will see in the sequel that the S-PROP solution is capable of satisfying, on average, almost the target satisfaction percentage.

In Figure 3.16b we present the percentage of satisfied UEs for the scenarios in Figure 3.16a that presented higher performance losses. Therefore, considering both cases (with all simulation rounds and the case with only unfeasible simulation rounds), we can see that the S-PROP solution can almost reach the required satisfaction target (95% and 100%). As we can see in Figure 3.16b, when we aim to satisfy 100% and 95% of the UEs, the S-PROP solution is capable of satisfying 98% and 94% of them considering the optimal β value for satisfied UEs and all simulation rounds. Considering only the unfeasible simulation rounds, we can see that the gap between the target and obtained satisfaction is reduced when the number of required satisfied UEs decreases. As explained before, a way to deal with these unsatisfied UEs is to satisfy them in the next TTIs.

In summary, from the analyses of the results, the S-PROP low-complexity algorithm achieves good performance compared to the S-OPT solution considering the problem objective and constraints. As shown in Section 3.4.3, the computational complexity of the S-PROP suboptimal algorithm is polynomial and much lower than that of the S-OPT solution, thus offering a good performance-complexity trade-off.

3.5 Conclusions

In this chapter, we proposed and evaluated a framework of RRA for hybrid precoding massive MIMO communication systems that consists of three parts. First, the clustering procedure partitions the UEs into clusters containing spatially correlated UEs using a clustering algorithm. This step reduces the search space to perform the SDMA groups. Secondly, the grouping procedure selects spatially compatible UEs from each cluster to form SDMA groups.

Finally, the scheduling procedure assigns RBs to the SDMA groups aiming at optimizing a predefined objective.

To evaluate our proposed framework, firstly we solve the problem of maximizing the system data rate considering one RB. Since this problem considers only one RB, it only applies the clustering and grouping procedure. In the clustering procedure, we partition UEs into clusters that are spatially compatible using the K-means clustering algorithm. The analog part of the hybrid precoder is obtained from the cluster centroids. In the grouping procedure, we select UEs from each cluster to build an SDMA group in order to maximize the capacity. In order to reduce the computional burden involved in SDMA grouping, a low-complexity metric to find suitable UEs from each cluster while avoiding computing digital precoders for every possible candidate group of UEs is employed. Then, we formulated an optimization problem using a spatial compatibility metric based on [24] to build SDMA groups. Moreover, a suboptimal algorithm was proposed to solve this problem, and it was compared against the optimal and baseline solutions. Simulation results indicate that we can obtain gains by exploiting spatial compatibility when compared to less intelligent strategies that randomly choose UEs from clusters to build the SDMA groups. Lastly, the choice of a suitable value for β (spatial separability versus channel gain) in the studied problems can lead to considerable additional gains.

Next, we extend the previous problem to solve the problem of maximizing the system data rate considering multiple RBs, services and QoS requirements. The clustering procedure is done the same way as the previous problem. The grouping process formulates an optimization problem using a spatial compatibility metric to build different SDMA groups to maximize the data rate and QoS requirements. The solution of this problem generates a set of SDMA groups suitable for all RBs exploiting the channel hardening characteristic. Finally, it was necessary to allocate the RBs to SDMA groups to meet QoS requirements while maximizing the data rate. Moreover, a suboptimal algorithm was proposed to solve the scheduling part, and it was compared against the optimal solution and an adaptation of a solution from the literature. Simulation results showed that our proposed framework presented a good performance especially in low and moderated system loads. In high loads, even when the proposed algorithm was not able to find a feasible solution, it provided good results in terms of UE satisfaction. We also show that a suitable trade-off between the spatial channel correlation and channel gain should be chosen to improve the system performance. Also, there may be an optimum trade-off to the outage rate and another to capacity, i.e., this choice depends on the system objective. Moreover, the spatial compatibility and channel hardening

characteristics can be exploited to drastically reduce the possible number of SDMA groups that need to be built in a system. Furthermore, the proposed suboptimal solution presented a good performance-complexity trade-off.

The content of this chapter can be extended in some directions. In the following, some of the possible future works are pointed out:

- Extend the adopted scenario to a more dynamic one where UEs are moving at different speeds. This scenario makes the channels from UEs change rapidly, making it necessary to calculate more often the clustering and covariance, which can lead to an unpractical scenario. It is interesting to evaluate how our proposed solutions perform in this more challenging scenario.
- Extend the scenario to consider a traffic model. One possibility is to adapt the proposed framework to consider the network traffic as information to decide which UEs are going to be scheduled.
- Extend the scenario to consider other QoS requirements, such as packet delay, latency and jitter.

Chapter 4

RRA in Massive MIMO Systems Using RL Tools

In the present chapter, we deal with RRA problems for massive MIMO networks proposing scheduling algorithms using RL tools to optimize the system performance. More specifically, we propose a framework that leverages RL in order to schedule UEs in a massive MIMO scenario with hybrid precoding. This way, we propose three learning-based scheduling algorithms by employing CMAB theory aiming at maximizing system data rate, fairness, and assuring QoS requirements, whose action space is reduced by taking advantage of the interference mitigation properties of ZF precoding and clustering described in Chapter 2.

4.1 Contributions and Chapter Organization

This chapter has the following main contributions:

- A framework that leverages RL in order to schedule UEs in a massive MIMO scenario with hybrid precoding that has the following advantages:
  - The framework is based on virtual learning agents, where the BS is the physical entity, and the UE clusters are the logical entities. It learns from past experience about the spatial compatibility of the different UEs inside a cluster how to select the UEs to achieve a given objective.
  - To perform scheduling, virtual agents do not require instantaneous CSI of UEs for the compatibility check, but instead the system sum data rate (reward) of UEs scheduled together in the past, thus reducing the signaling overhead (feedback costs). Furthermore, the

instantaneous CSI is only reported for the scheduled UEs, reducing even more the signaling overhead.

  - The framework is capable of supporting UEs with different data rate requirements (multiple services).

- The proposed framework supports three different objectives, which can dynamically configure/adapt the objective to consider throughput maximization, fairness guarantees, or balance between throughput maximization and QoS provisioning.

- Performance evaluation and comparison of the proposed framework in a massive MIMO scenario with hybrid precoding against reference solutions previously proposed in the literature.

This chapter is organized as follows. Section 3.2 shows how clustering and ZF digital precoding can be used to reduce the scheduling search space of our proposal. In the same section, we propose the three learning-based schedulers of our framework. Section 4.3 shows the numerical results of the proposed framework against reference solutions. Finally, Section 4.4 presents the main chapter conclusions.

4.2 Action Space

We assume that the BS is the physical learning agent responsible for maximizing the reward α by scheduling K UEs. The reward α is defined as the instantaneous system data rate, which is the sum of data rates achieved by the K scheduled UEs. The reward is the same for all three proposed schedulers These differ by the use of context information, as it will be seen later. Furthermore, we assume that an action consists of selecting K UEs that will be scheduled by the BS. Then, the number A of possible actions in the action space $\mathcal{A}$ is given by

$$A = \binom{J}{K}, \tag{4.1}$$

which increases combinatorially with J and K, making the action set size rapidly get impractical. To reduce the number of actions, we consider each cluster as a logical virtual agent by using the previous assumption presented in Chapter 3, that the signal transmitted from the BS serving UEs in cluster x produces negligible interference at the UEs in cluster y. Each virtual agent is responsible for performing an action, i.e., scheduling the UEs belonging to its own cluster. Therefore, we can define for each virtual agent c the set of actions

$\mathcal{A}_c$, whose size A_c is given by

$$A_c = \binom{J_c}{K_c}, \tag{4.2}$$

where J_c and K_c are the total number of UEs and the number of scheduled UEs of cluster c, respectively. Since $\sum_{c=1}^{C} A_c \ll A$, the action space is drastically reduced.

4.2.1 Maximum Throughput Solution

In the sequel, we describe the maximum throughput (MT) learning algorithm as a CMAB problem. Note that the term throughput refers to the throughput obtained in a long run, i.e., from the first TTI until the current TTI. Consequently, we need to estimate action values which are used to make the action selection decision. The action value of an action is defined as the mean received reward when that action is selected. This way, the incremental average updating method is used to define the action value vector $\boldsymbol{d}_c \in \mathbb{R}_+^{A_c \times 1}$ as follows [35, Eq. 2.4]

$$\boldsymbol{d}_c(a_c) = \boldsymbol{d}_c(a_c) + \frac{1}{\boldsymbol{n}_c(a_c)}(\alpha - \boldsymbol{d}_c(a_c)), \tag{4.3}$$

where a_c is a given action, $\boldsymbol{n}_c \in \mathbb{Z}_+^{A_c \times 1}$ is the vector containing the number of times that a given action was selected, and the $\boldsymbol{n}_c(g)$ and $\boldsymbol{d}_c$ refer to the element g from vectors $\boldsymbol{n}_c$ and $\boldsymbol{d}_c$, respectively. For example, $\boldsymbol{n}_c(a_c)$ refers to the number of times in cluster c that the virtual agent selected the action a_c that belongs to cluster c. Since the three proposed schedulers use the same reward, note that this same estimation of action values will also be used by the proportional fair and QoS solutions.

4.2.2 Maximum Throughput with Fairness Guarantees

Note that, since the reward contains the system data rate, the scheduler presented in Section 4.2.1 does not require any additional information. This is not the case of the next presented schedulers, which require more information about the system to achieve their objectives. Therefore, a context information is going to be used by the next proposed schedulers and its definition, as well as its usage, are going to be presented in this section and in Section 4.2.3.

The maximum throughput with fairness guarantees (MTFG) algorithm proposed here is modeled as a CMAB problem and aims to maximize the system throughput guaranteeing the fairness among UEs. Since we are working with FDD massive MIMO, obtaining the instantaneous CSI is impractical. Therefore, the outdated CSI, which we consider available and was used before by the clustering in Section 2.1, is the considered context information used by our

MTFG algorithm, which is used to obtain the UEs' scheduling priority. Note that we consider that the UEs average throughput is the sum of the throughput obtained by each UE divided by the number of UEs. The UE priority for being scheduled is a value between 0 and 1 that reflects the distance of the UE throughput in relation to the UEs average throughput, i.e., a UE throughput lesser in relation to the UEs average throughput results in a UE scheduling priority close to 1, and a UE throughput greater in relation to the UEs average throughput results in a UE scheduling priority close to 0. In the following, we describe how the UEs' priority is modeled to achieve maximum throughput and guarantee the fairness among UEs. We use a priority function in which the UE priority decreases rapidly when its throughput approaches or exceeds its target (sigmoidal function). Therefore, similarly to [41, Eq.40], we propose to use the mentioned function

$$P_j(v_j) = \frac{1}{1 + \mathrm{e}^{-\delta(\frac{v_j}{v^{\text{avg}}} - 1)}}, \tag{4.4}$$

where $\delta > 0$ controls the function shape, v^{avg} is the sum throughput obtained over the number of UEs, and v_j is the throughput of the j-th UE. Note that we normalize v_j by v^{avg} to map the throughput of v_j as a portion of the UEs' average throughput, i.e., between 0 and 2, which was selected to have a better sampling. $P_j(v_j)$ is a decreasing function of the UEs throughput with a controllable shape η and centered at v^{avg}, as shown in Figure 4.1. As in [41], we used $\delta = -9.1912$ to obtain the shape shown in Figure 4.1. The idea is prioritizing the UE with the lowest throughput in order to improve the system fairness.

Figure 4.1 – UE prioritization function for MTFG.

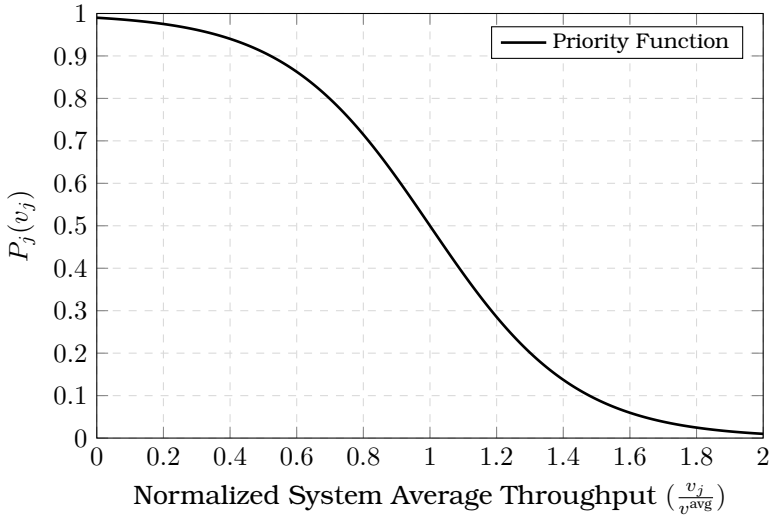

Source: Created by the author.

Therefore, we can define the mean priority $q_c(a_c)$ of UEs in the action a_c

belonging to cluster c as

$$q_c(a_c) = \frac{1}{K_c} \sum_{j \in \mathcal{U}_c(a_c)} P(v_j), \tag{4.5}$$

where $\mathcal{U}_c(a_c)$ is the group of UEs composing the action a_c in the cluster c. The UEs priorities and the action values will be jointly used to determine which actions are going to be selected in a given TTI. Therefore, we can define $\boldsymbol{q}_c \in \mathbb{R}^{A_c \times 1}$ as mean UEs priority vector of each action in a cluster c.

4.2.3 Maximum Throughput with QoS Guarantees

In the following, we describe how the UEs' priority is modeled aiming at maximizing the system throughput and guarantee the QoS requirements, namely maximum throughput with QoS guarantees (MTQG). Therefore, we replaced the variable v^{avg} that defines the center of our function (4.4) by v_j^{req}, which is the required throughput of UE j. As in Chapter 3, a UE is considered satisfied when it achieves a target throughput. With this in mind, we need a priority function capable of being adaptable to achieve a trade-off between throughput and QoS. Therefore, the UEs' priority depends on its current throughput, so the algorithm chooses the action with the best trade-off between the QoS requirements of UEs and the system throughput.

This can be achieved using the function defined in (4.4) and controlling its shape through the variable δ. Therefore, as it can be seen, depending on the P_j shape and current throughput, an unsatisfied UE ($v_j < v_j^{req}$) can have a priority to be scheduled between 0.5 and 1, while a satisfied UE can have a priority between 0 and 0.5. The shape of $P_j(v_j)$ is associated with the system satisfaction, where in Section 5.1 of [41] the authors obtained good results for $\delta = -9.1912$. In this work, we consider the system satisfaction as the ratio between the number of satisfied UEs and the total number of UEs. Following a similar approach as [41], we created 21 shapes for $P(\cdot)$ based on the value of δ, which are shown in Figure 4.2 for $\eta \in \{-10, -9, \ldots, 9, 10\}$ and $\delta = -9.1912 \times 2^{\Upsilon}$, where Υ determines the shape of the function P_j.

Therefore, in relation to Figure 4.2, if the system satisfaction is above μ and the worst satisfied UE has its throughput Ω greater than its target, the Υ value is reduced by 1 so as to make P_j in (4.4) approach a straight/flat line (light gray). The μ and Ω values are estimated by the network operator, e.g., based on the environment and past experience. When the function assumes a flat line shape, the UEs have the same priority of approximately 0.5, leading the scheduler to select UEs following a maximum throughput policy. Otherwise, the Υ value increases by 1 as to make the shape $P_j(v_j)$ in (4.4) approach a step function

Figure 4.2 – UE prioritization function for MTQG.

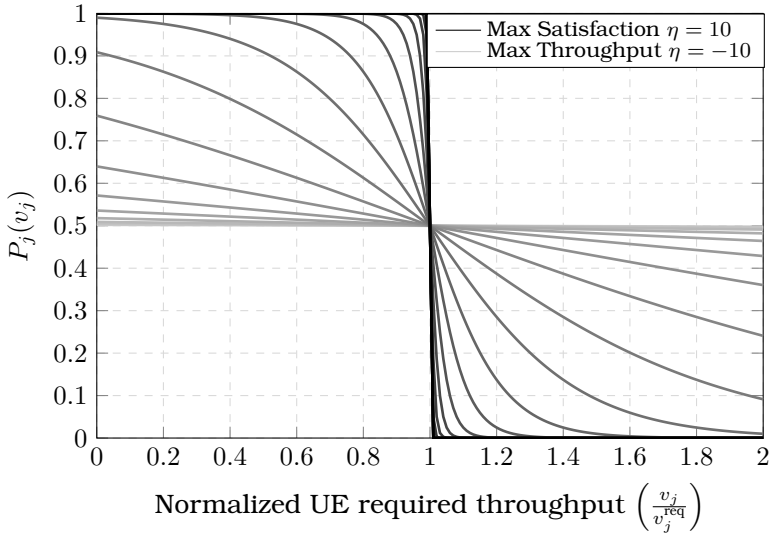

Source: Created by the author.

(dark gray). When the function assumes the step function shape, the unsatisfied and over-satisfied UEs have priorities of almost 1 and 0, respectively, leading the scheduler to select UEs following a maximum satisfaction policy.

4.2.4 Proposed Framework

The framework containing the MT, MTFG, and MTQG solution is presented in Algorithm 4. Note that, since all proposed schedulers use the same reward (system throughput), we can create a joint framework even if they have different goals. Therefore, the solutions MTFG and MTQG can reach their desired goals by combining this shared reward with (4.5). Also, for the MTQG solution, the changes in (4.4) need to be considered, as explained in Section 4.2.3. For each TTI and virtual agent, depending on the system operator objective (MT, MTFG or MTQG), our framework selects its actions based on the ϵ-greedy policy, which has two distinct phases: exploration (with probability ϵ) and exploitation (with probability $1 - \epsilon$). The ϵ value decays linearly at each TTI until it reaches the desired value, and this strategy is known in the literature as ϵ-decaying method [79]. This way, a random value between 0 and 1 at each TTI is generated, if this value is greater or equal than ϵ the algorithm will enter in the exploration phase. Otherwise, it will enter the exploitation phase. For more details on the ϵ-greedy strategy as well the ϵ-decaying method, please refer to [79]. In the exploration phase, a random action is selected from $\mathcal{A}_c$. An exploration phase is needed to get information about the unexplored actions or even those actions that are not selected so often. In the exploitation phase, if the system provider chooses to operate using the MT scheduling, the virtual agent chooses an action that maximizes the value of $\boldsymbol{d}_c$. Otherwise, if the system provider

chooses to operate using the MTFG or MTQG scheduling, the virtual agent computes its priority using (4.5) following the definitions of Section 4.2.2 and Section 4.2.3, respectively.

After that, the virtual agent selects the action that maximizes the trade-off between the UEs throughput and their priorities, which corresponds to the maximum value in the Hadamard (element-wise) product $\boldsymbol{q}_c \odot \boldsymbol{d}_c$. Then, the BS schedules the UEs chosen by the virtual agents. These scheduled UEs use the analog precoder to feed back their equivalent channel, which is used as CSI to calculate their digital precoders. Afterwards, the system data rate is calculated by the BS using (2.12).

In the next step, the system data rate associated with the action selected by each virtual agent, as well as the number of times that these actions were selected, are stored in $\boldsymbol{d}_c$ and $\boldsymbol{n}_c$, respectively. Moreover, if the framework is operating using the MTQG scheduling, the shape of the priority function needs to be managed. Therefore, let us introduce the variables μ and Ω. μ is a value between 0 and 1 that refers to the percentage of satisfied UEs required by the system operator. Ω is a value that refers to the throughput security threshold that the worst UE needs to have before the system starts to get concerned about the system satisfaction, i.e., the threshold that triggers the mechanism that changes the scheduling priority shape. The variables μ, Ω and Υ determine the shape of the function $P_j(v_j)$, which starts at a predetermined shape $\eta = 10$ (maximum priority) and may change as the system evolves. The change criteria of those parameters are shown afterward.

Hence, each virtual agent learns over time its best groups of UEs to maximize system throughput, a knowledge that is combined with the context information on prioritizing certain UEs to improve QoS provisioning. Algorithm 4 presents the proposed framework containing the MT, MTFG and MTQG solutions.

4.2.5 Signaling Overhead Reduction

In this chapter, at each TTI, the BS firstly schedules the UEs using one of our proposed algorithms presented in Section 4.2. Secondly, the scheduled UEs feed back their CSI using the analog precoders (2.6) and eigenvectors of equivalent channel (2.3) presented in Section 2.2. Finally, the digital precoder (2.9) is computed following Section 2.2, and the data is sent to the scheduled UEs using (2.12).

In general, most works in the literature (e.g., [29], [45], [47], [53]) consider that all UEs in the system feed back their instantaneous equivalent CSI before scheduling, providing information that helps the scheduler. Our scheme,

Algorithm 4 Proposed Framework.

Input: $\mathcal{A}_c$, C and T
Initialize: $\boldsymbol{q}_c = \mathbf{0}_{A_c \times 1}$ and $\boldsymbol{d}_c = \mathbf{0}_{A_c \times 1}$, $\forall c$
Initialize: set of scheduled UEs $\mathcal{S} = \emptyset$
Initialize: counter vectors $\boldsymbol{n}_c = \mathbf{0}_{A_c \times 1}$ of each action $\forall c$
Initialize: shape control variable $\eta = 10$ ▷ Max. priority.
for each TTI **do**
  for $c = 1$ to C **do**
    if system operator decides for MT scheduling **then**

$$a_c \leftarrow \begin{cases} \underbrace{\text{action that maximizes } (\boldsymbol{d}_c)}_{\text{Exploitation}}, & \text{probability } 1-\epsilon \\ \underbrace{\text{random action from } \mathcal{A}_c}_{\text{Exploration}}, & \text{probability } \epsilon \end{cases}$$

    else if system operator decides for MTFG scheduling **then**
      Calculate the vector of priorities $\boldsymbol{q}_c$ using (4.5) following Section 4.2.2

$$a_c \leftarrow \begin{cases} \underbrace{\text{action that maximizes } (\boldsymbol{q}_c \odot \boldsymbol{d}_c)}_{\text{Exploitation}}, & \text{probability } 1-\epsilon \\ \underbrace{\text{random action from } \mathcal{A}_c}_{\text{Exploration}}, & \text{probability } \epsilon \end{cases}$$

    else if system operator decides for MTQG scheduling **then**
      Calculate the vector of priorities $\boldsymbol{q}_c$ using (4.5) following Section 4.2.3

$$a_c \leftarrow \begin{cases} \underbrace{\text{action that maximizes } (\boldsymbol{q}_c \odot \boldsymbol{d}_c)}_{\text{Exploitation}}, & \text{probability } 1-\epsilon \\ \underbrace{\text{random action from } \mathcal{A}_c}_{\text{Exploration}}, & \text{probability } \epsilon \end{cases}$$

    end if
    $\mathcal{S} \leftarrow \mathcal{S} \cup \mathcal{A}_c(a_c)$ ▷ Schedule the UEs.
  end for
  Scheduled UEs $\mathcal{S}$ feed back their CSI
  Compute hybrid (analog and digital) precoder using (2.6) and (2.9)
  $d \leftarrow$ sum of scheduled UEs data rate using (2.12) ▷ Reward.
  for $c = 1$ to C **do**
    $\boldsymbol{n}_c(a_c) \leftarrow \boldsymbol{n}_c(a_c) + 1$ ▷ Number of times that a_c was chosen.
    $\boldsymbol{d}_c(a_c) \leftarrow \boldsymbol{d}_c(a_c) + \frac{1}{\boldsymbol{n}_c(a_c)}(\alpha - \boldsymbol{d}_c(a_c))$ ▷ Action values.
  end for
  if system operator decides for MTQG scheduling **then**
    if system satisfaction $\geq$ μ and the lowest satisfied UE throughput $\geq$ Ω (throughput requirement) **then**
      if $\eta \geq -10$ **then**
        $\eta = \eta - 1$ ▷ Prioritize more the throughput.
      end if
    else
      if $\eta \leq 10$ **then**
        $\eta = s + 1$ ▷ Prioritize more the satisfaction.
      end if
    end if
  end if
end for

however, needs only the equivalent instantaneous CSI of the K scheduled UEs. Therefore, it requires less signaling than those previous works. Figure 4.3 shows the main steps of all proposed algorithms.

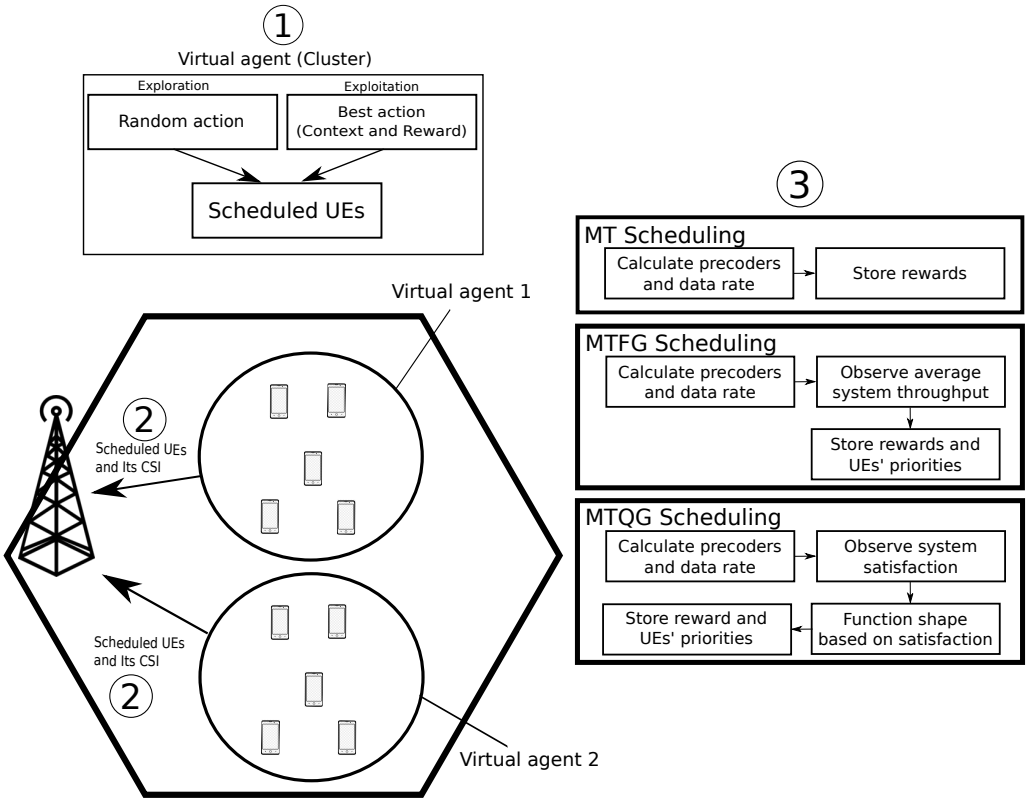

Figure 4.3 – Illustration of the main steps of the proposed scheduling algorithms. Firstly, the virtual agents select the UEs to be scheduled by the BS based on the exploration or exploitation strategy. Secondly, the selected UEs are scheduled by the BS and feed back their equivalent instantaneous CSIs. Finally, depending on the desired system performance the MT, MTFG or MTQG scheduling is executed.

4.3 Numerical Results

In this section, we describe our main assumptions as well as the scenario considered in our study. Afterwards, we compare the performance of the proposed algorithms against that of some baseline solutions previously proposed in the literature.

The scenario considered herein is shown in Figure 4.4, where a massive MIMO BS at coordinate $(0, 0)$ is equipped with an 8×8 UPA ($N = 64$), where x and y axis are the distances from the BS to the other elements of the scenario. It serves 20 UEs which are randomly distributed inside two hotspots, each with a radius of 15 m, located inside a $60°$ cell sector with 200 m of radius. The centers of the hotspots are 100 m away from the BS and $30°$ apart. Moreover, as in [8], [32], [53], [73], [74], we consider at most 10% of the number of transmit antennas as the quantity of available RF chains. Furthermore, the number of simulated UEs is limited by the complexity to obtain the optimal solution that has an exponential computational complexity.

We adopt the QuaDRiGa UMi LOS channel model [75] and assume the BS

Figure 4.4 – Scenario considering 2 hotspots with a determined angle θ between their centers.

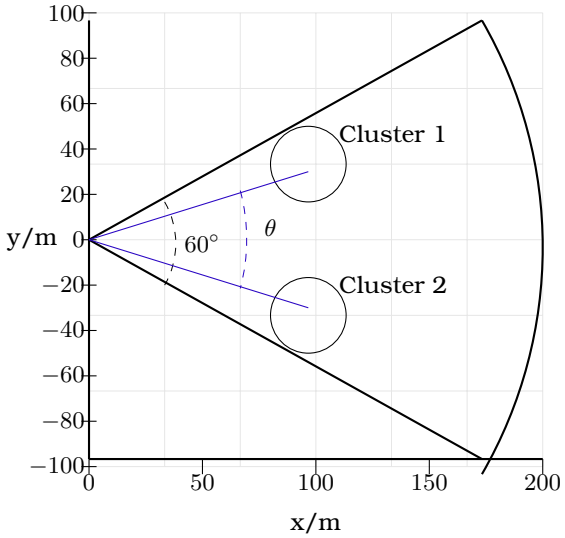

Source: Created by the author.

power to be evenly divided among 125 RBs. However, in this chapter, we are assuming only one RB available for transmission. The most relevant parameters used in our simulations are shown in Table 4.1.

Table 4.1 – Simulation Parameters for Chapter 4.

Parameter	**Value**
System bandwidth	100 MHz
System carrier frequency	28 GHz
Number of subcarriers per RB	12
Subcarrier spacing	60 kHz
TTI duration	0.25 ms
Number of OFDM symbols per TTI	14
Total transmit power	35 dBm
Noise figure	9 dB
Noise spectral density	-174 dBm/Hz
Shadowing standard deviation	3.1 dB
Cell radius	200 m
UEs Speed	0.83 and 16.67 m/s
Number of UEs	20
Number of clusters	2
Number of UEs per cluster	10
Number of UEs selected per cluster	2
Number of simulation rounds	100
Simulation duration	1 s

Source: Created by the author.

Herein, we consider two services with UEs requiring different throughput to be satisfied. For simplicity, we consider that each UE is using only one service. In order to differentiate the services, we consider that UEs from service 2 require 200 kbps more than the ones from service 1. Furthermore, we consider that the BS requires a system satisfaction $\mu = 90\%$, which we assume as the minimum acceptable satisfaction rate in our system. We also consider that

the UEs are randomly distributed uniformly among the services. Finally, we consider the value of $\Omega = 120\%$ of the worst satisfied UE throughput to trigger the change of shape conditions. The Ω value is chosen to make the framework adapt itself before the system satisfaction goes down under the required value μ. Note that these different service requirements are going to be used to evaluate the MTQG solution.

In order to get the system into a typically normal long-run condition for the RL algorithms, we consider a warm-up phase (which can be considered the RL training stage). Note that this warm-up phase is considered only for the RL schedulers since they perform decisions based on past experiences. In this phase, we consider that the UEs throughput requirement starts fulfilled and the ϵ values decay linearly from 100% to 5% over time. Thus, we consider that the warm-up phase has a duration of 100 TTIs. The motivation of having more exploration at the start is to avoid getting stuck into a local optimum by acquiring more information about the action space.

4.3.1 Max Rate Evaluation

In this section, we compare three solutions: the proposed MT algorithm with the solution proposed in Chapter 3 (BF) [32] – which employs a greedy algorithm to solve the scheduling problem –, and with the optimum solution (OPT) – which knows the equivalent instantaneous CSI to calculate all precoders and uses brute force enumerating all possible solutions choosing the best one. Notice that, due to the combinatorial size of the problem, the OPT solution has impractical computational complexity, which was calculated in (4.1). Also notice that all the simulated algorithms in this section use hybrid precoding, perform clustering before scheduling and, consequently, select only K_c UEs per cluster. Therefore, the interference among UEs of different clusters is supposed to be negligible for all simulated algorithms, as explained in Section 3.3.

In Figure 4.5, MT, BF, and OPT schedulers are compared in terms of system throughput for different UE speeds. The motivation to analyze scenarios with different speeds is to evaluate if there is a loss in the learning algorithm when the scenario gets more dynamic. The BF scheduler in Section 3.3 has a parameter β that establishes the trade-off between spatial correlation and channel gain. Note that the optimal value for this parameter can change with the UE distribution, so the system needs to find and adjust its value. To perform a fair comparison between schedulers, we consider that the optimal β is known by the system. As our proposed MT scheduler learns from the past, it is not sensitive to the UE distribution, differently from the BF solution. Another

Figure 4.5 – System throughput over the TTIs.
(a) UEs speed 3 km/h. (b) UEs speed 60 km/h.

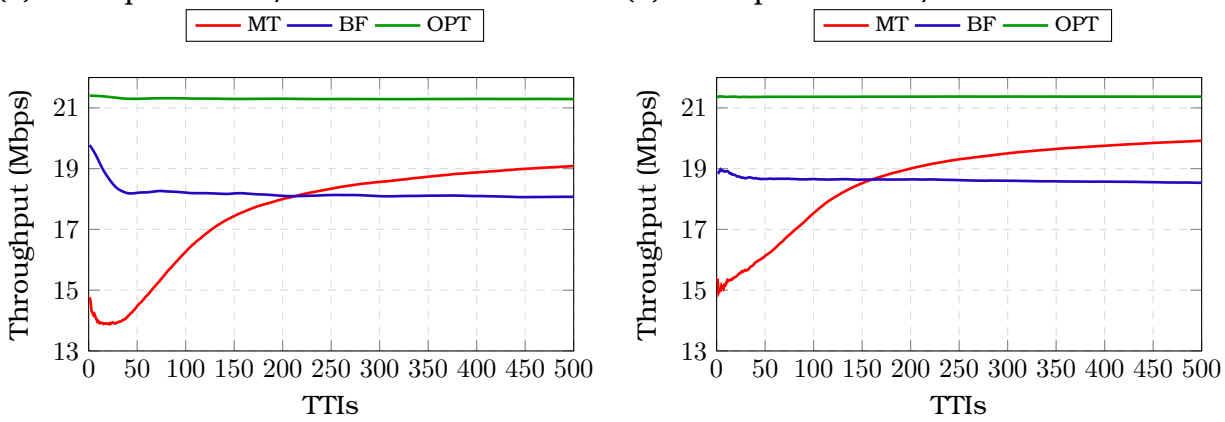

Source: Created by the author.

drawback of the BF scheduler in Section 3.3 is that it uses the covariance matrix to schedule the UEs. However, this information becomes outdated over time and needs to be estimated with a certain periodicity. In our simulations the same large-scale, long-term statistical CSI is used during the entire simulation. Note that these issues do not affect our proposed MT since the UEs are scheduled based on their past experience.

Focusing on the relative performance among algorithms, we can see that the MT scheduler needs only approximately 250 TTIs (62.5 ms) to outperform the BF solution. Furthermore, Figures 4.5a and 4.5b show that the OPT solution outperforms approximately 10% and 16% the MT and BF schedulers, respectively. Also, Figure 4.5b shows that the MT scheduler is robust to high mobility scenarios obtaining almost the same performance shown in Figure 4.5a. Note that, in the high mobility scenario the small-scale fading changes considerably for 100 TTIs at a speed of 60 km/h. Finally, in this scenario some UEs are going to get closer to the BS than in the low mobility scenario, therefore, these UEs are going to be scheduled by the MT and BF solutions achieving better performance.

4.3.2 Maximum Throughput with Fairness Guarantees Evaluation

In this section, we compare the proposed MTFG scheduler with the MT solution, which does not take into account any context information, and with the blind equal throughput (BET) [80], which uses the past average throughput as metric to schedule UEs. The BET scheduling stores the past average throughput and uses it as a metric to calculate the UEs scheduling priorities, providing fairness among UEs regardless of their channel conditions [80]. For more details on the BET algorithm, please refer to [80].

Figure 4.6 – System throughput over the TTIs for MT, MTFG, and BET algorithms.
(a) UEs speed 3 km/h. (b) UEs speed 60 km/h.

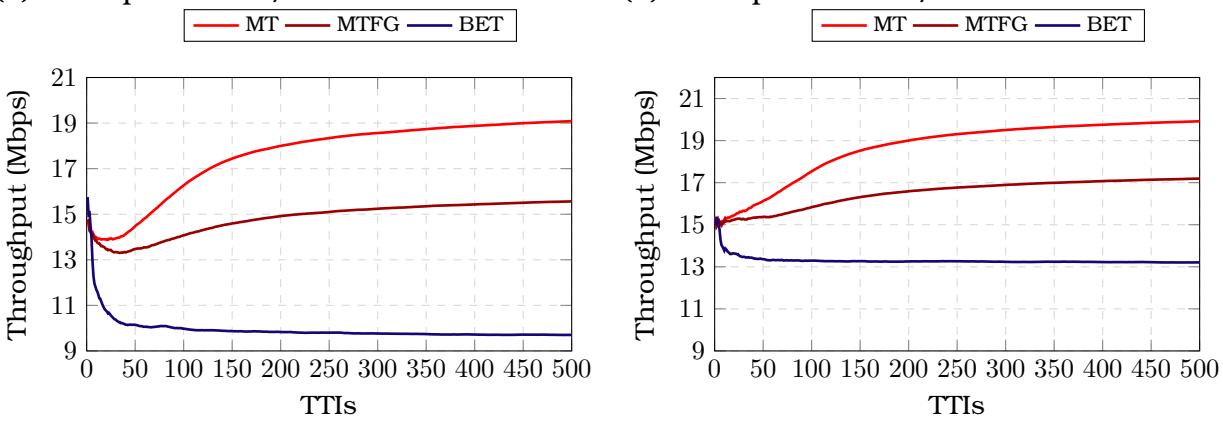

Source: Created by the author.

In Figure 4.6, MT, MTFG, and BET schedulers are compared in terms of system throughput for different UE speeds. As we can see, the MT scheduler achieves the best performance in terms of throughput. However, it will be seen later that seeking only for maximum throughput negatively affects the fairness among UEs. The MTFG scheduler solves this problem by giving priority to the UEs with lowest throughput, which is done through the priority function (4.4). Therefore, actions with highest values will be selected more often aiming at increasing the fairness among UEs, which negatively impacts the system throughput. Moreover, the BET scheduler has the worst performance due to its search for fairness, without concern over the system throughput achieved.

Focusing on the relative performance among schedulers in terms of throughput, we can see in Figures 4.6a and 4.6b that the MT scheduler outperforms the MTFG and BET by approximately 16% and 45%, respectively. Moreover, Figure 4.6b shows that the proposed scheduler can maintain its throughput performance even for higher mobility.

In Figure 4.7, MT, MTFG, and BET schedulers are compared in terms of Jain's fairness index for different UE speeds. As we can see, the performance of the schedulers in terms of fairness is the opposite of the one presented in Figure 4.6, as expected. The MT achieves the worst performance since it is concerned only about the system throughput. Moreover, in Figures 4.7a and 4.7b, the MTFG needs approximately 100 TTIs (25 ms) to achieve the same performance of the BET solution. Note that the MTFG scheduler achieves higher fairness among UEs at the price of a relatively small loss in throughput, thus offering a good fairness-throughput trade-off. Moreover, Figure 4.7b shows that the proposed MTFG can maintain its performance even for higher mobility.

Figure 4.7 – Jain's fairness index over the TTIs for MT, MTFG, and BET algorithms.
(a) UEs speed 3 km/h. (b) UEs speed 60 km/h.

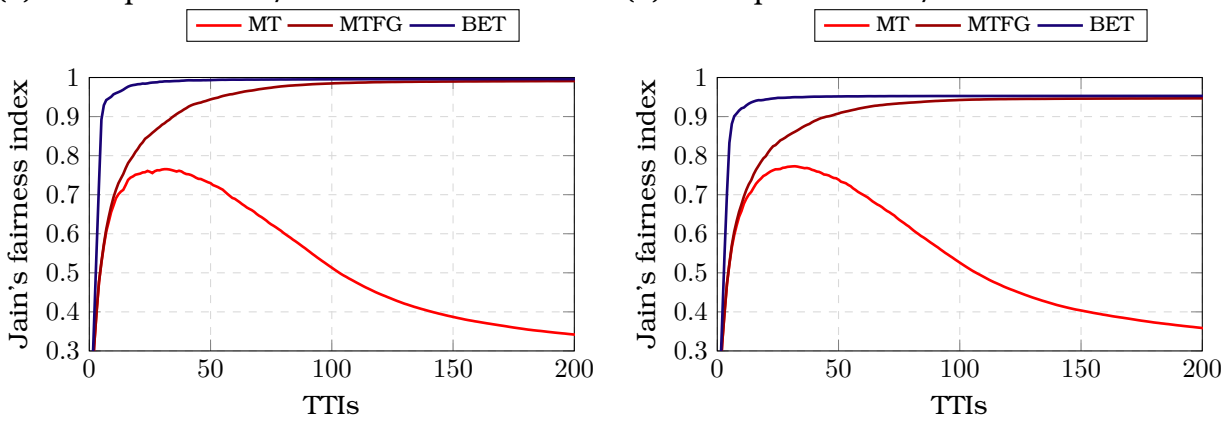

Source: Created by the author.

4.3.3 Maximum Throughput with QoS Guarantees Evaluation

In this section, we compare the scheduler MTQG with the QoS-aware proportional fair PF QoS (PF QoS) scheduler [80] and an adaptation of the JSM scheduler proposed in [41]. The proportional fair (PF) QoS is similar to the traditional PF scheduling. However, it works with two sets of UEs: i) the priority set with UEs that do not meet their QoS requirements, which own the highest priorities, and ii) the low priority set with the rest of the UEs (currently satisfied UEs). The JSM scheduler uses two policies based on the derivatives of the sigmoidal to obtain the UEs' priority. For more details on the JSM and PF QoS algorithms, please refer to [80] and [41], respectively. Moreover, the instantaneous CSI is used by the PF QoS and JSM schedulers to estimate the data rate, which is the information utilized to schedule the UEs. Therefore, for the sake of fairness in comparisons among different solutions, PF QoS and JSM schedulers use dominant eigenvalues and eigenvectors to estimate the data rate as the proposed schedulers, instead of using instantaneous CSI, since this is the same CSI employed by our proposed CMAB framework.

In Figure 4.8, the system satisfaction for MTQG, PF QoS, and JSM schedulers is shown for increasing values of the required throughput of service 1. As we can see, the PF QoS is the scheduler that achieves the worst performance for both UE speeds. This happens due to the simplicity of the scheduler and the inaccurate CSI available, which drastically decreases the performance. In Figure 4.8a, we can see that MTQG achieves the best performance and maintains higher satisfaction levels: above μ and close to 100%. However, the increase in the UEs' speed makes the MTQG and JSM schedulers achieve the same performance in Figure 4.8b. This happens due to the quick change of the channel state caused by the higher UEs' speed, which makes the best

Figure 4.8 – System satisfaction versus required throughput of service 1 for the MTQG, PF QoS, and JSM algorithms.
(a) UEs speed 3 km/h. (b) UEs speed 60 km/h.

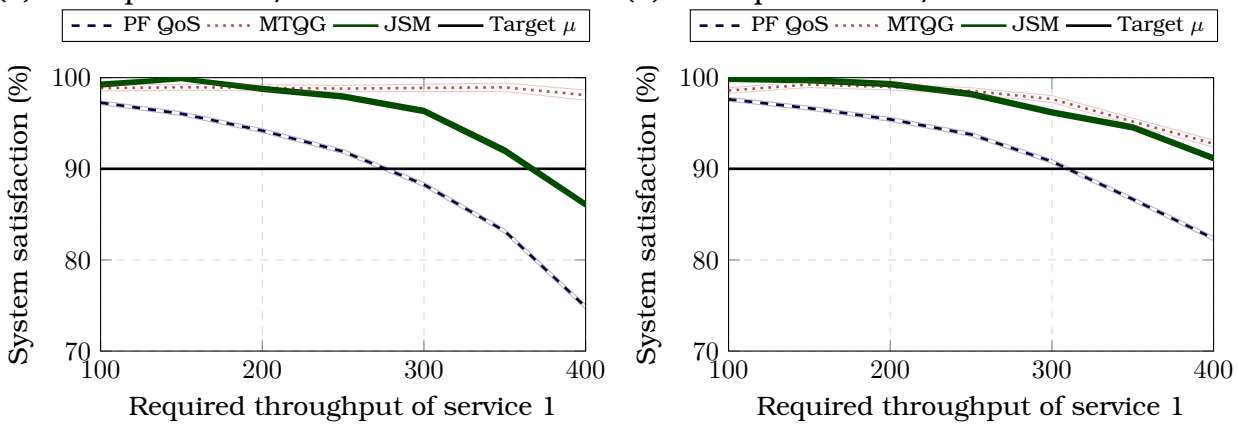

Source: Created by the author.

Figure 4.9 – System throughput versus required throughput of service 1 for the MTQG, PF QoS, and JSM algorithms.
(a) UEs speed 3 km/h. (b) UEs speed 60 km/h.

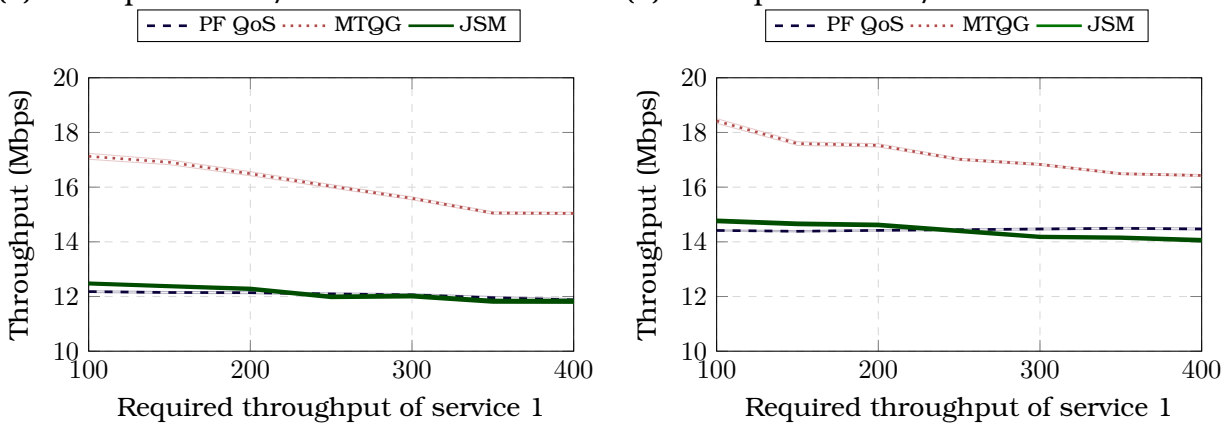

Source: Created by the author.

scheduling compositions change more often, leading to a more challenging scenario to be learned by the MTQG. Also, the performance loss of the baseline algorithms occurs because they do not take into account any information about the interference among scheduled UEs, increasing the probability of scheduling UEs with correlated channels in the same RB. On the other hand, MTQG learns about channel correlation through rewards and uses the same CSI as the baseline schedulers.

In Figure 4.9, MTQG, PF QoS, and JSM schedulers are compared in terms of system throughput for different values of required throughput for service 1. We recall that the required throughput of service 2 is 200 kbps higher than that of service 1. As it can be seen, the system throughput decreases as the required throughput increases, so that there is a trade-off between satisfaction and system throughput to which the algorithms are subjected. Moreover, the

MTQG scheduler achieves the highest system throughput independently of the service required throughput. The MTQG and JSM schedulers can maintain almost the same throughput over the required throughput. In Figure 4.8b, only the PF QoS scheduler decreases drastically its satisfaction compared to the JSM and MTQG solutions. Anyway, the MTQG scheduler provides gains in system throughput of up to 41% compared to PF QoS and JSM algorithms. Moreover, Figure 4.9b shows that the proposed algorithm can maintain its performance even for higher mobility.

4.4 Conclusions

In this chapter, we proposed and evaluated a framework of RRA for hybrid precoding massive MIMO communication systems using RL tools. In order to deal with the combinatorial search space of the scheduler, we create clusters of UEs with correlated statistical channels and propose a new strategy that considers each cluster as a virtual learning agent. We consider that an action is the selection of UEs to be scheduled. Therefore, not considering virtual agents leads to an unpractical number of possible actions. Also, the virtual agents select the UEs belonging to their own cluster, aiming at maximizing a pre-determined objective. Therefore, the BS is responsible for receiving the UEs selected by the virtual agents and for scheduling them.

We solved three RRA problems in our framework, which are throughput maximization only, throughput maximization considering fairness, and throughput maximization with QoS guarantees. The proposed framework dynamically adapts itself to solve the RRA problem desired by the operator. Also, the proposed solutions to those problems utilize the CMAB tool. This tool achieves good performance even when working with limited/scarce information, which is one of the challenges of massive MIMO. Therefore, we utilize only the statistical CSI to schedule the UEs, which reduces the signal overhead. Also, since we are proposing a CMAB framework that learns by trial and error, we reduce even more the signaling overhead by considering that only the scheduled UEs have to feed back their equivalent instantaneous CSI. Moreover, the precoders are calculated only for the scheduled UEs, which avoids the computation for every scheduling possibility. Simulation results show that the baseline algorithms are outperformed by the proposed solutions in low and high mobility scenarios. Also, the results show that the learning algorithms are robust even when the scenario gets more dynamic.

The contents of this chapter can be extended in some directions. In the following, some of the possible future works are pointed out:

- Extend the scenario to consider multiple RBs. One possibility is to apply the proposed CMAB framework iteratively at each RB and evaluate its performance. Another possibility is to adapt the proposed CMAB framework to consider multiple RBs.
- Consider another bandit algorithm instead of ϵ-greedy, such as upper confidence bandit or gradient bandit.
- Extend the scenario to consider a model of network traffic. One possibility is to adapt the proposed CMAB framework to consider the network traffic as context to decide which UEs should be scheduled.
- Extend the scenario to consider other QoS requirements, such as packet delay, latency and jitter.

Chapter 5

Conclusions

As presented in Chapter 1, the main purpose of this thesis is to study solutions based on optimization and RL to address RRA problems in massive MIMO networks. The review in Chapter 1 presented some solutions pointed by the research community and industry to meet the main requirements of 5G. The reviewed technologies are massive MIMO, mmWave and network slicing. Besides those technologies having their own benefits and challenges, this thesis focuses on massive MIMO technology. We highlighted the benefits of massive MIMO achieved by the higher number of antenna elements, such as the higher data rates and number of served UEs, and the channel hardening effect. Also we reviewed some of the challenges of FDD massive MIMO systems, such as the large amount of required RF chains and the limited feedback channel. These challenges do not happen for time division duplex (TDD) systems since they can take advantage of some features, such as channel reciprocity. However, most of the current wireless networks are based in FDD systems and it is still favored by network operators, reinforcing the study of FDD massive MIMO systems. We presented the hybrid precoding as a scheme adopted by the academy and industry to deal with the challenge of needing a large number of required RF chains. This scheme links a smaller number of RF chains to a large number of antennas. Lastly, in Chapter 1 we presented a review of RRA and RL techniques. More specifically, we highlighted the particular case of RL tools known as CMAB.

We present in Chapter 2 the system model considered for all the chapters of this thesis. In this chapter, the considered spatial covariance matrix and its eigendecomposition are described. Also, we describe the clustering procedure which is used in all the chapters of this thesis. This procedure divides the UEs into clusters containing spatially correlated UEs by using a clustering algorithm that subsequently reduces the SDMA grouping search space. After

that, we describe the hybrid precoding scheme and received signal models. Furthermore, we describe how the SINR and data rate are calculated.

In Chapter 3, we propose a framework using optimization tools to deal with RRA problems in massive MIMO networks. The proposed framework has three steps: clustering, grouping, and scheduling. The clustering step is done as explained previously. The grouping procedure utilizes intelligent strategies to build several efficient SDMA groups in terms of SE. Finally, in the scheduling procedure we assign RBs to build SDMA groups in the grouping step, aiming at optimizing a predefined objective.

This way, in Chapter 3 we first deal with the RRA problem of maximizing the data rate considering only one RB. Since this problem only has one RB, the grouping and scheduling procedure are done together. Therefore, we formulate this problem as a binary quadratic problem which was solved using BB and a proposed low complexity algorithm. Our proposed low complexity solution is evaluated against the BB and a baseline solution. Simulation results show that our proposed solution performs better in terms of SE than the baseline solution and offers a good trade-off between computation complexity and system performance against the BB algorithm. Moreover, we also show that a suitable trade-off between the spatial channel correlation and channel gain should be chosen to improve the system performance.

After that, in Chapter 3, we extended the previous problem to solve the RRA problem of maximizing the system data rate considering multiple RBs, services and QoS requirements. Here, since we considered multiple RBs, all the steps of the framework are utilized. The clustering step is done as explained previously. A binary quadratic problem that builds multiple groups and considers fairness is formulated and applied in the grouping step. The grouping step exploits the channel hardening characteristic generating a set of SDMA groups suitable for all RBs. In the scheduling step, the assignment of RBs to the previously generated SDMA groups is done aiming at maximizing the data rate and meeting the QoS requirements. We propose low complexity solutions to the grouping and scheduling steps evaluating them separately against optimal and baseline solutions. Simulation results show that our proposed framework achieves a good trade-off in terms of SE and outage against optimal and baseline solutions, especially in low and moderate system loads. Moreover, we also show that a suitable trade-off between the spatial channel correlation and channel gain should be chosen to improve the system performance.

In Chapter 4, we proposed a framework using CMAB tools to deal with RRA problems in massive MIMO networks. The proposed CMAB framework

dinamically configures/adapts itself to solve the RRA problems of maximizing the data rate, maximizing the data rate with fairness guarantees, or maximizing the data rate with QoS guarantees. We take advantage of the clustering and ZF precoding to reduce the scheduling search space. This way, we consider that the BS is the physical entity and the UEs' clusters are the logical entities (virtual agents). Therefore, since we are using CMAB theory, the virtual agents learn from the past experiences the best policy to schedule the UEs aiming at achieving one of the previously mentioned objectives. Also, the signaling overhead is reduced by considering that only the scheduled UEs have to feed back their equivalent instantaneous CSI, which is used to calculate the system data rate (reward). Simulation results show that the baseline algorithms are outperformed by the proposed solutions. Also, the results show that the learning algorithms are robust even when the scenario gets more dynamic (UEs moving at different speeds).

References

[1] W. Hong, Z. H. Jiang, C. Yu, D. Hou, H. Wang, C. Guo, Y. Hu, L. Kuai, Y. Yu, Z. Jiang, Z. Chen, J. Chen, Z. Yu, J. Zhai, N. Zhang, L. Tian, F. Wu, G. Yang, Z. C. Hao, and J. Y. Zhou, "The role of millimeter-wave technologies in 5G/6G wireless communications", *IEEE Journal of Microwaves*, vol. 1, no. 1, pp. 101–122, 2021. DOI: 10.1109/JMW.2020.3035541.

[2] H. Fourati, R. Maaloul, and L. Chaari, "A survey of 5G network systems: challenges and machine learning approaches", in *International Journal of Machine Learning and Cybernetics*, Aug. 2020. DOI: 10.1007/s13042-020-01178-4.

[3] N. Al-Falahy and O. Y. Alani, "Technologies for 5G Networks: challenges and opportunities", *IT Professional*, vol. 19, no. 1, pp. 12–20, 2017. DOI: 10.1109/MITP.2017.9.

[4] P. V. Klaine, M. A. Imran, O. Onireti, and R. D. Souza, "A survey of machine learning techniques applied to self-organizing cellular networks", *IEEE Communications Surveys Tutorials*, vol. 19, no. 4, pp. 2392–2431, 2017. DOI: 10.1109/COMST.2017.2727878.

[5] M. Agiwal, A. Roy, and N. Saxena, "Next Generation 5G Wireless Networks: A Comprehensive Survey", vol. 18, no. 3, pp. 1617–1655, 2016. DOI: 10.1109/COMST.2016.2532458.

[6] B. Wang, F. Gao, S. Jin, H. Lin, and G. Y. Li, "Spatial- and frequency-wideband effects in millimeter-wave massive MIMO systems", *IEEE Transactions on Signal Processing*, vol. 66, no. 13, pp. 3393–3406, Jul. 2018, ISSN: 1941-0476. DOI: 10.1109/TSP.2018.2831628.

[7] W. Roh, J. Y. Seol, J. Park, B. Lee, J. Lee, Y. Kim, J. Cho, K. Cheun, and F. Aryanfar, "Millimeter-wave beamforming as an enabling technology for 5g cellular communications: Theoretical feasibility and prototype results",

IEEE Communications Magazine, vol. 52, no. 2, pp. 106–113, Feb. 2014, ISSN: 0163-6804. DOI: 10.1109/MCOM.2014.6736750.

[8] W. V. F. Mauricio, T. F. Maciel, A. Klein, and F. R. M. Lima, "Learning-based scheduling: contextual bandits for massive MIMO systems", in *2020 IEEE International Conference on Communications Workshops (ICC Workshops)*, 2020, pp. 1–6. DOI: 10.1109/ICCWorkshops49005.2020.9145188.

[9] H. Yu, H. Lee, and H. Jeon, "What is 5G? Emerging 5G mobile services and network requirements", *Sustainability*, vol. 9, no. 10, Oct. 2017.

[10] I. A. Hemadeh, K. Satyanarayana, M. El-Hajjar, and L. Hanzo, "Millimeter-wave communications: Physical channel models, design considerations, antenna constructions, and link-budget", vol. 20, no. 2, pp. 870–913, 2018.

[11] M. R. Akdeniz, Y. Liu, M. K. Samimi, S. Sun, S. Rangan, T. S. Rappaport, and E. Erkip, "Millimeter wave channel modeling and cellular capacity evaluation", vol. 32, no. 6, pp. 1164–1179, 2014.

[12] X. Foukas, G. Patounas, A. Elmokashfi, and M. K. Marina, "Network slicing in 5G: survey and challenges", *IEEE Communications Magazine*, vol. 55, no. 5, pp. 94–100, 2017. DOI: 10.1109/MCOM.2017.1600951.

[13] ITU-R, "IMT vision – framework and overall objectives of the future development of IMT for 2020 and beyond", Recommendation ITU-R M.2083-0, 2015. [Online]. Available: https://www.itu.int/rec/R-REC-M.2083 (visited on 10/19/2018).

[14] ITU, *IMT-2020 network high level requirements - how african countries can cope*. [Online]. Available: https://www.itu.int/en/ITU-T/Workshops-and-Seminars/standardization/20170402/Documents/S2_4.%5C%20Presentation_IMT%5C%202020%5C%20Requirements-how%5C%20developing%5C%20countries%5C%20can%5C%20cope.pdf.

[15] E. Björnson, E. G. Larsson, and T. L. Marzetta, "Massive MIMO: Ten myths and one critical question", vol. 54, no. 2, pp. 114–123, 2016.

[16] V. F. Monteiro, I. L. da Silva, and F. R. P. Cavalcanti, "5G Measurement Adaptation Based on Channel Hardening Occurrence", *IEEE Communications Letters*, vol. 23, no. 9, pp. 1598–1602, 2019. DOI: 10.1109/LCOMM.2019.2926268.

[17] H. Q. Ngo and E. G. Larsson, "No downlink pilots are needed in TDD massive MIMO", *IEEE Transactions on Wireless Communications*, vol. 16, no. 5, pp. 2921–2935, May 2017, ISSN: 1536-1276. DOI: 10.1109/TWC.2017.2672540.

[18] D. C. Araújo, T. Maksymyuk, A. L. F. de Almeida, T. Maciel, J. C. M. Mota, and M. Jo, "Massive MIMO: survey and future research topics", *IET Communications*, vol. 10, no. 15, pp. 1938–1946, 2016. DOI: 10.1049/iet-com.2015.1091.

[19] R. W. Heath, N. González-Prelcic, S. Rangan, W. Roh, and A. M. Sayeed, "An overview of signal processing techniques for millimeter wave MIMO systems", *IEEE Journal of Selected Topics in Signal Processing*, vol. 10, no. 3, pp. 436–453, Apr. 2016, ISSN: 1932-4553. DOI: 10.1109/JSTSP.2016.2523924.

[20] E. Björnson, *When will hybrid beamforming disappear?* [Online]. Available: https://ma-mimo.ellintech.se/2019/05/02/when-will-hybrid-beamforming-disappear/.

[21] M. Rihan, T. Abed Soliman, C. Xu, L. Huang, and M. I. Dessouky, "Taxonomy and performance evaluation of hybrid beamforming for 5G and beyond systems", vol. 8, pp. 74 605–74 626, 2020.

[22] M. Soleimani, R. C. Elliott, W. A. Krzymie, J. Melzer, and P. Mousavi, "Hybrid beamforming for mmWave massive MIMO systems employing DFT-assisted user clustering", *IEEE Transactions on Vehicular Technology*, vol. 69, no. 10, pp. 11 646–11 658, 2020. DOI: 10.1109/TVT.2020.3015787.

[23] M. Dottling, M. Sternad, G. Klang, J. von Hafen, and M. Olsson, "Integration of spatial processing in the WINNER B3G air interface design", in *Proceedings of the IEEE Vehicular Technology Conference (VTC)*, vol. 1, 2006, pp. 246–250. DOI: 10.1109/VETECS.2006.1682813.

[24] T. F. Maciel and A. Klein, "On the performance, complexity, and fairness of suboptimal resource allocation for multiuser MIMO-OFDMA systems", vol. 59, no. 1, pp. 406–419, 2010, ISSN: 0018-9545. DOI: 10.1109/TVT.2009.2029438.

[25] M. Majidzadeh and M. Eslami, "A novel suboptimal SDMA grouping algorithm for multiuser MIMO-OFDMA systems", in *Proc. Iranian Conference on Electrical Engineering (ICEE)*, 2014, pp. 1805–1810. DOI: 10.1109/IranianCEE.2014.6999832.

[26] K. B. Letaief and Y. J. Zhang, "Dynamic multiuser resource allocation and adaptation for wireless systems", vol. 13, no. 4, pp. 38–47, 2006, ISSN: 1536-1284. DOI: 10.1109/MWC.2006.1678164.

[27] W. V. F. Mauricio, D. C. Araujo, T. F. Maciel, and F. R. M. Lima, "A framework for radio resource allocation and sdma grouping in massive mimo systems", *IEEE Access*, vol. 9, pp. 61 680–61 696, 2021. DOI: 10.1109/ACCESS.2021.3074360.

[28] M. Moretti, L. Sanguinetti, and X. Wang, "Resource Allocation for Power Minimization in the Downlink of THP-Based Spatial Multiplexing MIMO-OFDMA Systems ", vol. 64, no. 1, pp. 405–411, 2015. DOI: 10.1109/TVT.2014.2320587.

[29] J. Nam, A. Adhikary, J. Ahn, and G. Caire, "Joint spatial division and multiplexing: opportunistic beamforming, user grouping and simplified downlink scheduling", vol. 8, no. 5, pp. 876–890, Oct. 2014. DOI: 10.1109/JSTSP.2014.2313808.

[30] Y. J. Zhang and K. B. Letaief, "An Efficient Resource-Allocation Scheme for Spatial Multiuser Access in MIMO/OFDM Systems ", vol. 53, no. 1, pp. 107–116, 2005. DOI: 10.1109/TCOMM.2004.840666.

[31] S. Boyd and L. Vandenberghe, *Convex optimization*, 1st. Cambridge University Press, 2004.

[32] W. V. F. Mauricio, D. C. Araujo, F. H. C. Neto, F. R. M. Lima, and T. F. Maciel, "A low complexity solution for resource allocation and SDMA grouping in massive MIMO systems", in *Proceedings of the IEEE International Symposium on Wireless Communications Systems (ISWCS)*, Aug. 2018, pp. 1–6. DOI: 10.1109/ISWCS.2018.8491076.

[33] F. D. Calabrese, L. Wang, E. Ghadimi, G. Peters, L. Hanzo, and P. Soldati, "Learning radio resource management in RANs: framework, opportunities, and challenges", *IEEE Communications Magazine*, vol. 56, no. 9, pp. 138–145, Sep. 2018, ISSN: 0163-6804. DOI: 10.1109/MCOM.2018.1701031.

[34] I. Ahmed and H. Khammari, "Joint machine learning based resource allocation and hybrid beamforming design for massive MIMO systems", in *2018 IEEE Globecom Workshops (GC Wkshps)*, Dec. 2018, pp. 1–6. DOI: 10.1109/GLOCOMW.2018.8644454.

[35] R. S. Sutton and A. G. Barto, *Introduction to reinforcement learning*, 1st. Cambridge, MA, USA: MIT Press, 1998, ISBN: 0262193981.

[36] F. Hussain, S. A. Hassan, R. Hussain, and E. Hossain, "Machine learning for resource management in cellular and IoT networks: potentials, current solutions, and open challenges", *prePrint: arXiv*, 2019. arXiv: 1907.08965 [cs.NI].

[37] M. Dudk, D. J. Hsu, S. Kale, N. Karampatziakis, J. Langford, L. Reyzin, and T. Zhang, "Efficient optimal learning for contextual bandits", *CoRR*, vol. abs/1106.2369, 2011. arXiv: 1106.2369. [Online]. Available: http://arxiv.org/abs/1106.2369.

[38] M. Simsek, M. Bennis, and . Güvenç, "Learning based frequency and time-domain inter-cell interference coordination in hetnets", *IEEE Transactions on Vehicular Technology*, vol. 64, no. 10, pp. 4589–4602, 2015. DOI: 10.1109/TVT.2014.2374237.

[39] S. Jiang, Y. Chang, and K. Fukawa, "Distributed inter-cell interference coordination for small cell wireless communications: a multi-agent deep Q-learning approach", in *2020 International Conference on Computer, Information and Telecommunication Systems (CITS)*, 2020, pp. 1–5. DOI: 10.1109/CITS49457.2020.9232512.

[40] IBM, *IBM ILOG CPLEX Optimizer*. [Online]. Available: http://www-01.ibm.com/software/integration/optimization/cplex-optimizer/.

[41] R. P. Antonioli, E. B. Rodrigues, T. F. Maciel, D. A. Sousa, and F. R. P. Cavalcanti, "Adaptive resource allocation framework for user satisfaction maximization in multi-service wireless networks", *Telecommunication Systems*, vol. 68, no. 2, pp. 259–275, Jun. 2018, ISSN: 1572-9451. DOI: 10.1007/s11235-017-0391-3.

[42] F. Zhao, W. Ma, M. Zhou, and C. Zhang, "A graph-based QoS-aware resource management scheme for OFDMA femtocell networks", *IEEE Access*, vol. 6, pp. 1870–1881, 2018, ISSN: 2169-3536. DOI: 10.1109/ACCESS.2017.2780520.

[43] J. Wang, Y. Zhang, H. Hui, and N. Zhang, "QoS-aware proportional fair energy-efficient resource allocation with iimperfect CSI in downlink OFDMA systems", in *2015 IEEE 26th Annual International Symposium on Personal, Indoor, and Mobile Radio Communications (PIMRC)*, Aug. 2015, pp. 1116–1120. DOI: 10.1109/PIMRC.2015.7343465.

[44] T. Y. Young and T. W. Calvert, "Classification, estimation and pattern recognition", *American Elsevier*, 1974.

[45] A. Destounis and M. Maso, "Adaptive clustering and CSI acquisition for FDD massive MIMO systems with two-level precoding", in *2016 IEEE Wireless Communications and Networking Conference*, Apr. 2016, pp. 1–6. DOI: 10.1109/WCNC.2016.7564900.

[46] A. Maatouk, S. E. Hajri, M. Assaad, H. Sari, and S. Sezginer, "Graph theory based approach to users grouping and downlink scheduling in FDD massive MIMO", in *2018 IEEE International Conference on Communications (ICC)*, May 2018, pp. 1–7. DOI: 10.1109/ICC.2018.8422263.

[47] X. Sun, X. Gao, G. Y. Li, and W. Han, "Agglomerative user clustering and cluster scheduling for FDD massive MIMO systems", *IEEE Access*, vol. 7, pp. 86 522–86 533, 2019. DOI: 10.1109/ACCESS.2019.2923246.

[48] J. Chen and D. Gesbert, "Joint user grouping and beamforming for low complexity massive MIMO systems", in *2016 IEEE 17th International Workshop on Signal Processing Advances in Wireless Communications (SPAWC)*, Jul. 2016, pp. 1–6. DOI: 10.1109/SPAWC.2016.7536906.

[49] G. Wang, J. Zhao, X. Bi, Y. Lu, and F. Hou, "User grouping and scheduling for joint spatial division and multiplexing in FDD massive MIMO system", *Int. J. Communications, Network and System Sciences*, vol. 10, pp. 176–185, 2017. DOI: 10.4236/ijcns.2017.108B019.

[50] A. Maatouk, S. E. Hajri, M. Assaad, and H. Sari, "On optimal scheduling for joint spatial division and multiplexing approach in FDD massive MIMO", *IEEE Transactions on Signal Processing*, vol. 67, no. 4, pp. 1006–1021, Feb. 2019, ISSN: 1941-0476. DOI: 10.1109/TSP.2018.2886163.

[51] G. Bu and J. Jiang, "Reinforcement learning-based user scheduling and resource allocation for massive MU-MIMO system", in *2019 IEEE/CIC International Conference on Communications in China (ICCC)*, Aug. 2019, pp. 641–646. DOI: 10.1109/ICCChina.2019.8855949.

[52] R. Chataut and R. Akl, "Channel gain based user scheduling for 5G massive MIMO systems", in *2019 IEEE 16th International Conference on Smart Cities: Improving Quality of Life Using ICT IoT and AI (HONET-ICT)*, Oct. 2019, pp. 049–053. DOI: 10.1109/HONET.2019.8908036.

[53] H. Xu, T. Zhao, S. Zhu, D. Lv, and J. Zhao, "Agglomerative group scheduling for mmWave massive MIMO under hybrid beamforming architecture", in *2018 IEEE 18th International Conference on Communication Technology (ICCT)*, Oct. 2018, pp. 347–351. DOI: 10.1109/ICCT.2018.8600015.

[54] Z. Jiang, S. Chen, S. Zhou, and Z. Niu, "Joint user scheduling and beam selection optimization for beam-based massive MIMO downlinks", *IEEE Transactions on Wireless Communications*, vol. 17, no. 4, pp. 2190–2204, Apr. 2018, ISSN: 1558-2248. DOI: 10.1109/TWC.2018.2789895.

[55] N. W. Moe Thet, T. Baykas, and M. K. Ozdemir, "Performance analysis of user scheduling in massive MIMO with fast moving users", in *2019 IEEE 30th Annual International Symposium on Personal, Indoor and Mobile Radio Communications (PIMRC)*, Sep. 2019, pp. 1–6. DOI: 10.1109/PIMRC.2019.8904133.

[56] A. Ortiz, A. Asadi, M. Engelhardt, A. Klein, and M. Hollick, "CBMoS: combinatorial bandit learning for mode selection and resource allocation in D2D systems", *IEEE Journal on Selected Areas in Communications*, vol. 37, no. 10, pp. 2225–2238, Oct. 2019, ISSN: 1558-0008. DOI: 10.1109/JSAC.2019.2933764.

[57] P. K. Tathe and M. Sharma, "Dynamic actor-critic: reinforcement learning based radio resource scheduling for LTE-advanced", in *2018 Fourth International Conference on Computing Communication Control and Automation (ICCUBEA)*, Aug. 2018, pp. 1–4. DOI: 10.1109/ICCUBEA.2018.8697808.

[58] I. Comsa, S. Zhang, M. E. Aydin, P. Kuonen, Y. Lu, R. Trestian, and G. Ghinea, "Towards 5G: a reinforcement learning-based scheduling solution for data traffic management", *IEEE Transactions on Network and Service Management*, vol. 15, no. 4, pp. 1661–1675, Dec. 2018, ISSN: 2373-7379. DOI: 10.1109/TNSM.2018.2863563.

[59] D. C. Araújo, E. Karipidis, A. L. F. de Almeida, and J. C. M. Mota, "Hybrid beamforming design with finite-resolution phase-shifters for frequency selective massive MIMO channels", in *2017 IEEE International Conference on Acoustics, Speech and Signal Processing (ICASSP)*, Mar. 2017, pp. 6498–6502. DOI: 10.1109/ICASSP.2017.7953408.

[60] T. Y. Young and T. W. Calvert, "Classification, estimation and pattern recognition", *American Elsevier*, 1974.

[61] F. H. Costa Neto, D. Costa Araújo, and T. Ferreira Maciel, "Hybrid beamforming design based on unsupervised machine learning for millimeter wave systems", *International Journal of Communication Systems*, 2020. DOI: 10.1002/dac.4276.

[62] Y. Xu, G. Yue, and S. Mao, "User grouping for massive MIMO in FDD systems: new design methods and analysis", *IEEE Access*, vol. 2, pp. 947–959, 2014, ISSN: 2169-3536. DOI: 10.1109/ACCESS.2014.2353297.

[63] G. W. Milligan and M. C. Cooper, "An examination of procedures for determining the number of clusters in a data set", *Psychometrika*, vol. 50, no. 2, pp. 159–179, Jun. 1985, ISSN: 1860-0980. DOI: 10.1007/BF02294245. [Online]. Available: https://doi.org/10.1007/BF02294245.

[64] L. Kaufman and P. Rousseeuw, *Finding groups in data: an introduction to cluster analysis*. Wiley, 1990.

[65] G. H. Golub and C. F. van Loan, *Matrix Computations*, Fourth. JHU Press, 2013, ISBN: 1421407949 9781421407944. [Online]. Available: http://www.cs.cornell.edu/cv/GVL4/golubandvanloan.htm.

[66] T. H. Cormen, C. E. Leiserson, R. L. Rivest, and C. Stein, *Introduction to Algorithms, Third Edition*, 3rd. The MIT Press, 2009, ISBN: 0262033844.

[67] E. Castaneda, A. Silva, A. Gameiro, and M. Kountouris, "An overview on resource allocation techniques for multi-user MIMO systems", vol. 19, no. 1, pp. 239–284, Firstquarter 2017. DOI: 10.1109/COMST.2016.2618870.

[68] T. M. Cover and J. A. Thomas, *Elements of information theory*, 2nd, J. W. bibinitperiod Sons, Ed. 2006, ISBN: 978-0471241959.

[69] V. Kumar and N. B. Mehta, "Modeling and analysis of differential CQI feedback in 4G/5G OFDM cellular systems", *IEEE Transactions on Wireless Communications*, vol. 18, no. 4, pp. 2361–2373, Apr. 2019, ISSN: 1536-1276. DOI: 10.1109/TWC.2019.2903047.

[70] F. R. M. Lima, T. F. Maciel, W. C. Freitas, and F. R. P. Cavalcanti, "Improved spectral efficiency with acceptable service provision in multiuser MIMO scenarios", vol. 63, no. 6, pp. 2697–2711, 2014, ISSN: 0018-9545. DOI: 10.1109/TVT.2013.2293333.

[71] G. Sierksma, *Linear and integer programming: theory and practice, Second Edition*, ser. Advances in Applied Mathematics. Taylor & Francis, 2001, ISBN: 9780824706739.

[72] R. C. Browning, E. A. Baker, J. A. Herron, and R. Kram, "Effects of obesity and sex on the energetic cost and preferred speed of walking.", *Journal of applied physiology*, vol. 100 2, pp. 390–8, 2006.

[73] Z. Wang, M. Li, Q. Liu, and A. L. Swindlehurst, "Hybrid precoder and combiner design with low-resolution phase shifters in mmWave MIMO systems", *IEEE Journal of Selected Topics in Signal Processing*, vol. 12, no. 2, pp. 256–269, May 2018, ISSN: 1941-0484. DOI: 10.1109/JSTSP.2018.2819129.

[74] Z. Cheng, Z. Wei, and H. Yang, "Low-complexity joint user and beam selection for beamspace mmWave MIMO systems", *IEEE Communications Letters*, vol. 24, no. 9, pp. 2065–2069, 2020. DOI: 10.1109/LCOMM.2020.2995400.

[75] S. Jaeckel, L. Raschkowski, K. Börner, and L. Thiele, "QuaDRiGa: a 3-D multicell channel model with time evolution for enabling virtual field trials", vol. 62, no. 6, pp. 3242–3256, Jun. 2014, ISSN: 0018-926X. DOI: 10.1109/TAP.2014.2310220.

[76] V. F. Monteiro, I. L. da Silva, and F. R. P. Cavalcanti, "5G measurement adaptation based on channel hardening occurrence", *IEEE Communications Letters*, vol. 23, no. 9, pp. 1598–1602, 2019.

[77] T. Van Chien, "Spatial resource allocation in massive mimo communications : From cellular to cell-free", PhD thesis, Linköping University, Faculty of Science Engineering, 2020, p. 66, ISBN: 9789179299415. DOI: 10.3384/diss.diva-162582.

[78] A. A. Zaidi, R. Baldemair, H. Tullberg, H. Bjorkegren, L. Sundstrom, J. Medbo, C. Kilinc, and I. D. Silva, "Waveform and numerology to support 5G services and requirements", vol. 54, no. 11, pp. 90–98, 2016. DOI: 10.1109/MCOM.2016.1600336CM.

[79] O. Caelen and G. Bontempi, "Improving the exploration strategy in bandit algorithms", in *Learning and Intelligent Optimization*, V. Maniezzo, R. Battiti, and J.-P. Watson, Eds., Berlin, Heidelberg: Springer Berlin Heidelberg, 2008, pp. 56–68, ISBN: 978-3-540-92695-5.

[80] F. Capozzi, G. Piro, L. A. Grieco, G. Boggia, and P. Camarda, "Downlink packet scheduling in LTE cellular networks: key design issues and a survey", *IEEE Communications Surveys Tutorials*, vol. 15, no. 2, pp. 678–700, Second 2013. DOI: 10.1109/SURV.2012.060912.00100.